

UNCLASSIFIED

AD NUMBER

AD460405

NEW LIMITATION CHANGE

TO

**Approved for public release, distribution
unlimited**

FROM

**Notice: All release of this document is
controlled. All certified requesters shall
obtain release approval from Secretary of
Defense, Attn: ARPA-AGILE, Defense
Advanced Research Projects Agency, DARPA,
3701 North Fairfax Drive, Arlington, VA,
22203-1714.**

AUTHORITY

DARPA ltr, 20 Nov 2001

THIS PAGE IS UNCLASSIFIED

AD 469405

USATRECOM TECHNICAL REPORT 64-74

XV-8A FLEXIBLE WING AERIAL UTILITY VEHICLE

FINAL REPORT

By

F. Landgraf

P. F. Girard

PROPERTY OF U. S. ARMY

TRECOM

February 1965 TECHNICAL LIBRARY

AD - 469405

U. S. ARMY TRANSPORTATION RESEARCH COMMAND

FORT EUSTIS, VIRGINIA

CONTRACT DA 44-177-AMC-874(T)

RYAN AERONAUTICAL COMPANY

SPONSORED BY:
ADVANCED RESEARCH
PROJECTS AGENCY



DDC Availability Notice

All distribution of this report is controlled. Qualified DDC users shall request through Secretary of Defense, ATTN: ARPA-AC (LE), Washington, D. C. 20310.

Release or announcement to the public is not authorized.

Reproduction Limitations

Reproduction of this document in whole or in part is prohibited except with permission of the Secretary of Defense.

Disclaimer

The findings in this report are not to be construed as an official Department of the Army position, unless so designated by other authorized documents.

When Government drawings, specifications, or other data are used for any purpose other than in connection with a definitely related Government procurement operation, the United States Government thereby incurs no responsibility nor any obligation whatsoever, and the fact that the Government may have formulated, furnished, or in any way supplied the said drawings, specifications, or other data is not to be regarded by implication or otherwise as in any manner licensing the holder or any other person or corporation, or conveying any rights or permission, to manufacture, use, or sell any patented invention that may in any way be related thereto.

Disposition Instructions

Destroy this report when it is no longer needed. Do not return it to the originator.

HEADQUARTERS
U S ARMY TRANSPORTATION RESEARCH COMMAND
FORT EUSTIS, VIRGINIA 23604

This report is a summary presentation of the aerodynamic analysis, stress analysis, structural tests, and initial flight evaluation of a Flexible Wing Aerial Utility Vehicle that is designated the XV-8A. The XV-8A was designed and built by Ryan Aeronautical Company in accordance with the requirements of Contract DA 44-177-AMC-874(T), which was initiated by the U. S. Army Transportation Research Command and funded by the Advanced Research Projects Agency.

The conclusions reached in this report are concurred in by this Command. Based on these conclusions, the aircraft has been modified, and a follow-on flight test program has been conducted to determine the performance and handling qualities (reference USATRECOM Technical Report 64-55).

This Command gratefully acknowledges the assistance provided during this project by the Airborne Operations Section, Yuma Proving Ground, Yuma, Arizona.

Task ID121401A14172
Contract DA 44-177-AMC-874(T)
USATRECOM Technical Report 64-74

February 1965

XV-8A
FLEXIBLE WING AERIAL UTILITY VEHICLE

REPORT NO. 65B003

This research was supported by the Advanced Research Projects Agency of the Department of Defense and was monitored by the U.S. Army Transportation Research Command (USATRECOM) under Contract DA 44-177-AMC-874(T).

Prepared by
RYAN AERONAUTICAL COMPANY
SAN DIEGO, CALIFORNIA

for
U.S. ARMY TRANSPORTATION RESEARCH COMMAND
FORT EUSTIS, VIRGINIA

ABSTRACT

This report entitled XV-8A FLEXIBLE WING AERIAL UTILITY VEHICLE is a final report based upon the Contractor's abridged Report No. 64B08 dated August 1964 which contained 96 pages, 29 illustrations and 13 tables. The contract number was DA 44-177-AMC-874(T), ARPA Order 294-62 Amendment No. 3, Unclassified. This final report and the abridged preliminary report discussed procedures and accomplishments of the design, fabrication and test program of the XV-8A for the following phases:

1. Investigation of the feasibility of construction of a Flexible Wing Light Utility Vehicle that was simple to operate and capable of transporting a 1,000-pound payload for a distance of 100 miles at a speed of 50 miles per hour.
2. The design, building and testing of two vehicles.
3. The structural tests at the Contractor's plant and the flight tests at the U.S. Army Proving Ground, Yuma, Arizona.
4. The conclusion that the vehicles are feasible, and that further tests are recommended.

FOREWORD

The design, fabrication, and test program discussed in this report was conducted under the provisions of Contract DA 44-177-AMC-874(T) between the U.S. Army Transportation Research Command and the Ryan Aeronautical Company.

The vehicle described herein is a second generation outgrowth of a flexible wing manned test vehicle previously developed by Ryan Aeronautical Company. Tests on the original vehicle were made under the provisions of Contract DA 44-177-TC-721 as reported in TCREC Technical Report 62-25.

Structural tests described herein were conducted at the contractor's plant at San Diego, California. Taxi tests and flight tests were conducted at the Yuma Proving Ground, Yuma, Arizona.

CONTENTS

	<u>Page</u>
ABSTRACT	iii
FOREWORD	v
LIST OF ILLUSTRATIONS	ix
LIST OF TABLES	xi
LIST OF SYMBOLS	xii
SUMMARY	1
CONCLUSIONS	2
RECOMMENDATIONS	4
DESCRIPTION	5
AERODYNAMICS ANALYSIS	25
STRESS ANALYSIS	44
STRUCTURAL TESTS	53
FLIGHT-TEST EVALUATION	76
MAINTENANCE REQUIREMENTS	92
BIBLIOGRAPHY	93
DISTRIBUTION	95

ILLUSTRATIONS

<u>Figure</u>		<u>Page</u>
1	In-Flight View, Flexible Wing Aerial Utility Vehicle	11
2	Final Assembly Model 164	13
3	Aerial Utility Vehicle Platform Assembly	15
4	Wing Assembly and Installation	17
5	Main Landing Gear and Brake Assembly	19
6	Fuel System Installation	21
7	Controls Installation	23
8	Performance Data	27
9	Stability and Control Data	30
10	V-n Diagram for Symmetrical Flight	46
11	Reference Data for Weight and Center of Gravity Calculations	51
12	Loading and Burn-Off Curve	52
13	Whiffle Tree Configuration	54
14	Static Test Setup	55
15	Keel Deflection	55
16	Cockpit Controls Proof Loading Test Configuration	58
17	Control Column, Control Wheel and Brake Pedal Deflection	59
18	Keel Deflection Under Load	59

ILLUSTRATIONS (Continued)

<u>Figure</u>		<u>Page</u>
19	Deflection Point and Strain Gauge Location, Ruddervator	61
20	Shot Bag Configuration, Ruddervator	61
21	Ruddervator Failure	62
22	Ruddervator Failure, Shot Bags Removed	62
23	Ruddervator Deflection Data	63
24	Drop Test Configuration	66
25	Landing Gear Test Setup and Axle Failure	68
26	Landing Gear Test, Strain Gauge Location	74
27	Landing Gear Test, Load Vs. Strain	74
28	Landing Gear Test, Load Vs. Deflection	75
29	Performance Data, Level Flight	85

TABLES

<u>Table</u>		<u>Page</u>
1	Longitudinal Dynamic Stability Data	41
2	Lateral-Directional Dynamic Stability Data	42
3	Summary - Critical Loads and Factors of Safety	47
4	Weight and Center of Gravity Calculations	49
5	Actual Weighing Results	50
6	Weight Adjustments	50
7	Wing and Platform Test Data	57
8	Keel Deflection Load Results	60
9	Drop Test Configuration No. 1	69
10	Drop Test Configuration No. 2	70
11	Drop Test Configuration No. 3	71
12	Drop Test Configuration No. 4	72
13	Drop Test Configuration No. 5	73

LIST OF SYMBOLS

BHP	brake horse power
cg	center of gravity
C_A	axial force coefficient, $\frac{A}{qS_W}$
C_D	drag coefficient, $\frac{D}{qS_W}$
C_{D_0}	drag coefficient at zero lift
$C_{\frac{1}{2}}$	cycles to damp to 1/2 amplitude
C_h_α	hinge moment coefficient due to angle of attack, $\frac{\partial C_h}{\partial \alpha}$
C_K	wing keel length, feet
C_L	lift coefficient, $\frac{L}{qS}$
C_{L_q}	rate of change of lift coefficient with pitch velocity per radian
C_{L_α}	lift-curve slope, $\frac{dC_L}{d\alpha}$, per radian or degree
$C_{L_{\delta_e}}$	rate of change of lift coefficient with elevator deflection $\frac{dC_L}{d\delta_e}$, per degree
C_t_β	rate of change of rolling moment coefficient with side slip angle, $\frac{dC_t}{d\beta}$, per radian or degree
C_m	pitching moment coefficient, $\frac{M}{qSC}$

$C_m C_L$	rate of change of pitching moment with lift coefficient, $\frac{dC_m}{dC_L}$, per degree
C_{m_0}	pitching moment coefficient at zero lift
C_{m_T}	pitching moment coefficient due to thrust
C_{m_α}	rate of change of pitching moment coefficient with angle of attack, $\frac{dC_m}{d\alpha}$, per degree
$C_{m_{\delta_e}}$	rate of change of pitching moment coefficient with elevator deflection, $\frac{dC_m}{d\delta_e}$, per degree
C_N	normal-force coefficient, $\frac{N}{qS_W}$
$C_n \beta$	rate of change of yawing moment with side slip angle, $\frac{dC_n}{d\beta}$, per radian or degree
C_R	specific range, number miles/pound of fuel
$C_Y \beta$	rate of change of side force with sideslip angle, $\frac{dC_Y}{d\beta}$, per radian degree
D	drag, pounds
F_S	control stick, force, pounds
F_X	force along X axis, pounds
F_Z	force along Z axis, pounds
FS	fuselage station, inches
GW	gross weight, pounds
g	acceleration of gravity, $\frac{32 \text{ ft}}{\text{sec}^2}$

HM	hinge moment, foot-pounds
HP_{exc}	excess horsepower, $HP_{avail} - HP_{req'd}$
I_X	moment of inertia about X axis, slug-ft ²
I_Y	moment of inertia about Y axis, slug-ft ²
I_Z	moment of inertia about Z axis, slug-ft ²
I_{XZ}	product of inertia, slug-ft ²
i_{TH}	incidence of thrust line relative to body center line, degrees
i_W	incidence of wing relative to body center line, degrees
I	rolling moment, foot-pounds
L_S	length of control stick, feet
L_{TH}	distance from center of gravity to thrust line, feet
M	pitching moment, foot-pounds
m	mass, slugs
N	normal force, pounds
n_Y	side load factor
n_Z	vertical load factor
q	free stream dynamic pressure, $1/2 \rho v^2$, $\frac{lb}{ft^2}$
R/C	rate of climb, feet/minute
S_{GR}	takeoff or landing ground run, feet

s_w	flat-plan wing area, 450 square feet
s_t	tail area, square feet
SFC	specific fuel consumption
SR	specific range, nautical miles
T	thrust
THP	thrust horsepower
$t_{\frac{1}{2}}$	time to dampen to 1/2 amplitude, seconds
V	velocity, feet/second or knots
v_{LO}	lift off velocity
W	weight, pounds
X	distance from cg measured along X stability axis, negative in sign if measured to point aft of cg
x_w	distance from cg to wing moment center along X stability axis
x_{ac}	distance from wing apex to longitudinal aerodynamic center of wing measured aft along keel
x_t	tail moment arm measured along X axis, feet/second square
\ddot{x}	acceleration along X axis, feet/second square
Z	distance from cg measured along Z stability axis, negative in sign if measured to point above cg in feet
\ddot{z}	acceleration along Z axis
z_t	tail moment arm measured along Z axis, feet
z_w	distance from cg to wing moment center along Z stability axis

α	angle of attack, degrees
α_{OL}	angle of attack at zero lift, degrees
β	angle of sideslip, radians or degrees
Σ	summation symbol
Γ	dihedral angle, degrees
γ	flight path angle, degrees
δ_e	elevator deflection, degrees or radians
δ_s	control-stick deflection, degrees or radians
ϵ	downwash angle, degrees
Θ	angular displacement of X axis and about Y axis, radians
μ	rolling-friction coefficient
μ_β	braking-friction coefficient
ρ	air density, slugs/feet ³
σ	air density ratio, $\frac{\rho}{\rho_0}$

SUBSCRIPT SYMBOLS

B	body
GR	ground run
TD	touchdown
TO	takeoff
t	tail
w	wing

SUMMARY

Preliminary design studies and the final detail design of a Flexible Wing Light Utility Vehicle were carried out, and two test vehicles were fabricated. Structural adequacy was determined by stress analysis and appropriate static and dynamic tests. A limited flight test program was conducted to determine the handling qualities and performance of the vehicle. Initial tests revealed a deficiency in longitudinal control power which was corrected by incorporation of an auxiliary elevator at the aft end of the fuselage. Roll control power was satisfactory, and roll control forces were light. A minor modification in the roll control linkage further lightened these forces.

Positive static longitudinal stability was demonstrated within the range of center of gravity positions tested. It was determined, however, that it would be advisable to move the wing forward 12 inches with respect to the cargo platform in order to improve the landing attitude with center of gravity forward.

The tricycle landing gear incorporating an oleo nose strut and fiber glass springs at the main wheels has performed very well. The fiber glass springs have required no maintenance.

Engine cooling by means of individual exhaust aspirated stacks proved to be entirely adequate as originally designed and fabricated. The engine fuel system has operated with complete reliability. Engine starting by manually turning the propeller has presented no difficulty at any time, starting generally being accomplished in the first quarter turn.

Additional flight testing will be required to fully evaluate the potential capabilities of the XV-8A vehicle.

CONCLUSIONS

From experience gained during the design, fabrication and test program on the XV-8A aircraft, the following conclusions were made:

1. It is feasible to build a vehicle of the type under consideration that will carry disposable load equal to its empty weight.
2. The performance of the fiber glass main landing gear springs in conjunction with the nose wheel oleo strut is excellent. In still air, low-speed ground handling characteristics of the XV-8A are very good.
3. When taxiing at low speed in crosswinds of 5 knots or more with the wing at high incidence, high lateral control forces are required to restrain the wing from canting downwind. These forces can be minimized by precanting the wing in the upwind direction before turning to the crosswind direction.
4. The roll control system, incorporating movable tips at the aft ends of the leading edge spars and a wing roll axis substantially parallel to the flight path, provides powerful control with low pilot effort and little or no adverse yaw.
5. The wing should be moved forward 12 inches with respect to the cargo platform in order to improve the landing attitude with forward center of gravity.
6. Within the range of center of gravity positions tested, the vehicle is statically stable about all axes.
7. With the auxiliary horizontal control surface, longitudinal control at landing approach speed is adequate. Control forces, however, are lower than desirable in comparison to roll control forces.
8. A damping device as installed on the nose wheel is adequate to prevent shimmy.

9. Spanwise battens installed along the outboard portion of the wing trailing edge are effective in preventing trailing edge flutter.
10. Improved longitudinal control results when the wing pitch trim system is interconnected with the pilot's control column so as to produce $\pm 1\frac{1}{2}$ degrees of wing incidence change when the control column is moved through its full travel of ± 19 degrees. Incorporation of such a system would require that the most advantageous position of the wing pivot point be chosen, in order to avoid excessive control force.

RECOMMENDATIONS

The following recommendations are made based on the experience gained thus far from the XV-8A test program:

1. The wing should be moved forward 12 inches with respect to the cargo platform, temporary outboard trailing edge battens and auxiliary horizontal tail surface should be replaced with permanent units, and the aluminum alloy aileron hinges should be replaced by steel parts to improve rigidity and reliability.
2. Tests should be made with progressively decreased freedom of motion of the wing about the roll axis with the objective of eliminating this motion entirely if satisfactory roll control can be obtained by means of the ailerons alone.
3. All tests made thus far have been with the "two-control" system, rigged so as to produce no interaction between the roll and yaw systems. Further tests should be made to evaluate the several degrees of interaction that may be rigged into the system, as well as the system in which the yaw control is independently operated by means of the rudder pedals. The objective of these tests would be to determine the optimum control system configuration for the intended vehicle mission.
4. Additional flight testing should be done to obtain quantitative evaluation of flying qualities and performance.

DESCRIPTION

Figure 1 shows the vehicle in flight. Figure 2 shows the arrangement of the vehicle described herein. It consists basically of a cargo platform suspended below a Rogallo-type flexible wing. A pilot's seat and the necessary flight controls are provided at the forward end of the platform. An engine, a pusher propeller, and a V-tail are mounted at the rear of the platform. Provision is made for manually folding the wing and tail surfaces.

Dimensions and Weights

Keel and leading edge length	26 feet
Leading edge sweep angle	50 degrees
Canopy area (flat) 45 degree sweep;	
6 percent scallop	450 square feet
Vehicle overall length	26 feet
Vehicle overall height (wing horizontal)	14.54 feet
Vehicle overall width (wing extended)	33.4 feet
Vehicle overall width (wing folded)	8 feet
Propeller diameter	
(Hartzell two-blade metal)	7 feet
Main landing gear tread	9 feet
Wheel base	10.63 feet
Designed gross weight	2300 pounds
Empty weight (actual)	1115 pounds

STRUCTURAL DETAILS

Platform

The basic body structure is a flat deck with a raised platform at the forward end which supports the pilot's seat, nose wheel, control mechanism, instrument panel and nose fairing (Figure 3). The usable cargo area, 64 inches wide and 80 inches long, is fitted with twelve standard flush-type cargo tie-down rings. Transverse beams are incorporated at the forward end of the cargo area, at the main landing gear, and at the rear where the tail surface loads are carried. Removable doors in the bottom skin provide access to the fuel tank, piping, control pulleys, and cables. The fiber glass fairing at the forward end of the cockpit is removable for access to the back of the pilot's instrument panel. The pilot's seat, a built-in portion of the vehicle structure, is equipped with

a standard seat belt and shoulder harness. Space for a back-pack-type parachute is provided.

Wing Support

A forward A-frame and an aft tripod constructed of aluminum alloy tubing attaches the wing to the body structure (Figure 2).

Wing Keel

The wing keel is a tapered, sheet aluminum alloy box type structure which attaches to the roll control structure with a hinged fitting installed at the keel 46 percent station.

Wing Leading Edge

The wing leading edges are hollow aluminum alloy spars having a symmetrical streamlined cross section. The spars are tapered toward both ends from a maximum section near the spreader bar attachment. The wing membrane is attached along the trailing edge. The aft 13-1/2 percent of the leading edge is hinged to permit ±5-degree motion in a chordwise direction. A cable and pulley system is used to control the position of the hinged portion of the leading edge in flight.

Wing Spreader Bar

The wing spreader bar is a transverse truss work of steel and aluminum tubing attached to the wing keel and leading edges. It resists the inward and upward forces due to membrane tension and transmits lift loads to the wing support structure. By removing two quick-release pins at the joint between the leading edges and the spreader bar, two men can fold the spreader bar and bring the wing leading edges inboard.

Wing Membrane

Fabric for the wing membrane is square-weave Daeron cloth coated on both sides with olive drab polyester resin (Figure 4). The treated fabric has a tensile strength of not less than 200 pounds per inch in the warp direction and not less than 120 pounds per inch in the fill direction. Number 6 machine screws, spaced 3 inches apart, are used to attach the wing membrane to the aft edge of the leading edge and the keel. The screws pass through a metal reinforcing strip, bonded and stitched into the hem.

A reinforcing cable, sewn in the hem along the trailing edge of the membrane, is adjustable while on the ground for roll trim.

Tail Surfaces

The twin tails mounted at 35 degrees dihedral are shown in Figure 2. The movable surfaces incorporate aluminum alloy spars and fabric-covered ribs. The fixed surfaces are similarly constructed, except that metal skins are used to obtain maximum torsional stiffness. Hinged attachment fittings permit folding the tail portions up and inboard for transportation and storage. As a result of preliminary tests, an auxiliary horizontal control surface hinged to the aft end of the control platform was incorporated in the final design.

Landing Gear

The tricycle-type landing gear (Figure 2 and Figure 5) uses main and nose-wheel tires and wheels of the same size and type (7.00 x 6), in the interest of keeping required spares to the minimum. The tread of the main landing gear is 9.0 feet; wheelbase is 10.63 feet. Landing loads at the main wheels are absorbed by cantilever fiber glass springs extending from both sides of the platform structure. Single-disc-type brakes in the main wheels are hydraulically actuated by a master cylinder located in the pilot's cockpit. Landing loads on the nose wheel are absorbed by an oleo-type shock absorber incorporated in the nose landing gear. The nose wheel may be steered through an angle of 25 degrees either side of center by operating foot pedals in the pilot's cockpit.

PROPELLION SYSTEM

Engine

The engine specifications are as follows:

Model No.	IO-360A
Type	6-cylinder, Horizontally Opposed, Air Cooled
Continuous Horsepower,	
Rated Maximum	195
R. P. M., Maximum Continuous . .	2,800
Fuel Octane Rating	100/130
Fuel Control System	Continuous Flow, Injector

Four flexible rubber mounts are used to attach the engine to a steel tube truss near the aft end of the platform structure. An exhaust aspirated cooling system is used. Ten quarts of oil are carried in the engine sump. Oil flow through the air-cooled, engine-mounted oil cooler is regulated by a built-in thermal device.

Propeller

The BHC-C2YF-1A, 7-foot-diameter, all-metal propeller is installed as a pusher. The propeller is operated at fixed pitch by locking the blades at the angle for best all-around performance.

Fuel

A 25-gallon aluminum alloy fuel tank is mounted below the floor of the cargo platform near the center of gravity. (See Figure 6). A float-type fuel quantity gage is used. The tank is removable through a door on the bottom of the platform. Fuel from the tank flows through an emergency shutoff valve and fuel strainer to an engine-driven vane-type pump which maintains a constant pressure of 8 p.s.i. at the inlet to the engine-driven fuel metering pump. The metering pump supplies fuel to individual-cylinder fuel-injector nozzles at the pressure required for the particular throttle setting and engine speed. A hand pump, mounted on the right side of the pilot's seat, supplies about 2-1/2 p. s. i. pressure to the fuel metering pump for engine starting.

Control System

For ease of operation by pilots with minimum training, the Aerial Utility Vehicle has been designed as a "two-control" aircraft. Longitudinal control is accomplished by means of the tail surfaces previously described, actuated by fore and aft motion of a control column in the pilot's cockpit (Figure 7). Roll control results from displacing the wing about the roll axis. This action is achieved partly by direct control force applied to the wing and partly by means of servo tabs built into the aft ends of the wing leading edge, both actuated by means of a wheel at the top of the pilot's control column. In order to counteract the adverse yaw associated with wing roll, the control mechanism incorporates means to actuate the two ruddervators differentially when roll control is applied. An adjustable stop is provided to limit the amount of up elevator control so as to avoid flying at wing

angles of attack beyond 34 degrees. A pitch trim wheel is provided on the left side of the pilot's cockpit. It regulates the incidence of the wing to effect longitudinal trim for any flight speed and center of gravity position within the design limits. A pair of foot pedals for nose wheel steering and main wheel braking completes the cockpit control installation.

Roll Control

To reduce pilot roll control force requirements, an aerodynamic boost system is incorporated. The aft tip portion of each wing leading edge spar is hinged to permit ± 5 degrees motion in a chordwise direction. These tips are differentially actuated by the initial movement of the control wheel to produce an effect similar to that of ailerons on a conventional wing. The rolling moment due to tip displacement is in a direction to assist the desired wing roll. When the tips reach the limit of their displacement, further motion of the control wheel follows the rolling motion of the wing, or augments it, depending on the amount of force applied.

Yaw Control

A mechanism under the floor of the pilot's cockpit interconnects the aileron control system with the ruddervator system to move the tail surfaces differentially and thus produce a yawing moment. The link between the aileron system and the ruddervator system can be connected in any one of several sets of holes to permit rigging of varying amounts of yaw control into the system.

Longitudinal Control

A tubular steel control column is hinged to the floor of the pilot's cockpit. An arm on the bottom of the column extends below the floor, where it connects to the control interconnect mechanism described under "Control System, Yaw Control." A system of cables, bell cranks, and push rods moves the tail surfaces up or down in unison when the control column is moved fore and aft.

Longitudinal Trim

The vehicle may be trimmed longitudinally by turning the trim wheel on the left-hand side of the pilot's seat. This wheel rotates a cable

drum through a set of reduction gears. The revolving cable drum reels a cable out on one side while taking up the cable on the opposite side. The cables are attached to the wing keel, one forward of the main pivot and one aft. Forward rotation at the wheel rim produces a nose-down moment and vice versa. An irreversible clutch in the wheel hub locks the wheel against rotation when torque is applied from the direction of the cable drum, but permits free rotation when torque is applied at the handwheel.

Roll Trim

A small-diameter steel cable is incorporated in the trailing edge of each lobe of the wing canopy. Tightening the cable increases the lift of the wing lobe. The cables are independently adjustable to provide roll trim.

Yaw Trim

No provision is made for yaw trim.

Nose Steering Wheel

Foot pedals in the pilot's cockpit are connected by means of cables to steering arms extending from each side of the nose wheel oleo piston tube. Stops at the pedals limit the steering motion to ± 25 degrees.

Brakes

Both rear wheel brakes are operated from a single hydraulic master cylinder connected to an auxiliary pedal mounted on the right steering pedal (Figure 5 and Figure 7).

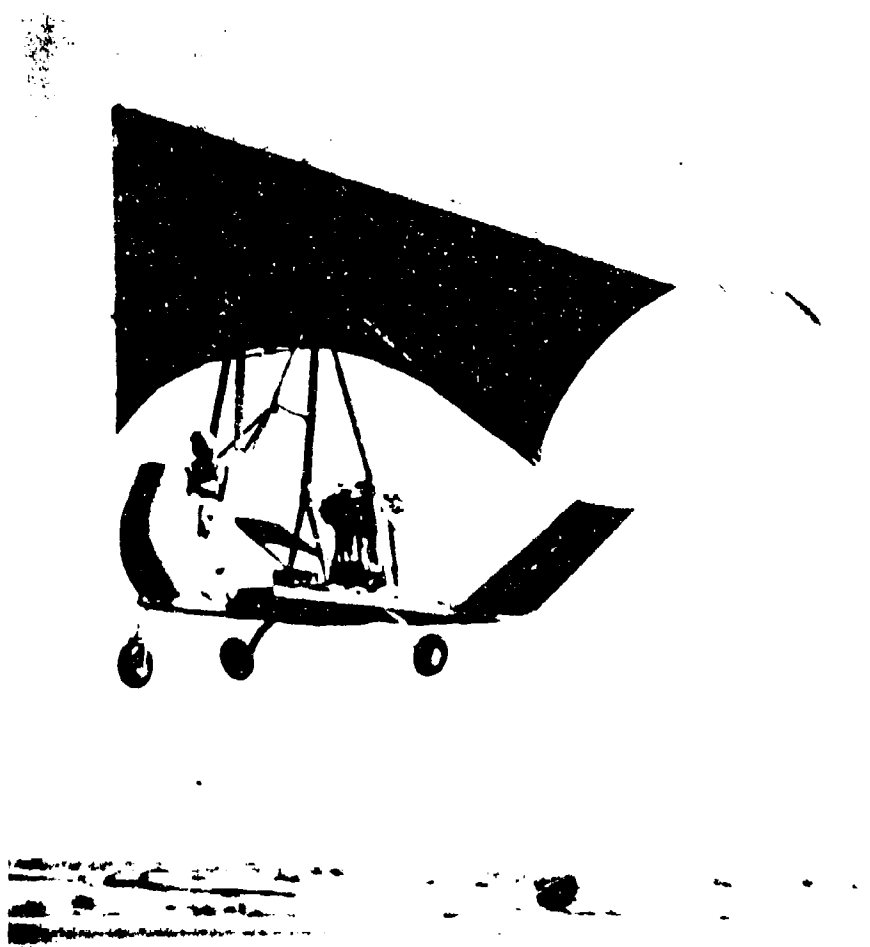
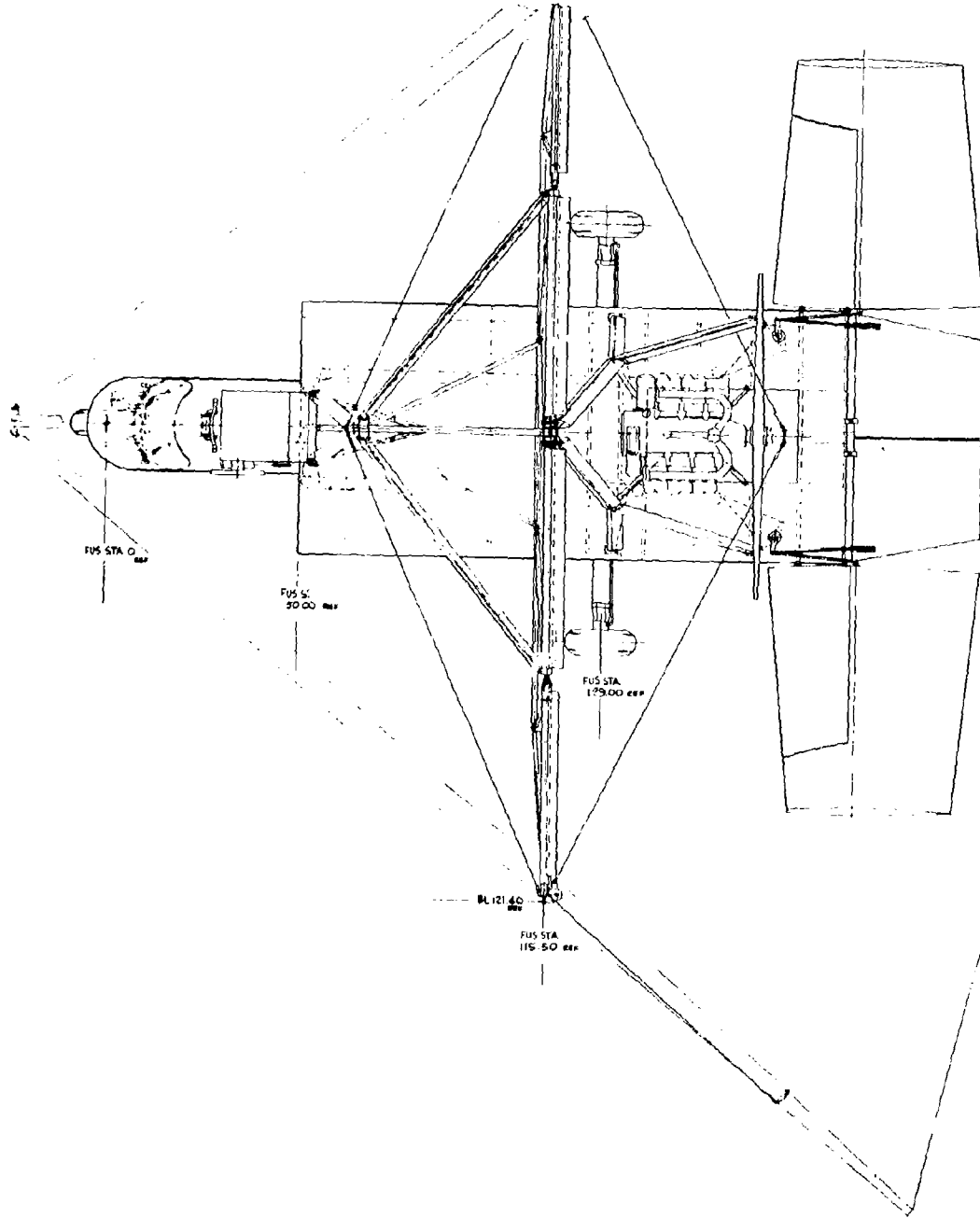


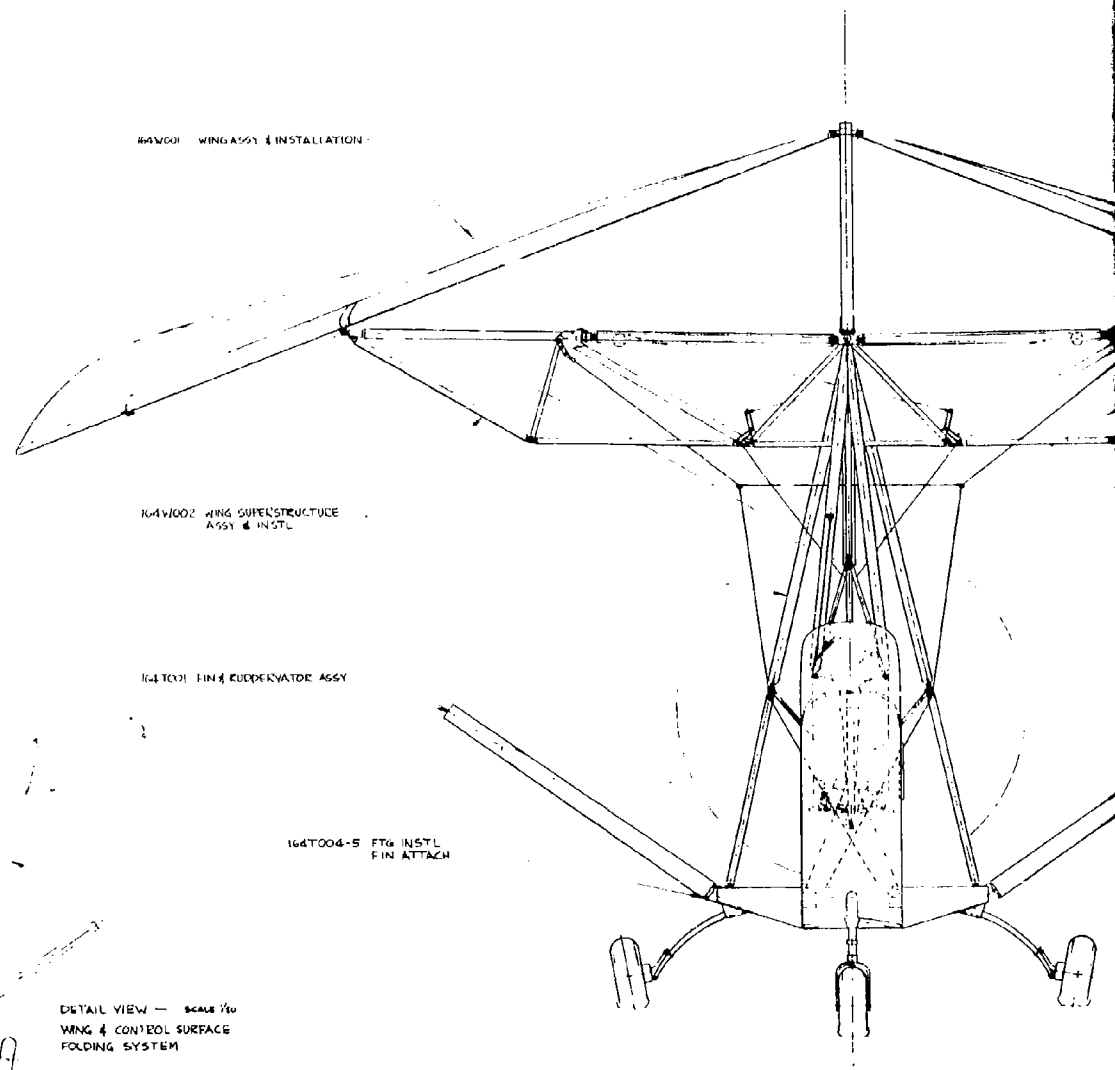
Figure 1. In-Flight View - Flexible Wing Aerial Utility Vehicle



164V001 WING ASSY & INSTALLATION

BLO } d AGFT

WING SHOWN AT
ZERO INCIDENCE



164V002 WING SUPERSTRUCTURE
ASSY & INSTL

164T001 FIN & RUDDERVATOR ASSY

164T004-5 FTG INSTL
FIN ATTACH

DETAIL VIEW - SCALE 1:6
WING & CONTROL SURFACE
FOLDING SYSTEM

2

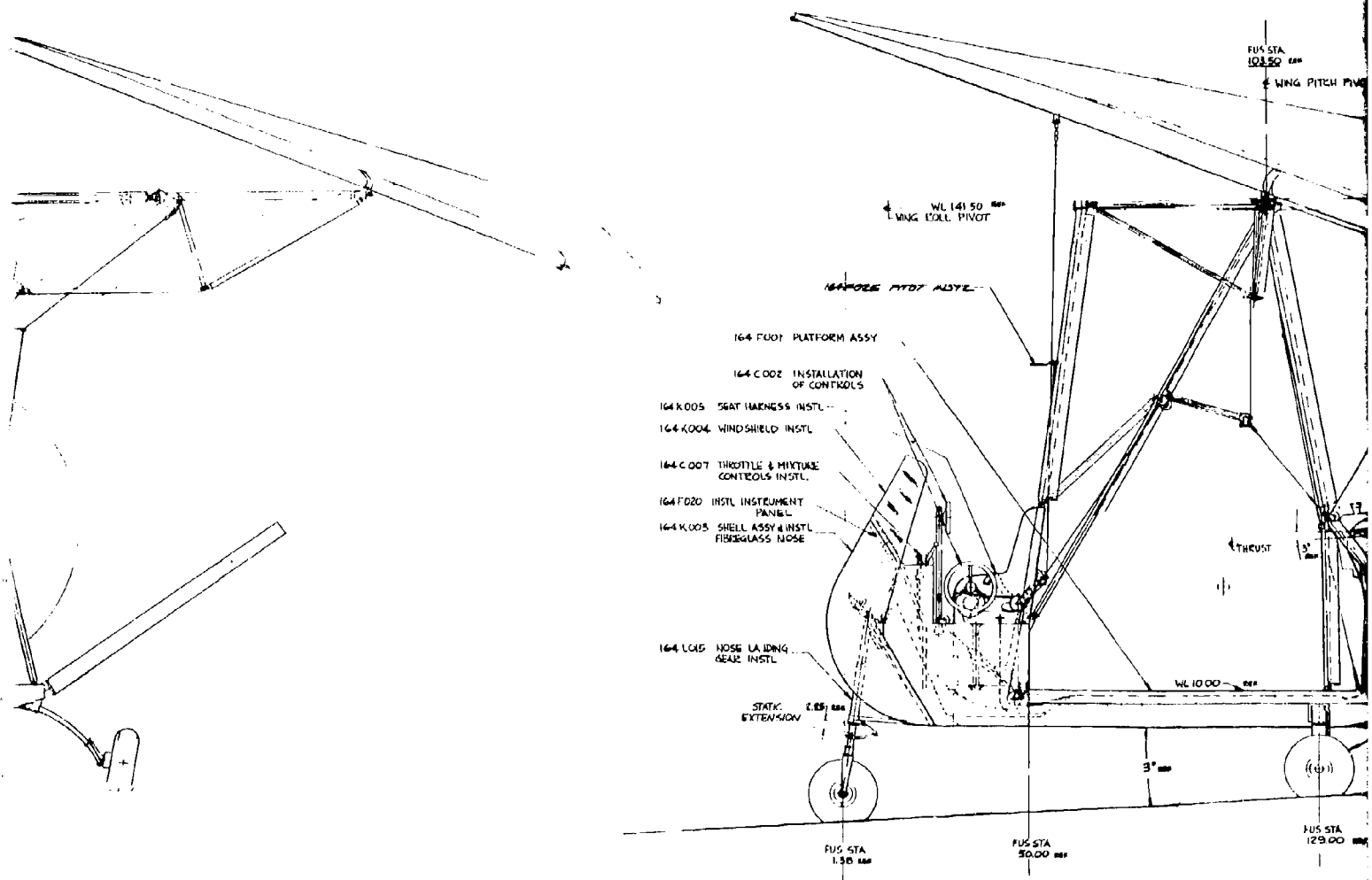


Figure 2. Final Asse

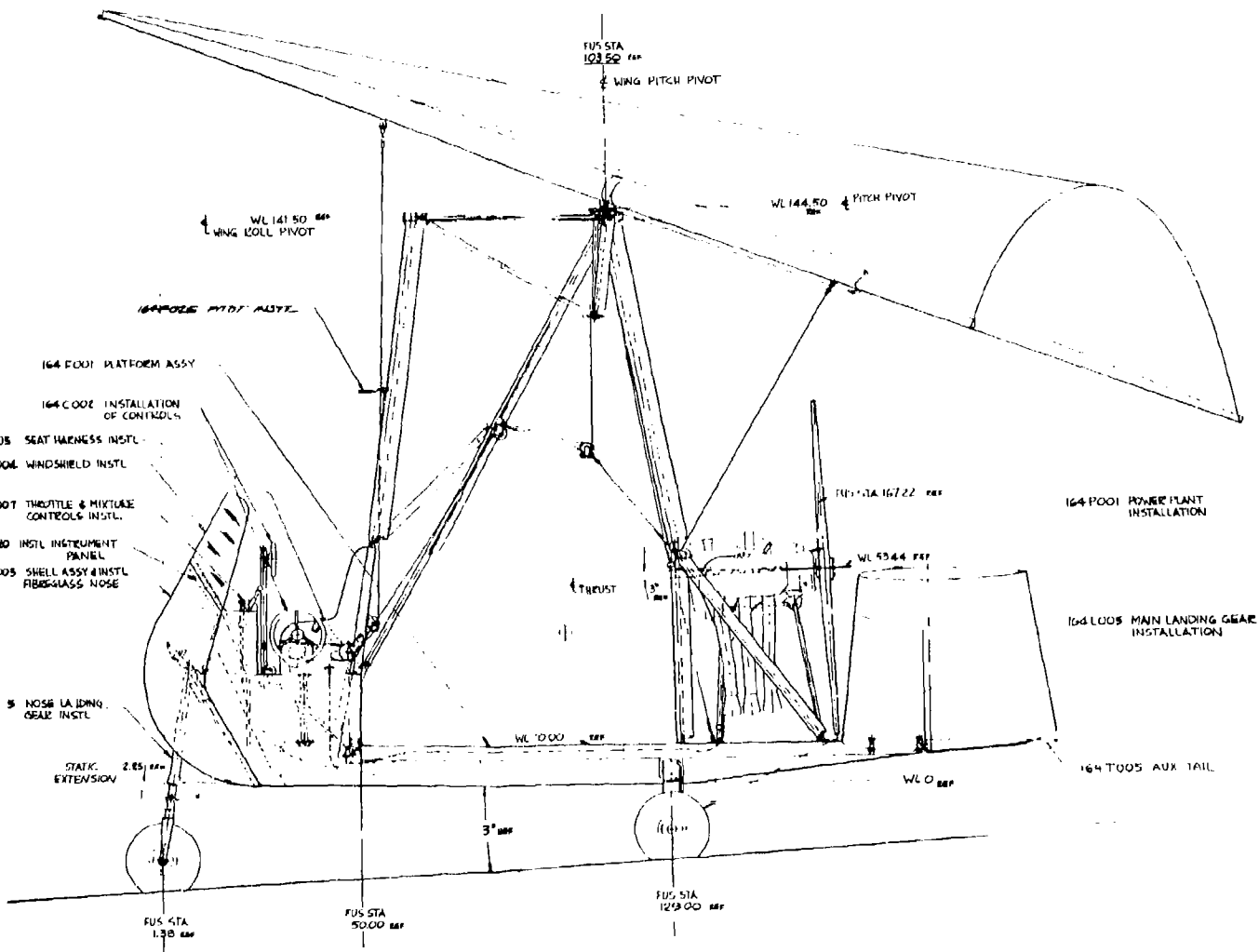
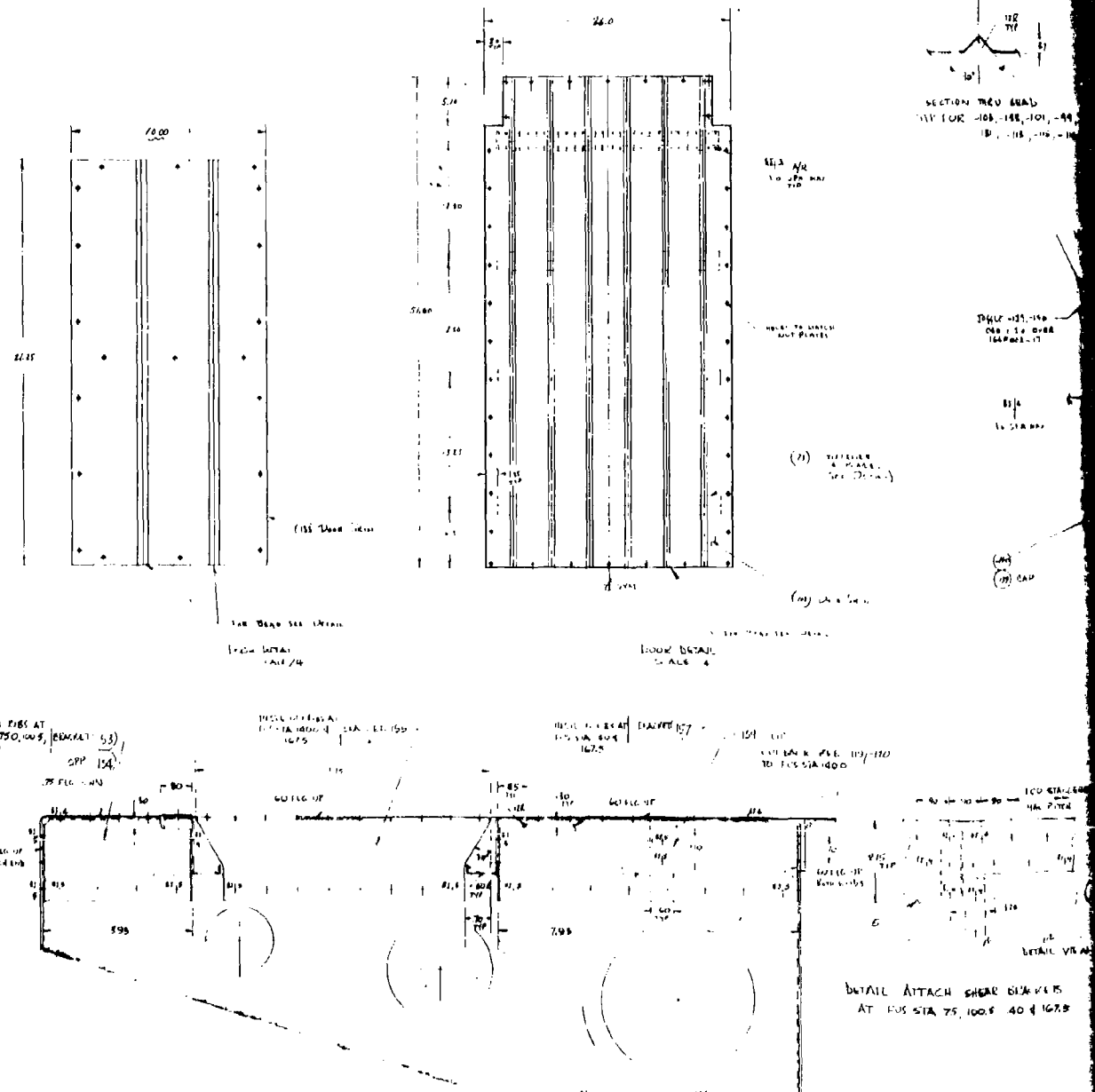
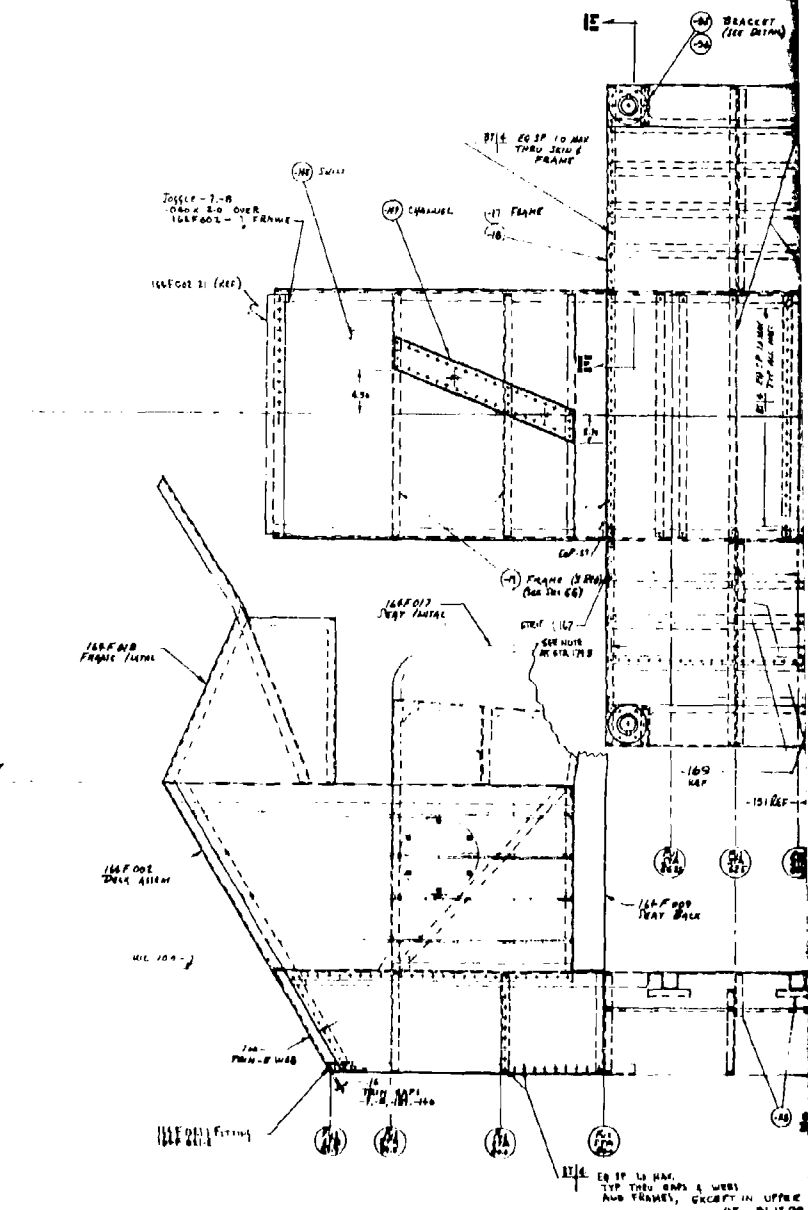
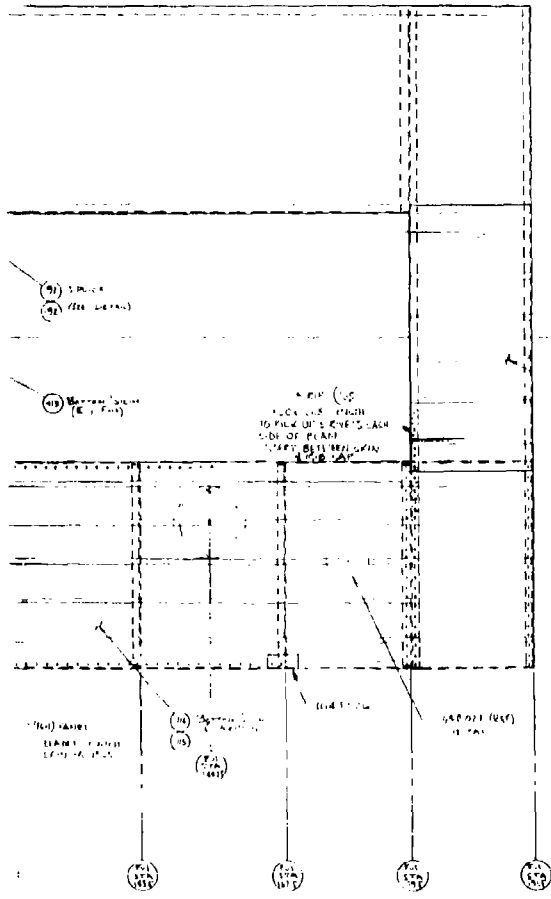


Figure 2. Final Assembly, Model 164





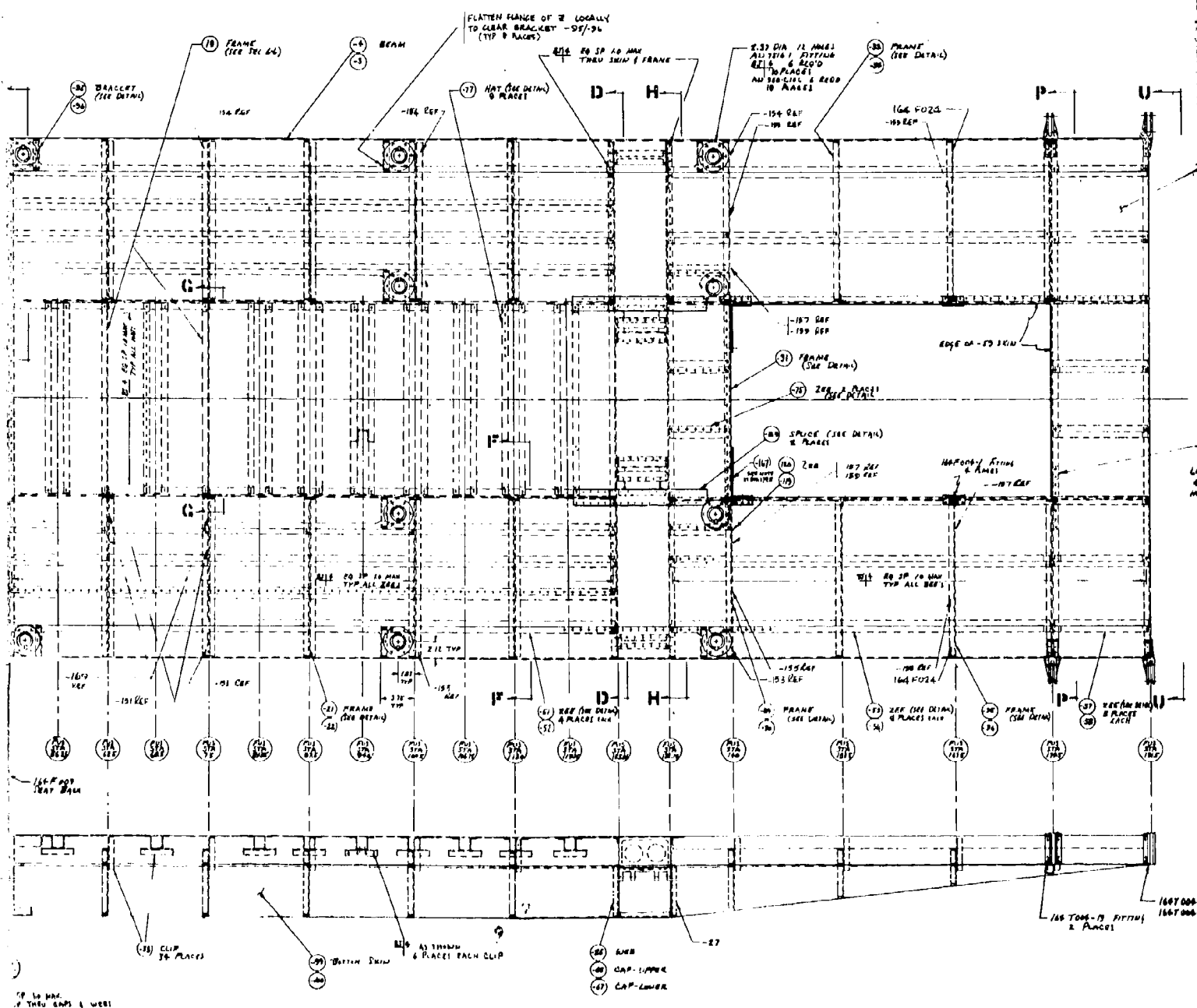


Figure 3. Aerial Utility Vehicle Platform Assembly

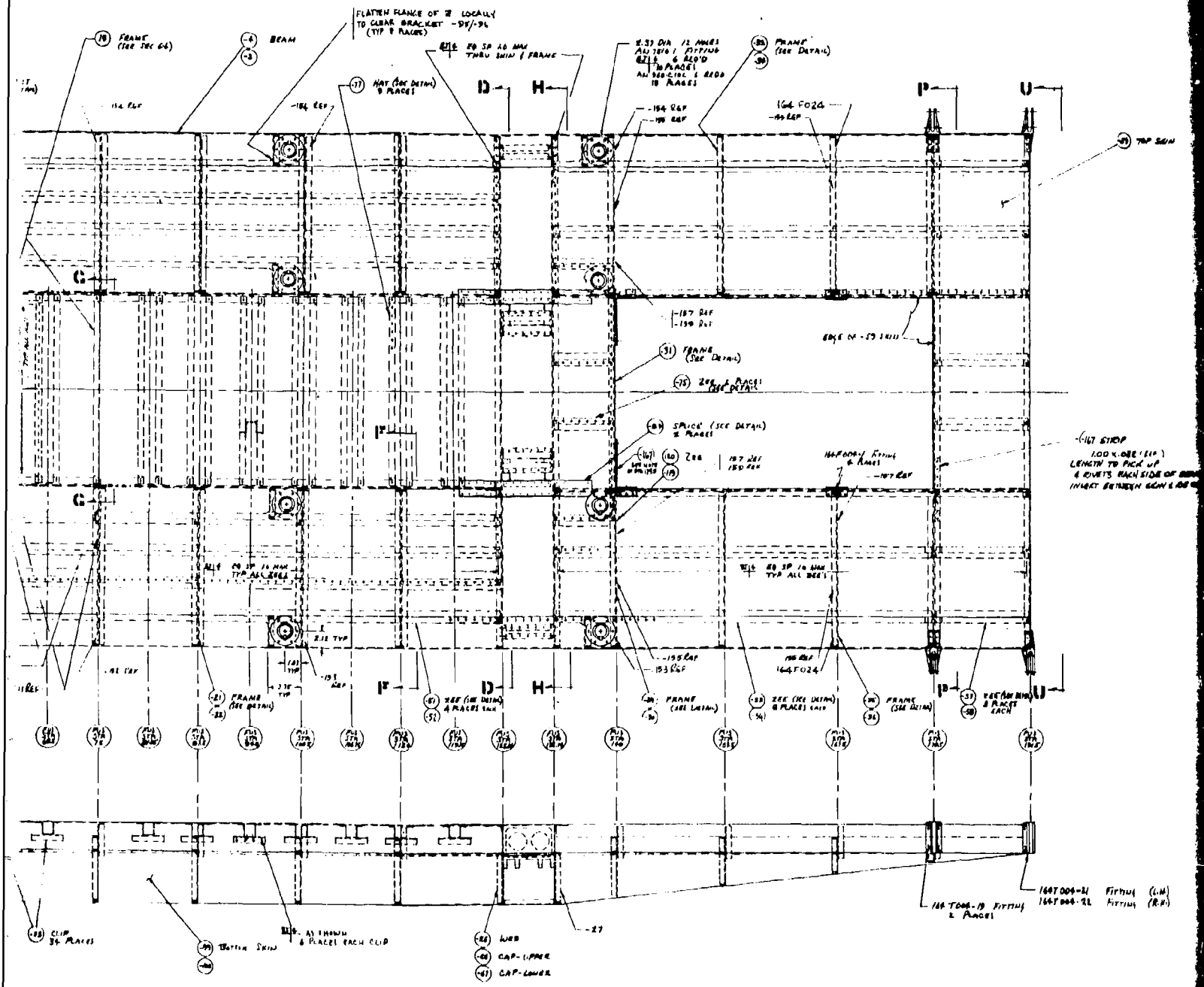
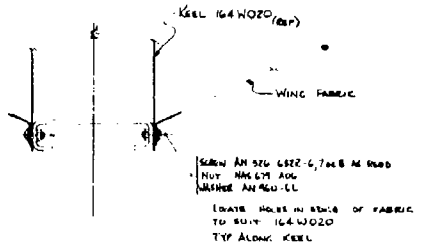
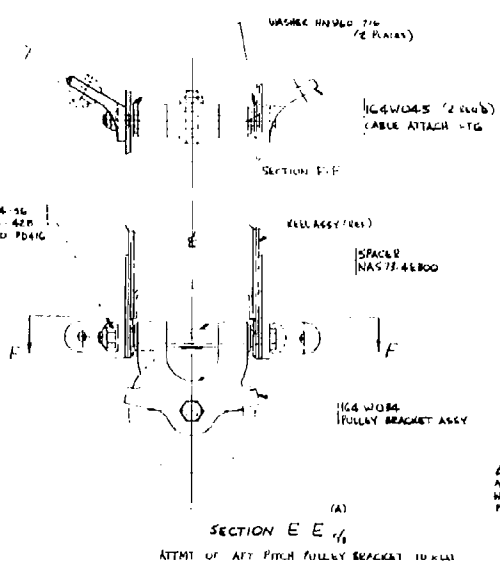


Figure 3. Aerial Utility Vehicle Platform Assembly



SECTION B-B_g FULL SCALE (ROTATED FOR CONVENIENCE)
ATTMT OF FABRIC TO KEEL

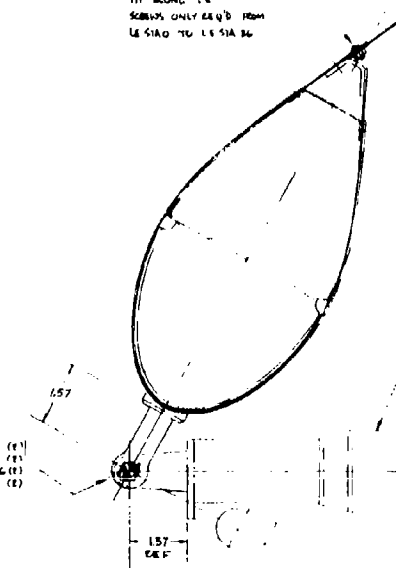


ATTEMPT OF ATTACH PITCH TUBEY BRACKET TO KLM

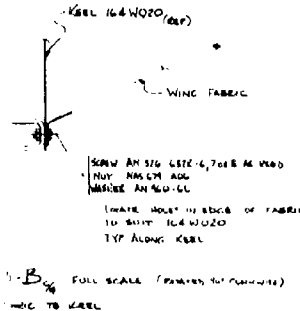
AN-F60-682E 5-SREW
NAS67M A06 NUT
AN 960-6L WASHER

LOCATE HOLES IN EDGE
OF PANEL TO SUIT KNOWBUL
TOP BLOWN LE

SCREWS ONLY E80'D FROM
LE SIAO TO LE SIA BG



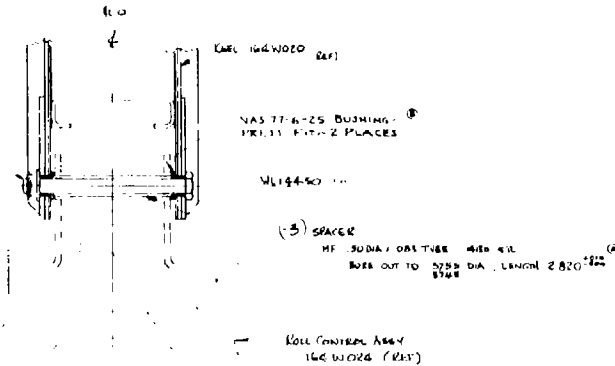
SECTION D-D_{NB} FULL SCALE
ATTMT OF L.E TO SPREADER ARM



AN SIG CLEVIS, 7028 AL HEAD
NYL NACM ADG
WASHER AN460-2
PIN AN 980-1-3
MAKES HOLES IN EDGE OF FABRIC
TO SUIT 164 W020
TYP ALONG KEEL

1/1-B_{1/2} FULL SCALE (ROTATED 90° COUNTERCLOCKWISE)
ATTACH TO KEEL

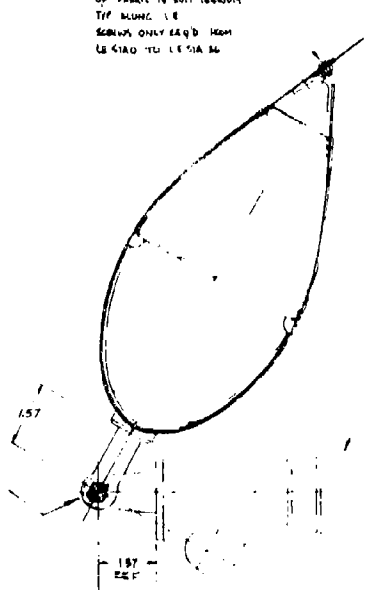
BOLT NAS 106-SLD
NUT AN 820-6
WASHER AN460-PD616
PIN AN 980-1-3



M111 DIA 1.025
DIA .975, LENGTH 2.820^{.975}
BORE OUT TO .975

(3) SPACER
M111 DIA 1.025
DIA .975, LENGTH 2.820^{.975}
BORE OUT TO .975

A_{1/2} ACP - BLO



SECTION D-D_{1/2} FULL SCALE (ROTATED 90° COUNTERCLOCKWISE)
ATTACH OF LE TO SPREADER ARM

SECTION C-C_{1/2} FULL SCALE (ROTATED 90° COUNTERCLOCKWISE)

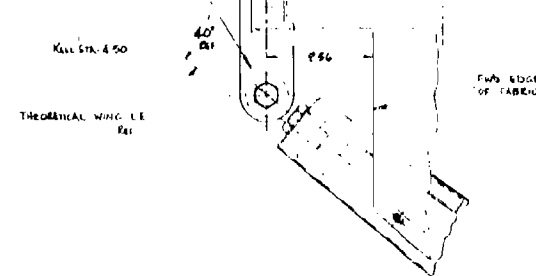
ATTACHMNT OF KEEL TO KEELED CONTROL ASSY

C

BOLT NAS 106-SLD
NUT AN 820-6
WASHER AN460-PD616
PIN AN 980-1-3

KEEL STAO (ref)

THEORETICAL WING LE (ref)



DETAIL A_{1/2} FULL SCALE
ATTACHMNT OF LE TO KEEL

2

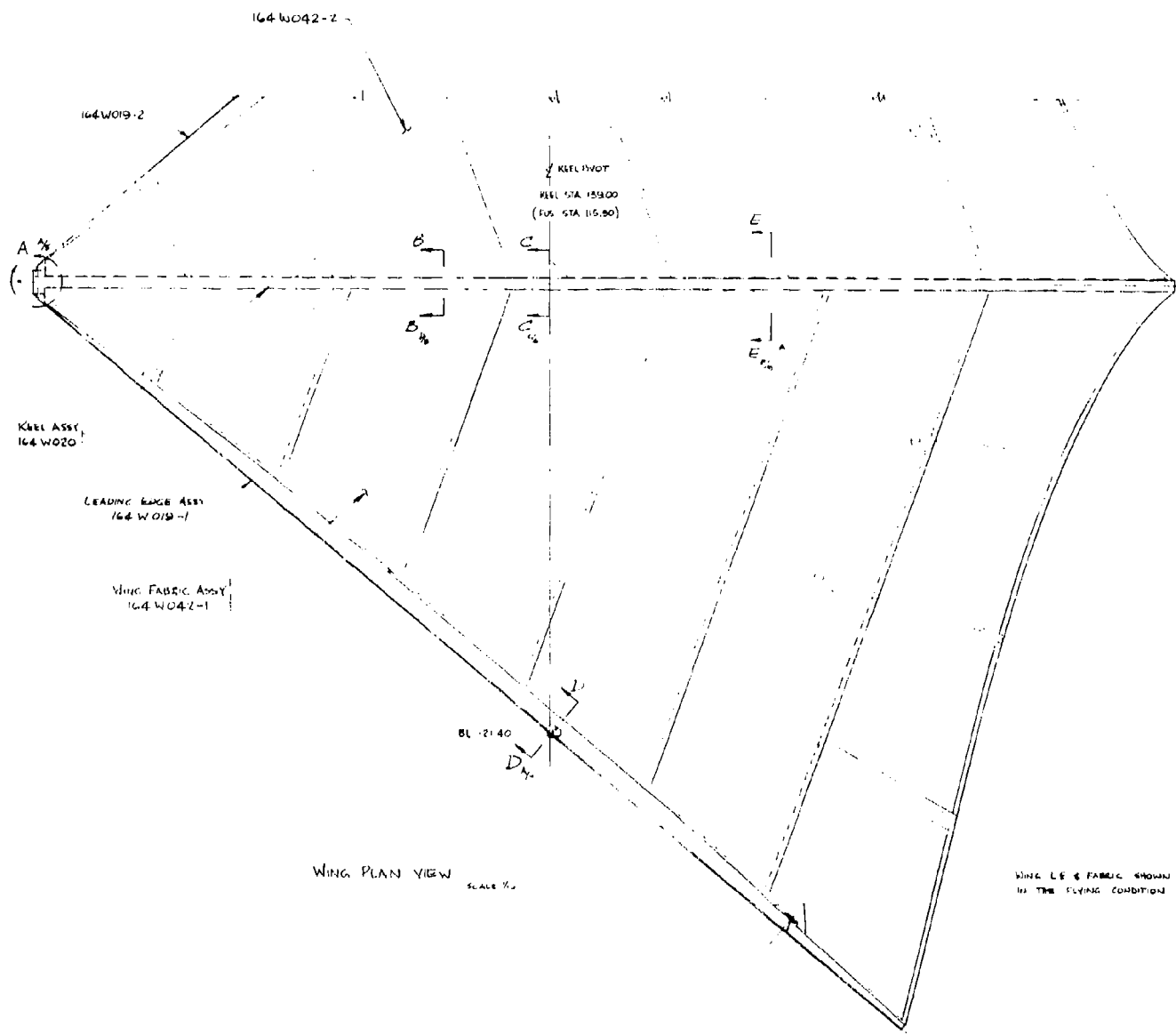


Figure 4. Wing Assembly and

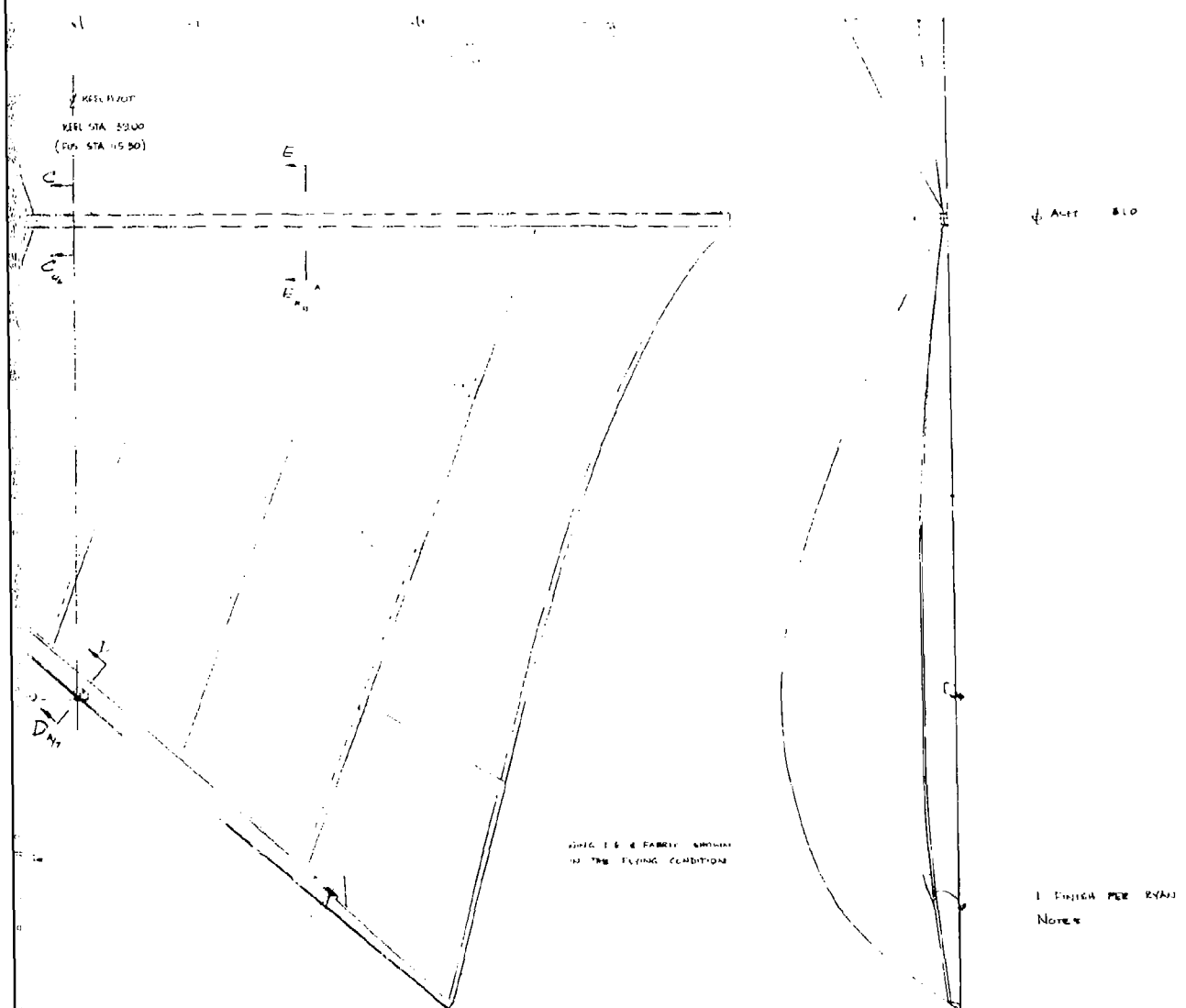
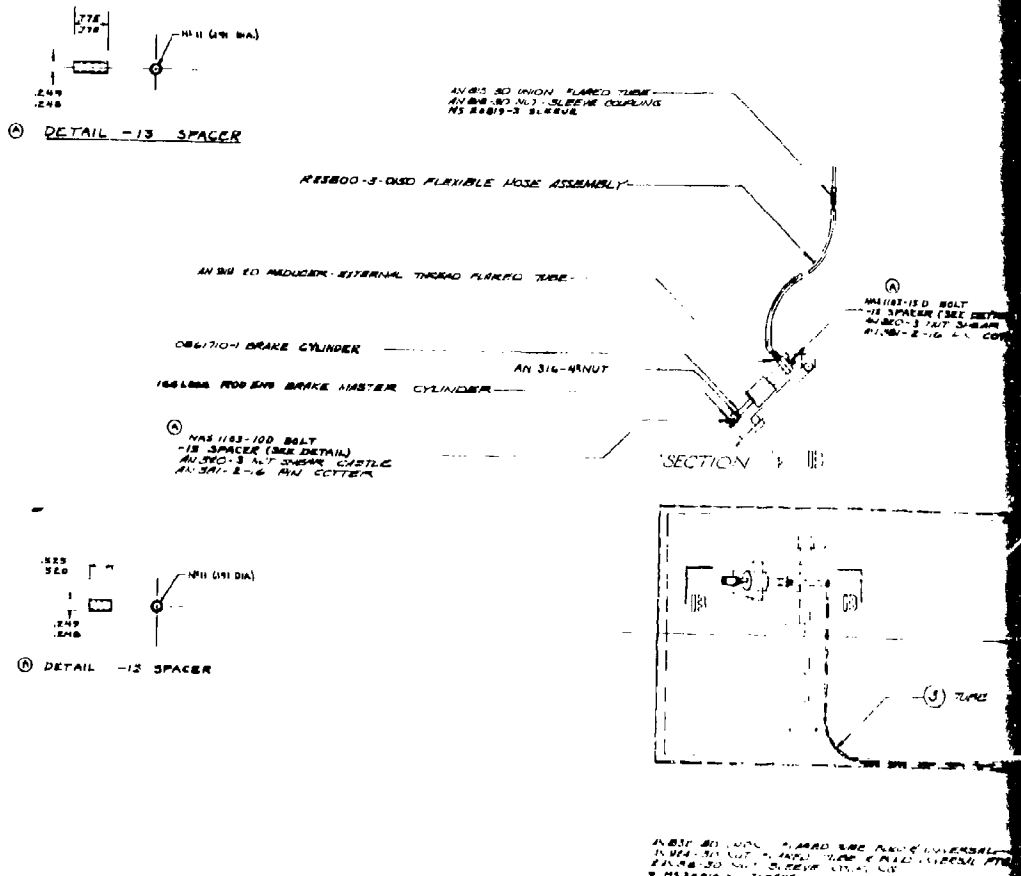


Figure 4. Wing Assembly and Installation



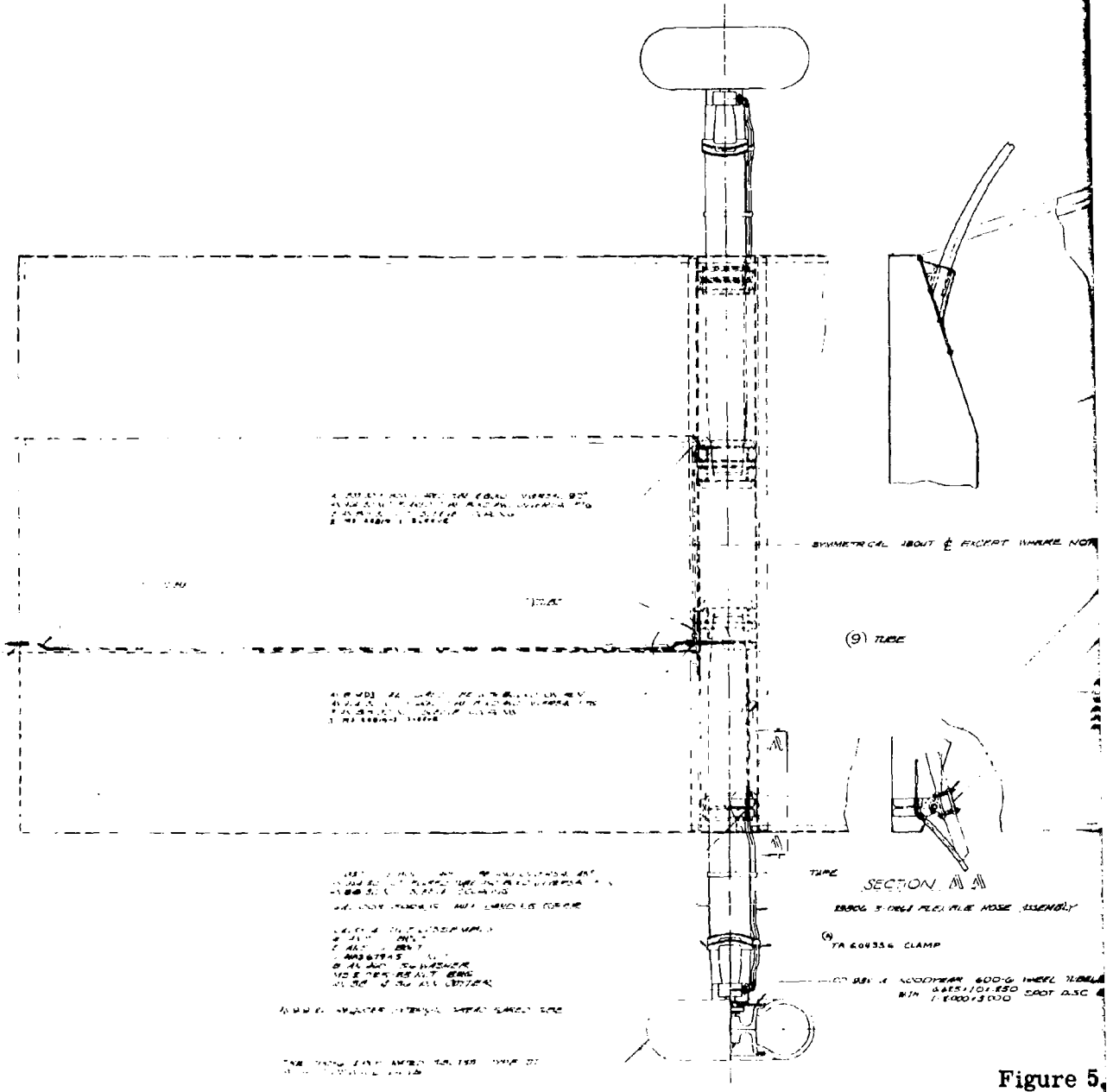


Figure 5.

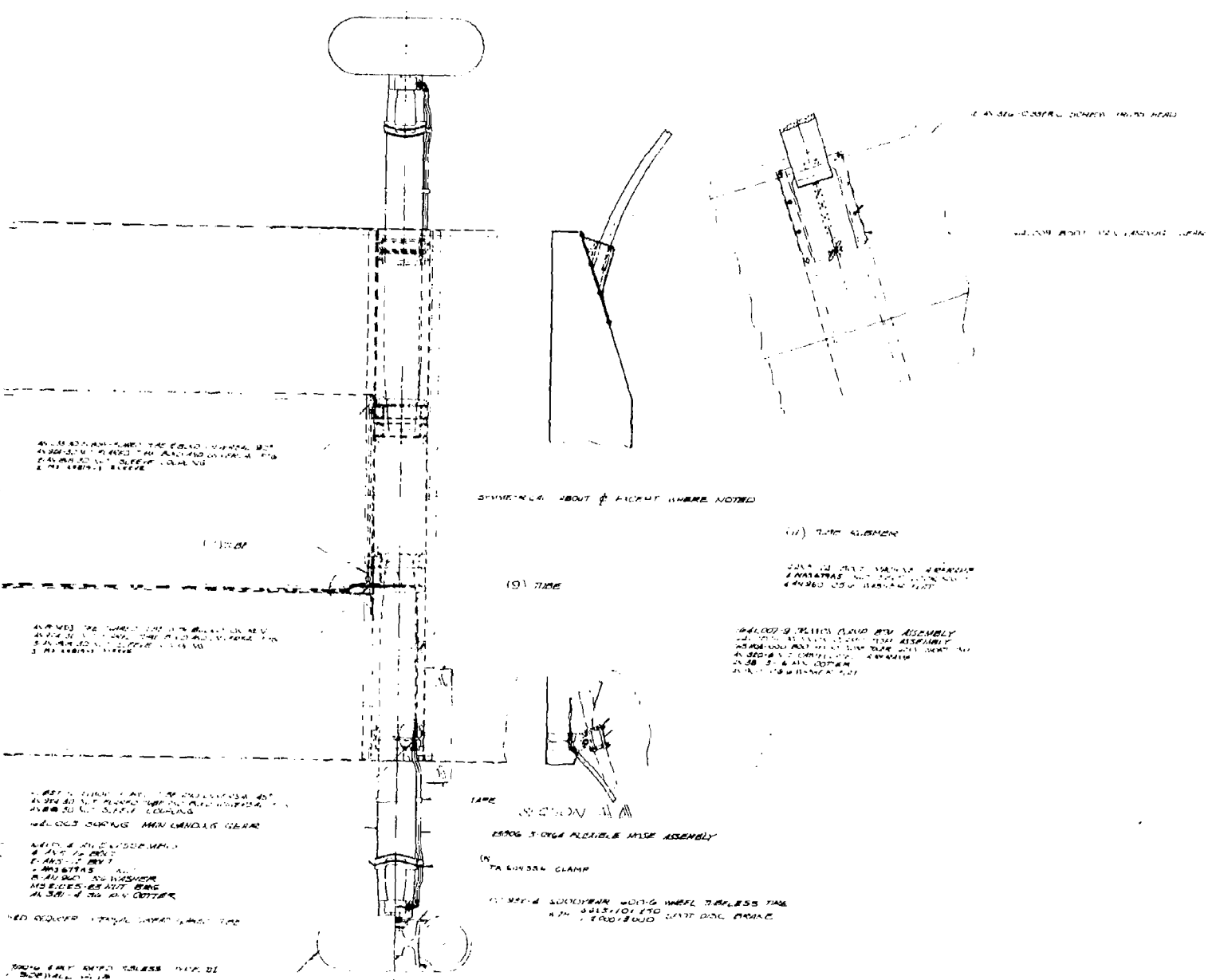


Figure 5. Main Landing Gear and Brake Assembly

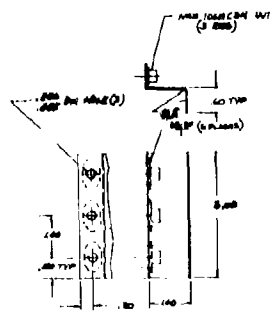


FIGURE 67-100

⑥ ID OF -57 TUBE TO MATCH
OD OF FILLER NECK (2.31 INCH)

3984255 FILLER NECK (REP)

⑤ AND
CUT HOLE IN PAD SO FILLER
NECK IS POSITIONED AROUND PLATE PIPES
AS SHOWN BEHIND TO FUSE
SEAL

⑦ SEAL JOINT WITH
DEVCON 'F' PUTTY



CLIP
(AS SHOWN)

VIEW C [A]
FIG. 398

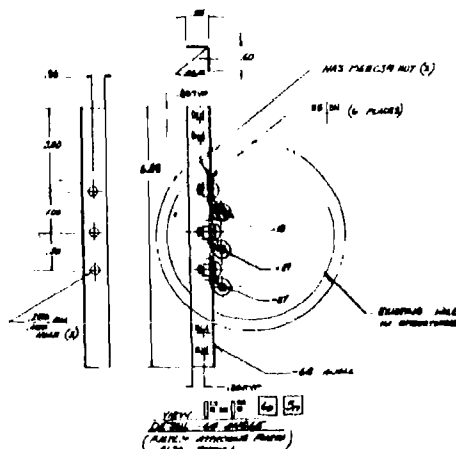
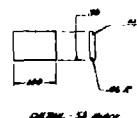
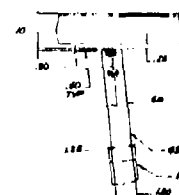
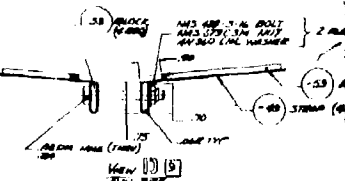


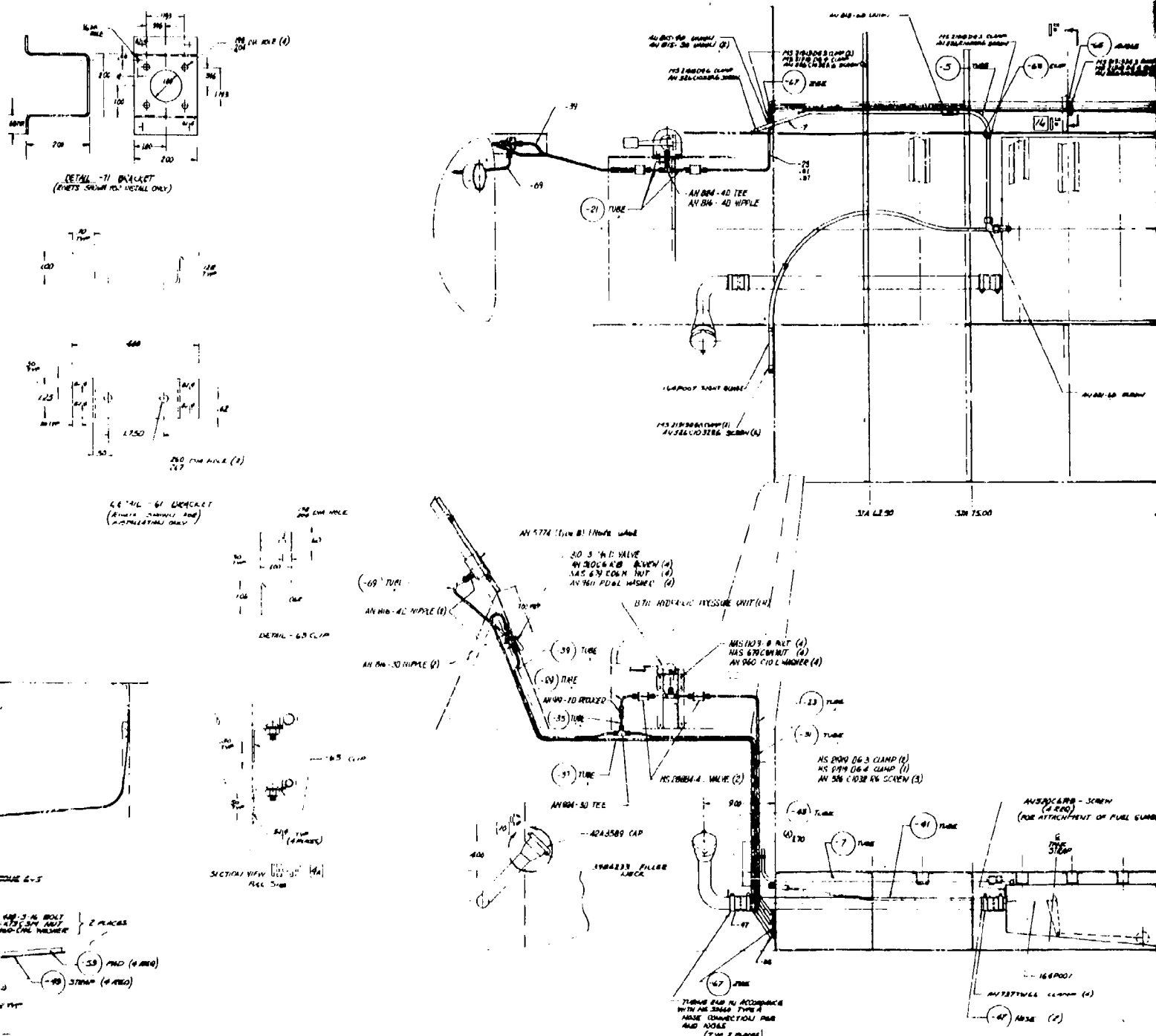
FIGURE 67-100



TOP EDGE OF FUEL TANK
SHOULD STICK OUT SOME 6-8
IN LOCATIONS



VIEW D [B]
FIG. 398



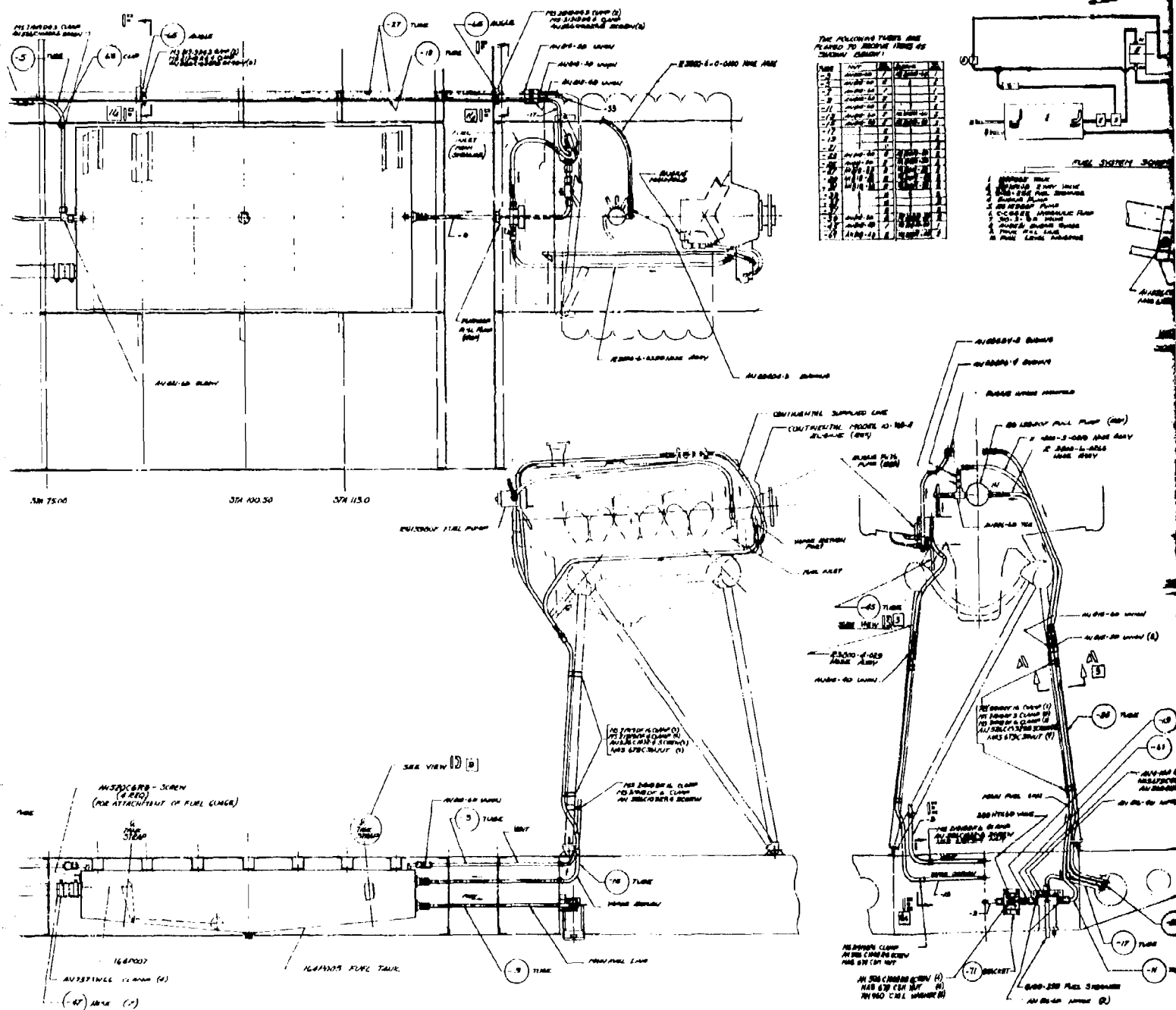


Figure 6. Fuel System Installation

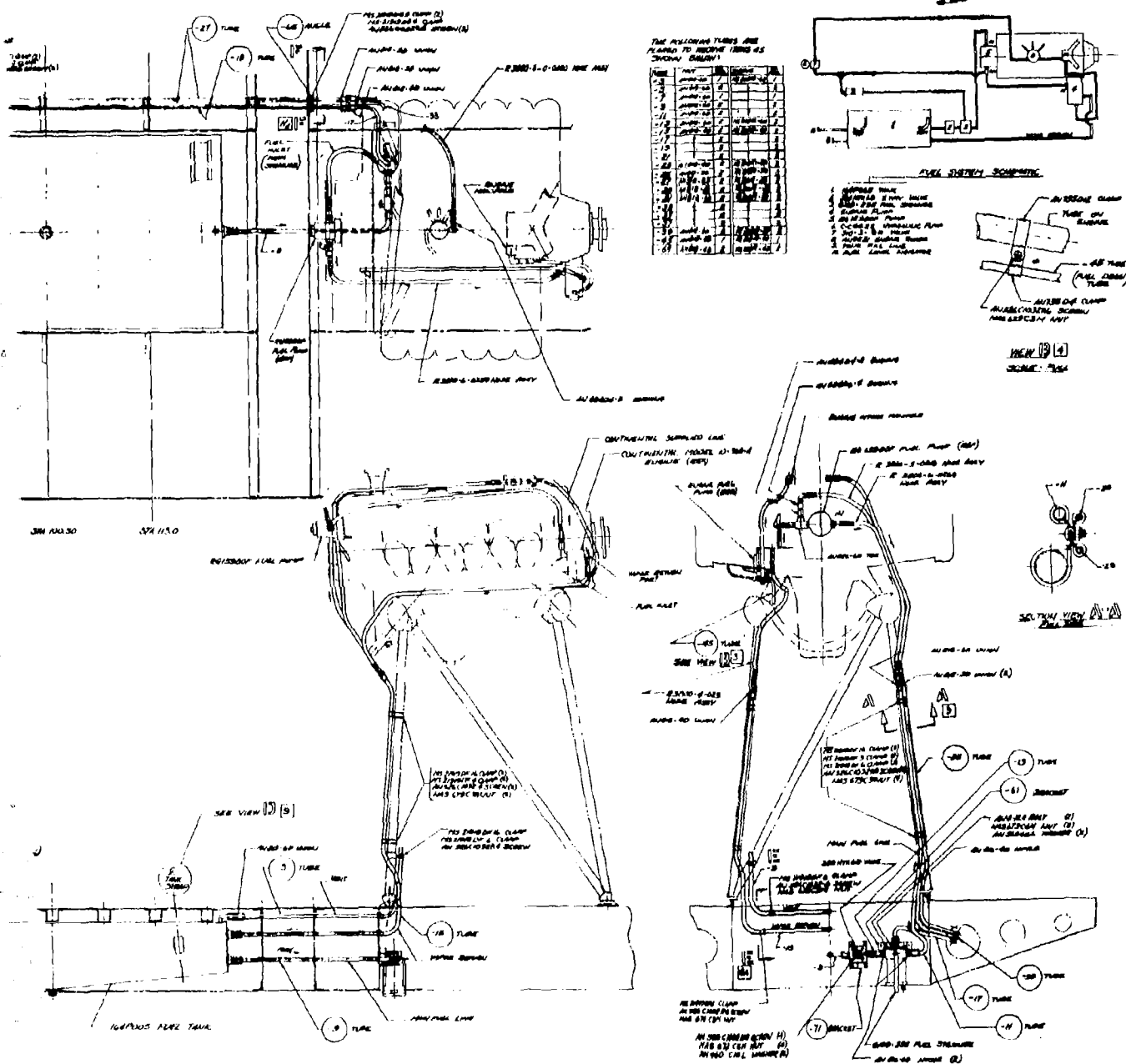
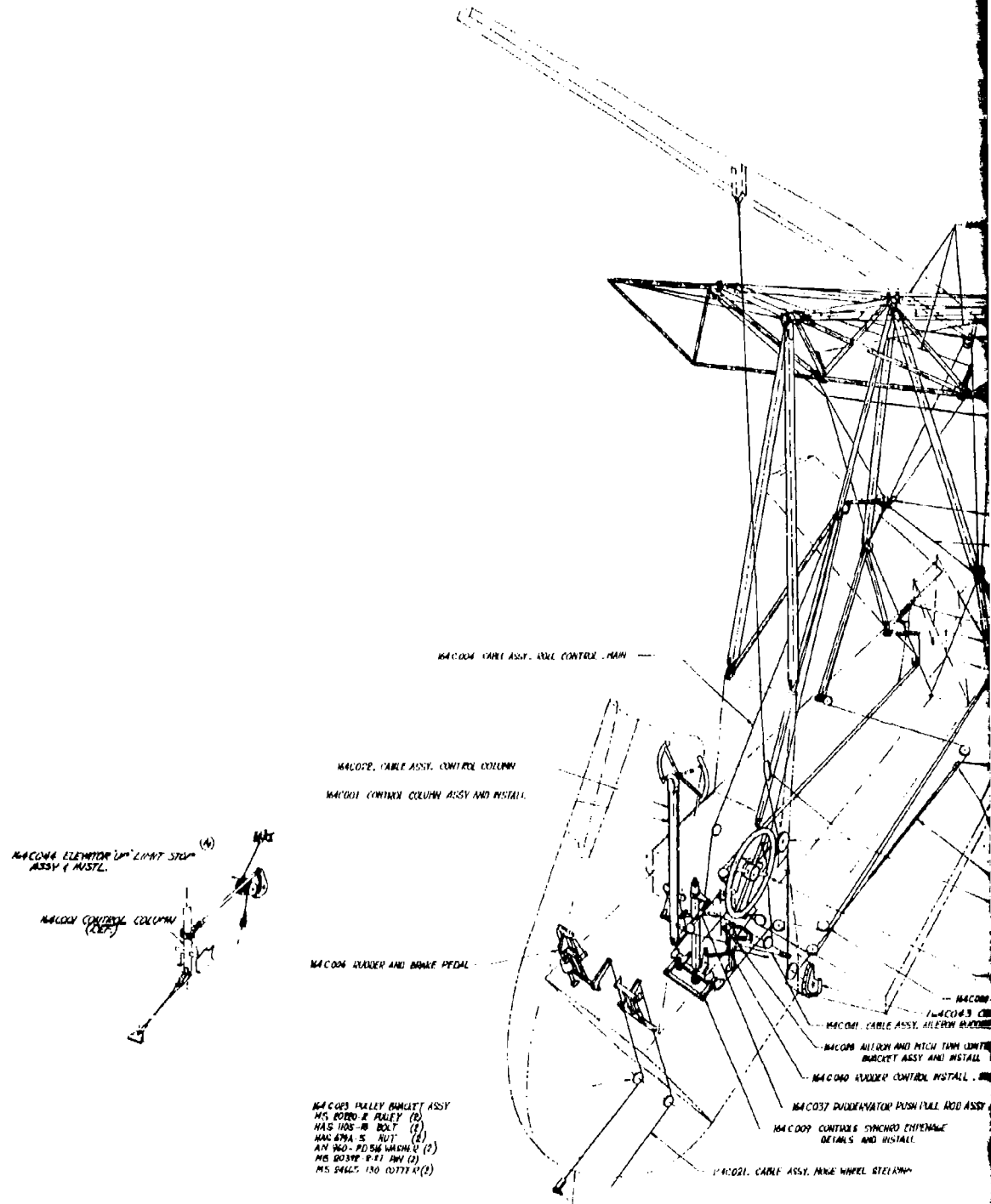


Figure 6. Fuel System Installation



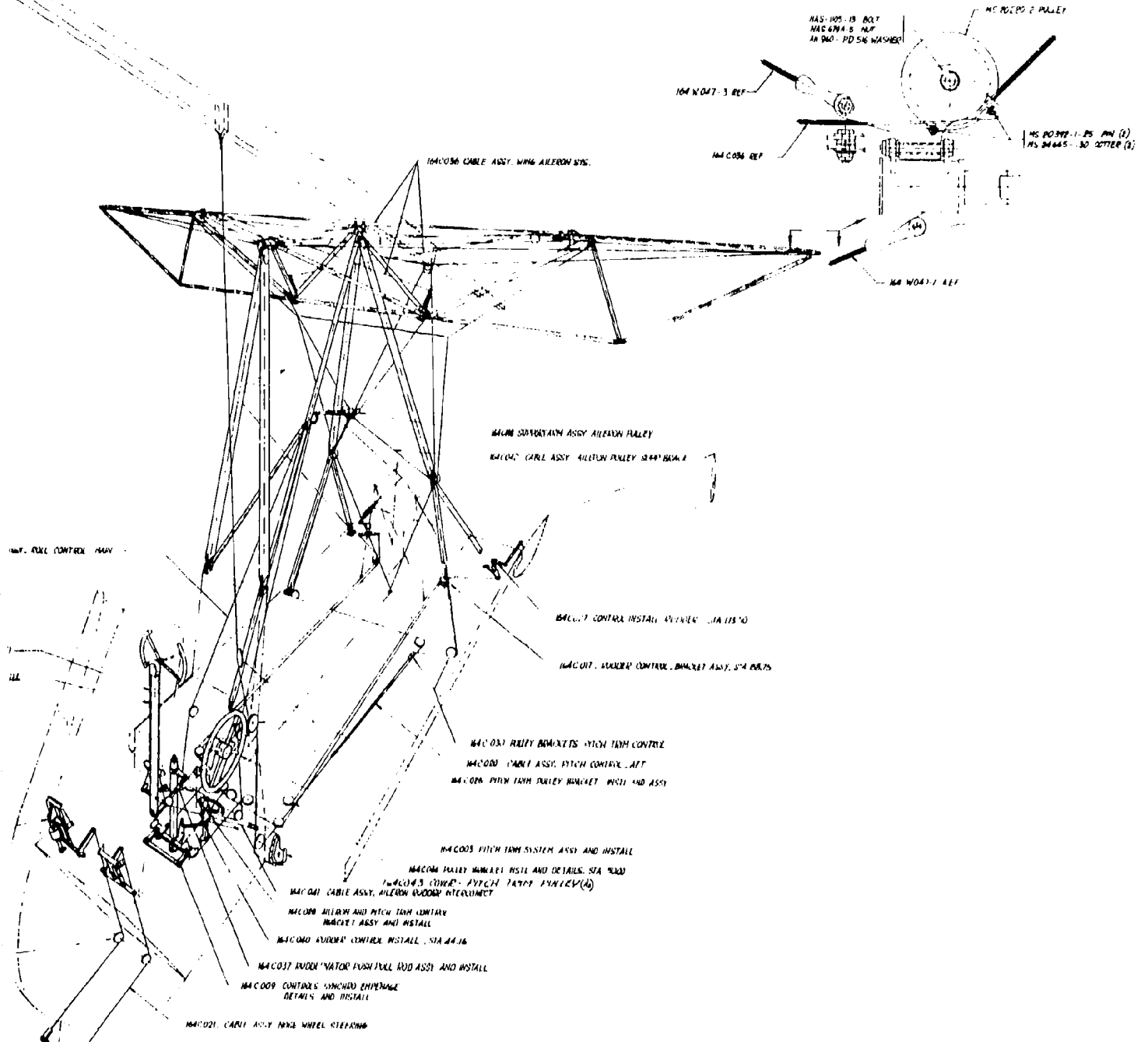


Figure 7. Controls Installation

AERODYNAMICS ANALYSIS

PERFORMANCE

Methods of Analysis and References

This section summarizes the performance capabilities and the stability-and-control characteristics of the Ryan Model 164 Utility aircraft. Included are the lift and drag bases and the methods of analyses used. All data are estimated data calculated prior to flight test of the aircraft.

Drag and Lift

Wing drag and lift were obtained from Ryan and NASA wind-tunnel test data. Drag of the body, struts, and other untested components was calculated using standard estimating techniques.

The drag polar for the complete aircraft is presented in Figure 8A and the corresponding lift curve in Figure 8B. Maximum lift-to-drag ratio of the aircraft is estimated to be 3.93.

Power Required and Available

Power available was calculated using the engine manufacturer's specifications. NASA propeller charts for a two-bladed fixed-pitch propeller of activity factor 90 were used to determine propeller efficiencies. Figure 8C shows power required and available at sea level, standard day conditions.

Takeoff

Ground roll and total distance over a 50-foot obstacle are plotted in Figure 8D, as a function of gross weight. Takeoff distances were calculated using the following equation:

$$\text{ground roll} = \frac{(0.0443)(W)(V_{LO})^2}{T - (C_D - \mu C_L)qS - \mu W}$$

$$\text{Air distance over 50-foot obstacle} = \frac{50}{\tan \gamma}$$

$$\text{where } \gamma = \arcsin \frac{R/C}{V}$$

Rate of Climb

Rates of climb at sea level are plotted versus velocity in Figure 8E for gross weights of 1,300, 1,800, and 2,300 pounds. Maximum rates of climb are 690 and 300 feet per minute at gross weights of 1,800 and 2,300 pounds respectively. Rates of climb were determined as follows:

$$R/C = \frac{(HP \text{ available} - HP \text{ required}) (33,000)}{W}$$

Range

Specific range is plotted in Figure 8F, as a function of velocity, for sea level, standard day conditions. Maximum specific range is 0.712 and 0.818 nautical mile per pound of fuel at gross weights of 1,800 and 2,300 pounds respectively. Specific range in nautical miles per pound of fuel was determined from the following equation:

$$SR = \frac{\text{Velocity}}{\text{Fuel Flow}} = \frac{V \text{ knots}}{SFC \times BHP}$$

Landing

The landing performance of the aircraft has been calculated in two segments: (1) distance from 50-foot obstacle to touchdown, and (2) ground roll distance. The distance from a 50-foot obstacle will vary greatly with approach speed and pilot technique. Landings simulated on the analog computer indicated air distances of 300 feet. Optimizing the approach technique will reduce this value; however, 300 feet will be assumed to be representative until additional data are obtained from flight tests. The estimated ground roll distance is plotted versus weight in Figure 8G, showing roll distance from approximately 70 to 120 feet for a braking coefficient of 0.35. Roll distance was calculated with the following equation:

$$S_{GR} = \frac{0.043 W V_{TD}^2}{(C_D - C_L) \mu q_s + \mu W} - (q_s \text{ at } 0.7 V_{TD})$$

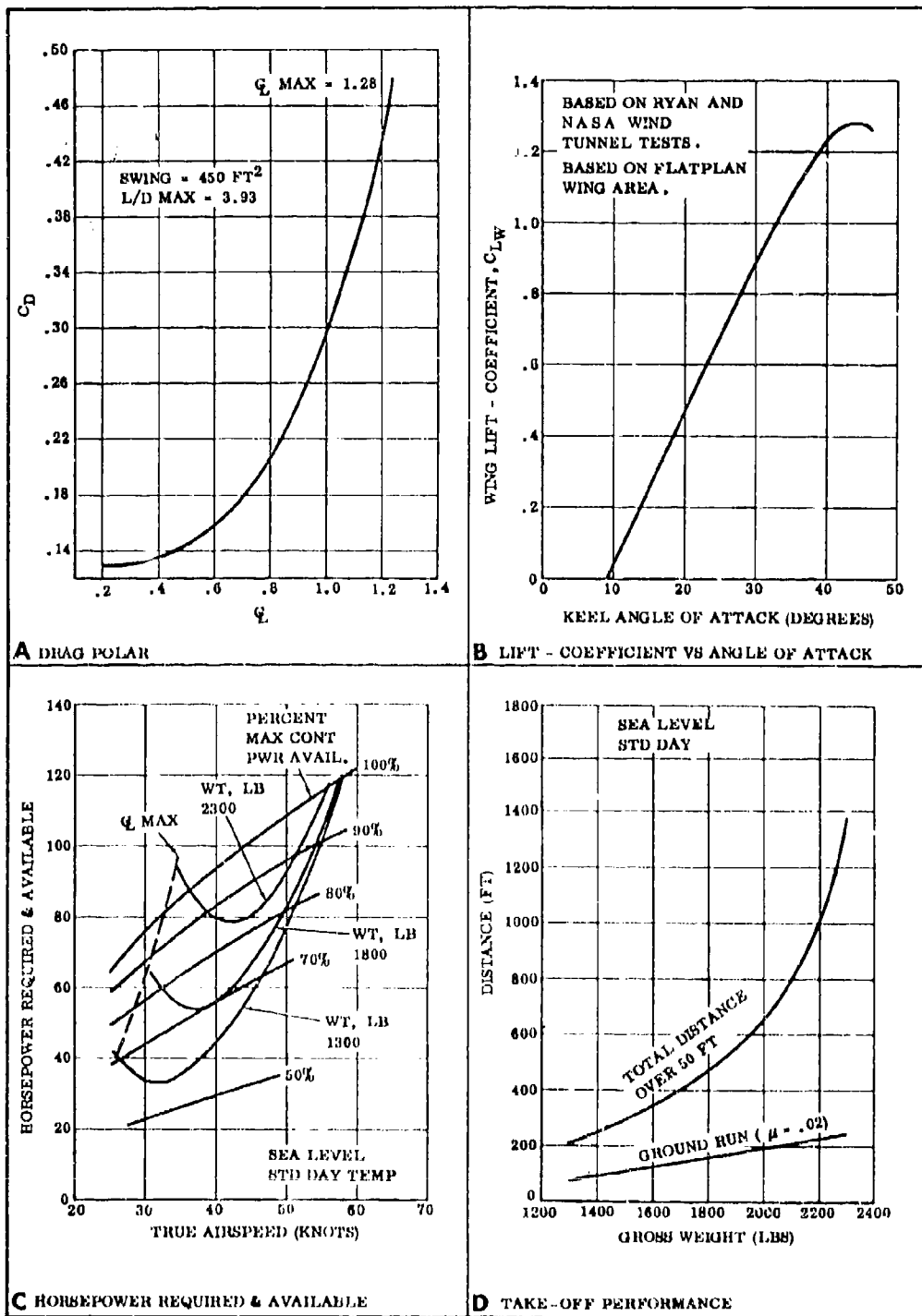


Figure 8. Performance Data (Sheet 1 of 2)

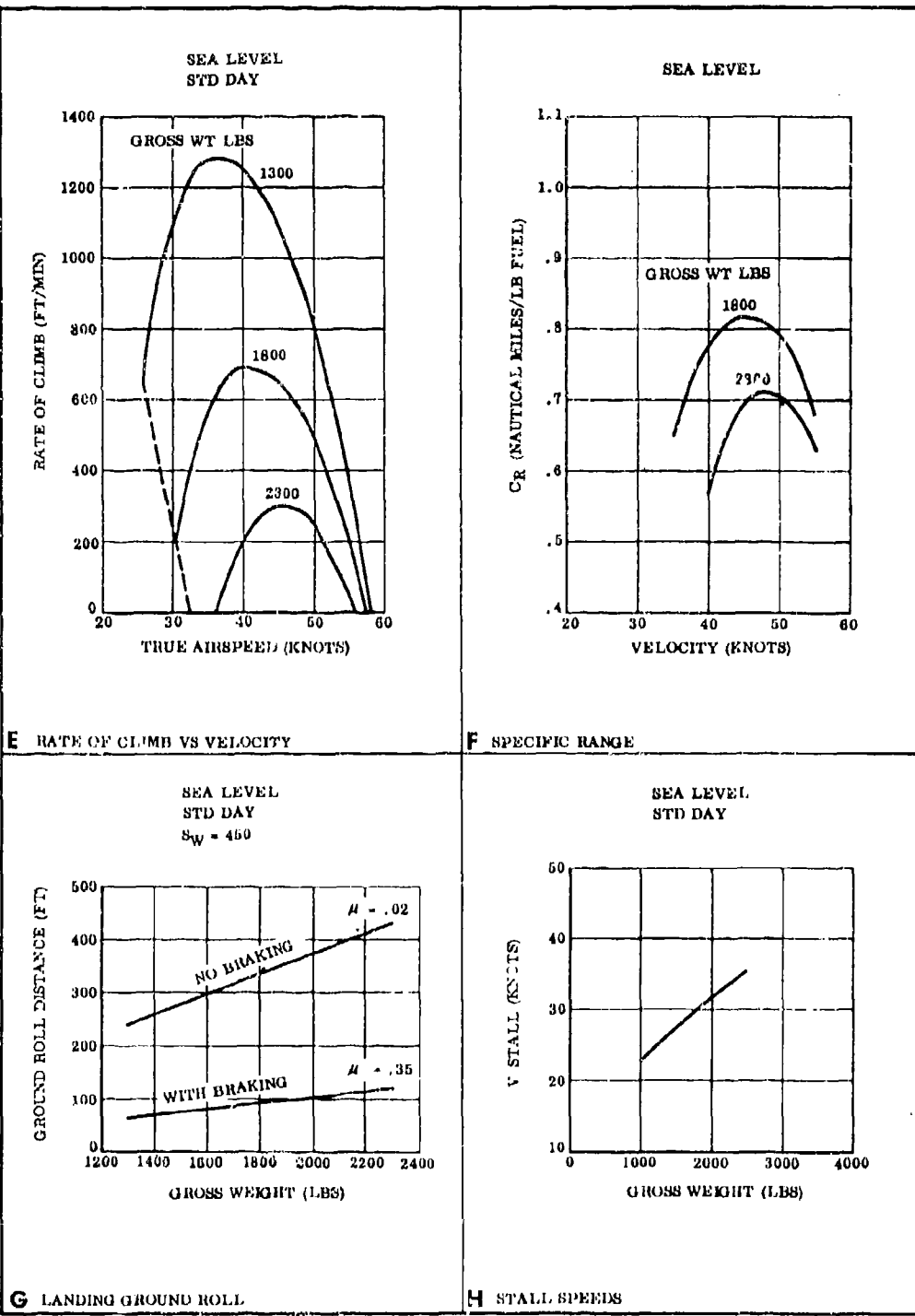


Figure 8. Performance Data (Sheet 2 of 2)

Stall Speed

Stall speeds are presented in Figure 8H for sea level, standard day conditions. Stall speed at the designed gross weight of 2,300 pounds is 34.3 knots. Stall speeds were calculated as follows (stall velocities in knots):

$$V_{\text{stall}} = \sqrt{\frac{GW \cos \gamma (295)}{C_{L\max} \sigma S_W}}$$

STABILITY AND CONTROL

Methods of Analysis and References

The stability and control section includes an analysis of the longitudinal trim requirements, the estimated stability and control characteristics, and results of an analytical investigation of power-off emergency landings.

Wing Longitudinal Characteristics

The wing longitudinal characteristics were estimated from Ryan and NASA wind-tunnel tests of Flexible Wing models and from data obtained from the Ryan Flexible Wing test bed. Characteristics of untested components were estimated using standard estimating techniques. Lift coefficients for the wing alone are presented in Figure 9A as a function of angle of attack. The wing drag polar is shown in Figure 9B.

Tail Longitudinal Characteristics

Studies have indicated that a tail mounted directly behind the propeller and designed to provide adequate longitudinal control in the power-off condition could easily pitch the aircraft to the stall angle of attack when power is on. This is possible because of the large increase in elevator effectiveness resulting from the increased dynamic pressure at the tail created by the propeller slipstream.

A 51-square-foot V-tail has been selected as the longitudinal-control device. This configuration allows the tail surfaces to be mounted clear of the propeller slipstream. Elevator effectiveness is thus made independent of power effects.

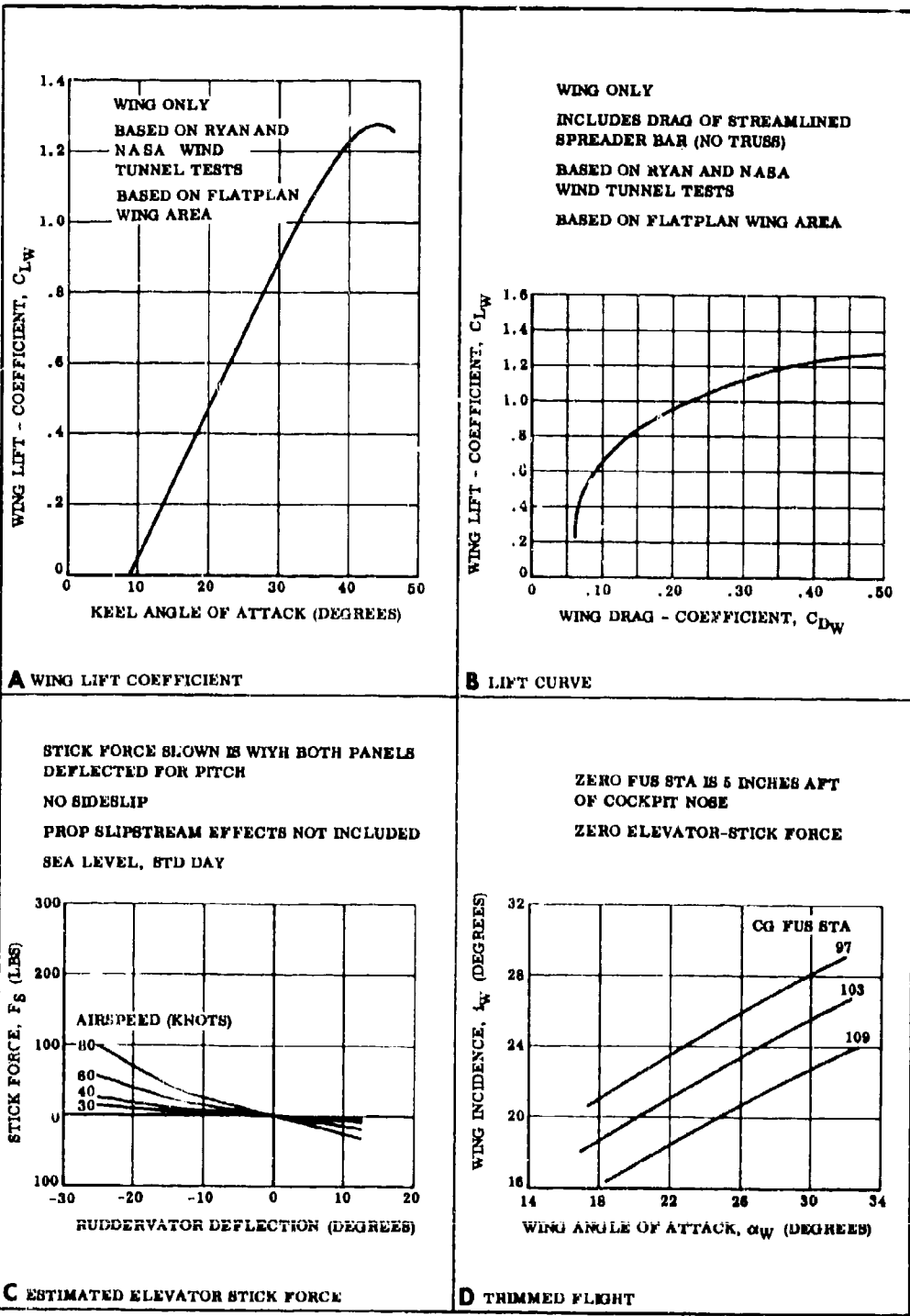


Figure 9. Stability and Control Data (Sheet 1 of 5)

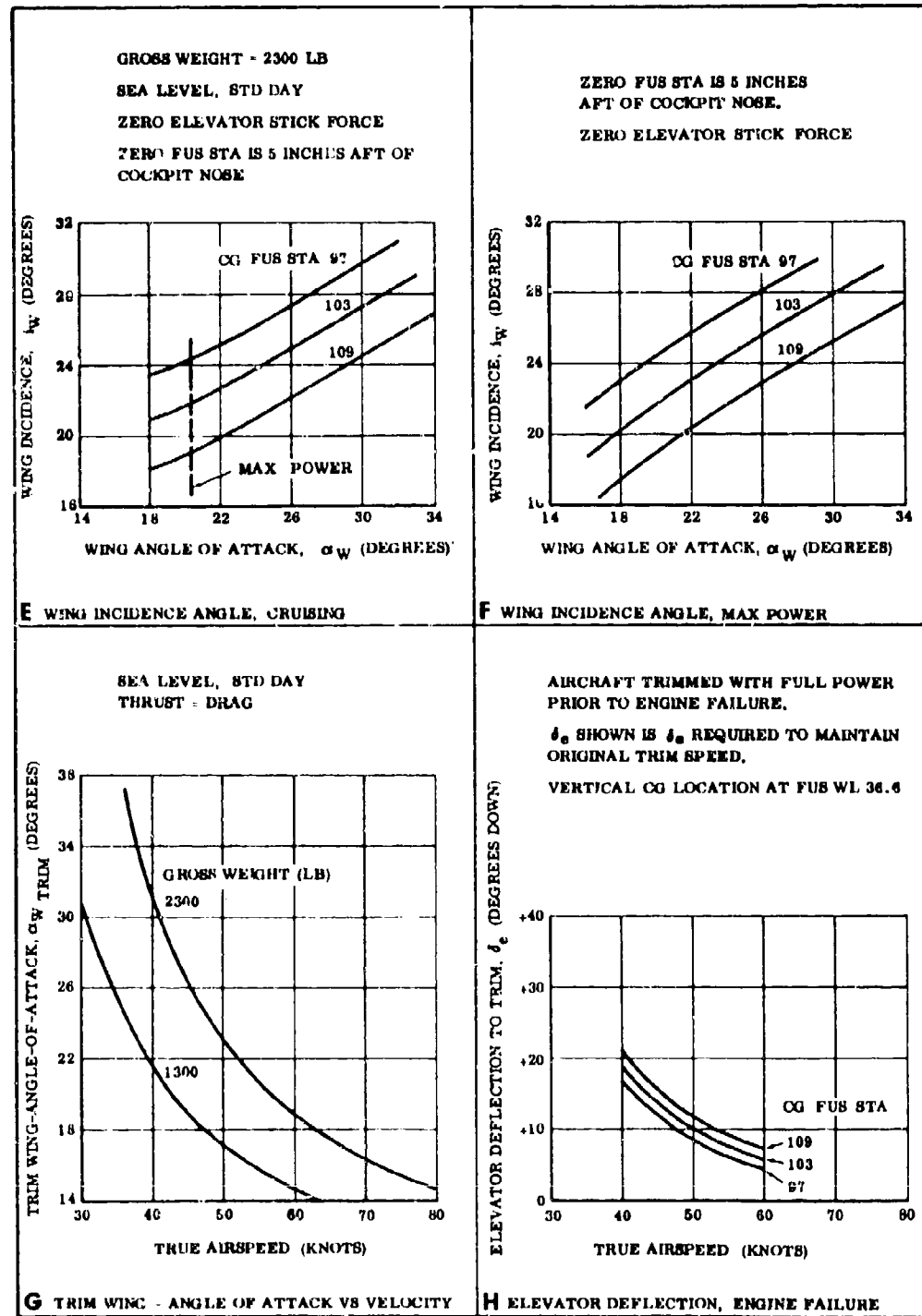


Figure 9. Stability and Control Data (Sheet 2 of 5)

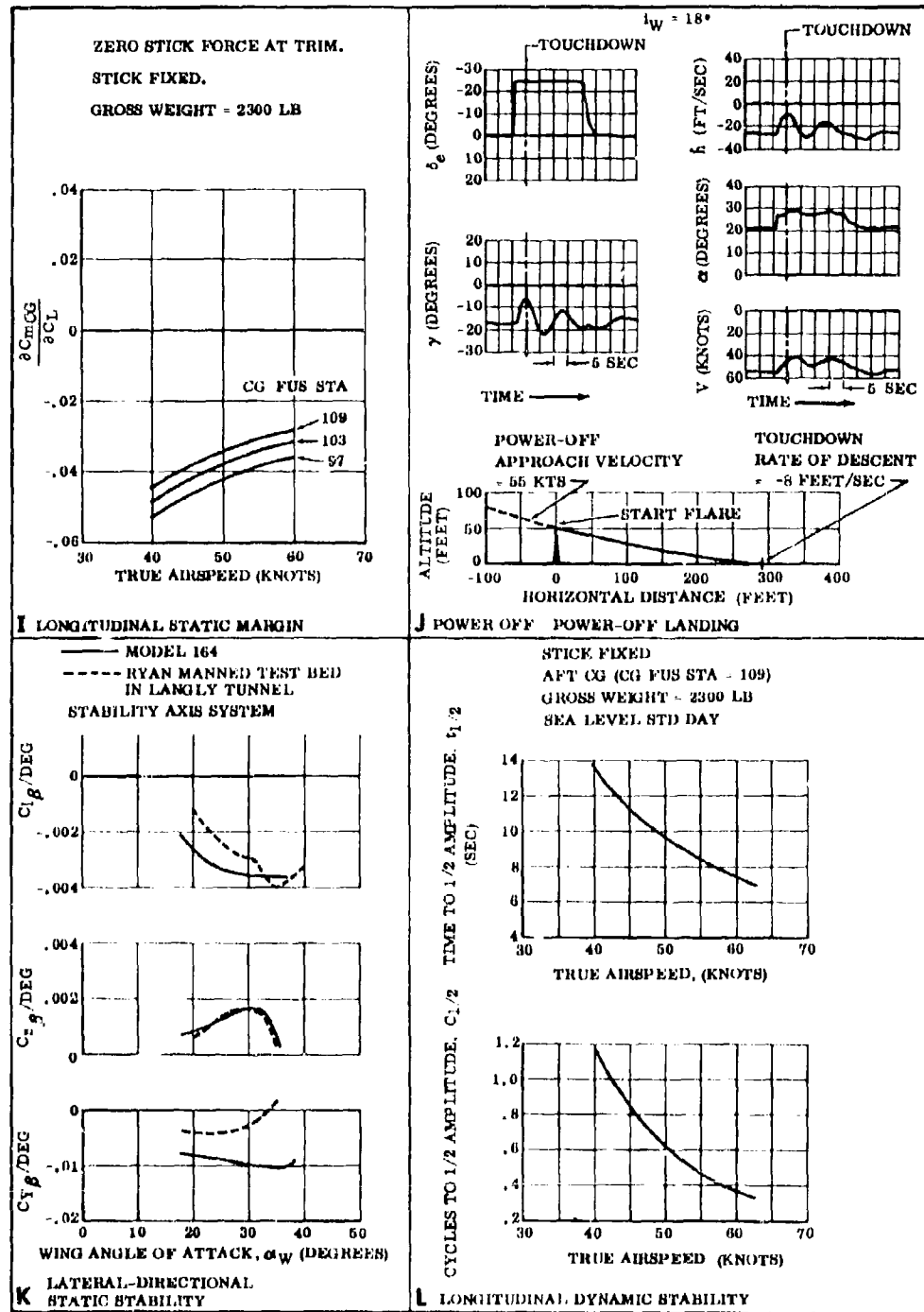


Figure 9. Stability and Control Data (Sheet 3 of 5)

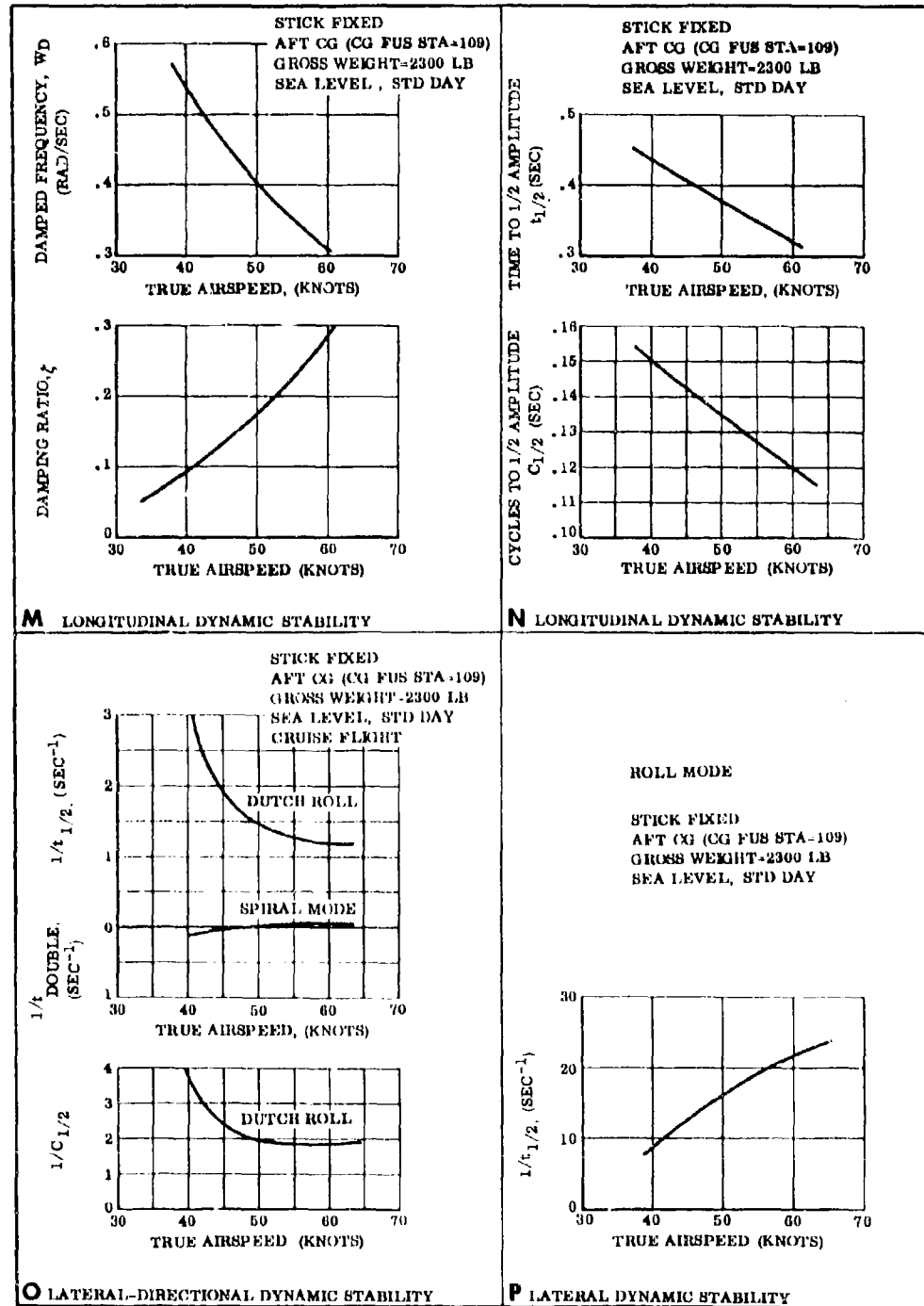


Figure 9. Stability and Control Data (Sheet 4 of 5)

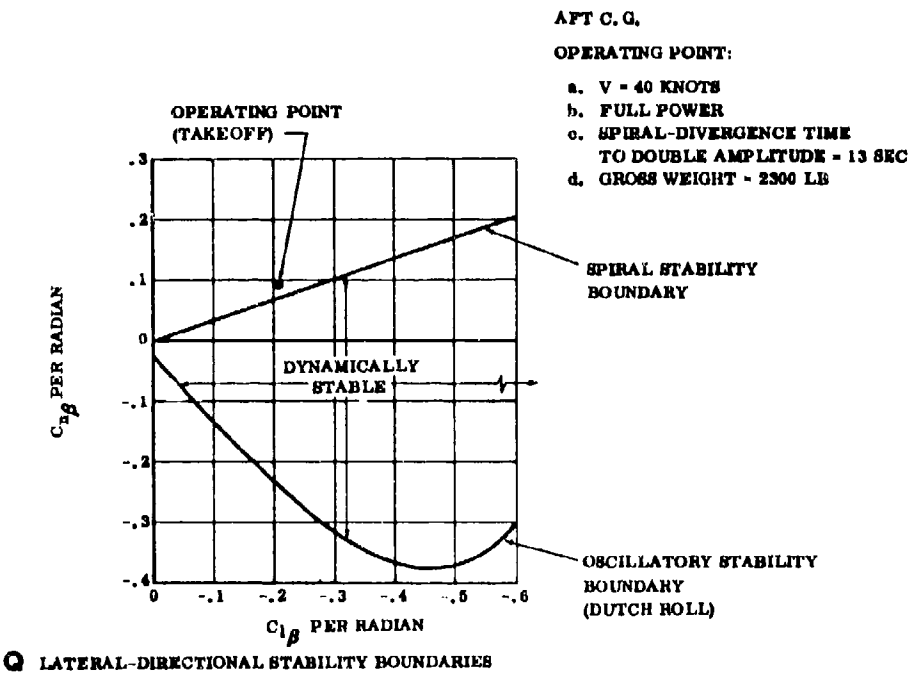


Figure 9. Stability and Control Data (Sheet 5 of 5)

The following criteria were considered in selecting the area and dihedral angle of the V-tail:

1. Maximum wing angle of attack with full up-elevator should not exceed the angle for encountering pitch-up or stall.
2. The tail should be capable of increasing angle of attack by at least 7 degrees with maximum elevator deflection.
3. Tail size cannot exceed space and weight limitations.

A longitudinal 3-degrees-of-freedom analog simulation was performed to evaluate various tail sizes and dihedral angles in order to select a vee-tail that would best satisfy the above listed criteria. Evaluation of the analog output resulted in selecting the following tail geometry:

Total tail area	51 square feet
Movable area (including balance area)	34.8 square feet
Horn balance area	4.72 square feet
Fixed area	16.2 square feet
Geometric aspect ratio	1.6 (1 side)
Airfoil	NASA 0009

The equations of motion used in the longitudinal simulation were written in the wind-axis system as follows:

$$\begin{aligned} \ddot{Z} = \frac{\Sigma F_Z}{m} = - & \left[C_L \frac{(\alpha_B + i_W + \alpha_{OL}) + C_L \frac{\alpha_B}{\alpha_B} + C_L q_{W,B} \left(\frac{\dot{\alpha}_C K}{ZV} \right)}{\alpha_W} \right] \frac{qS_W}{m} - \\ & \left[C_L \frac{(\alpha_B + i_t - \epsilon) + C_L \frac{\delta_e}{\delta_e} + C_L q_t \left(\frac{\dot{\alpha}_C}{ZV} \right)}{\alpha_t} \right] \frac{qS_t}{m} - \\ & \frac{T}{m} \sin (\alpha_B + i_{TH}) + g \cos \gamma - v \dot{v} \\ \ddot{X} = \frac{\Sigma F_X}{m} = - & \left[C_D \frac{0}{W} + K_D \frac{1}{1} (\alpha_B + i_W) + K_D \frac{2}{2} (\alpha_B + i_W)^2 + \right. \\ & \left. K_D \frac{3}{3} (\alpha_B + i_W)^3 + C_D \frac{0}{B,t} + C_D \frac{2}{2} \alpha_B^2 \right] \frac{qS}{m} + \\ & \frac{I}{m} \cos (\alpha_B + i_{TH}) - g \sin \gamma - v \dot{v} \end{aligned}$$

$$\ddot{\Theta} = \frac{\Sigma M}{I_Y} = \left[C_{m_0_W} + C_{N_W} \frac{X_W}{C_K} + C_{A_W} \frac{Z_W}{C_K} + C_{m_0_B} + C_{m_{\alpha_B}} \alpha_B + C_{m_{q_W, B}} \left(\frac{\dot{\alpha}_K}{ZV} \right) + C_{L_t} \frac{X_t}{C_K} \frac{S_t}{S} \right] \frac{qSC_K}{I_Y} + \frac{TZ_{TH}}{I_Y}$$

$$C_{D_W} = C_{D_0_W} + K_{D_1} (\alpha_B + i_W) + K_{D_2} (\alpha_B + i_W)^2 + K_{D_3} (\alpha_B + i_W)^3$$

where X_W and Z_W are distances from aircraft center of gravity to wing aerodynamical center, measured parallel and perpendicular to keel, respectively. K_{D_1} , K_{D_2} , and K_{D_3} are coefficients to curve-fit equation for C_{D_W} .

Elevator Stick Force

The elevator stick forces were determined as follows:

$$\text{Work done at the stick} = \text{work done at the elevator}$$

$$\frac{F_S \ell_S \delta_S}{2} = \frac{H M \delta_e}{2}$$

where ℓ_S is length of stick in feet, and δ_S and δ_e are the angular rotations of the stick and elevator, respectively, in radians. The above equation reduces to:

$$F_S = H M \frac{\delta_e}{\ell_S \delta_S}$$

Figure 9C presents the estimated elevator stick forces as a function of control surface deflection, for several airspeeds.

Longitudinal Trim

The wing-incidence angles required to trim the aircraft with zero stick-force are presented in Figures 9D through 9F for maximum power, cruise power, and power-off conditions. Trim angles of attack are plotted versus velocity in Figure 9G. The trim points were obtained from a longitudinal-trim digital computer program which

yields pitching moment coefficient versus angle of attack for a range of incidence angles.

The longitudinal trim program utilizes the following equation to solve the pitching moment coefficients about the aircraft center of gravity.

$$C_{m_{eg}} = C_{m_0_W} + C_{N_W} \frac{X_W}{C_K} + C_{A_W} \frac{Z_W}{C_K} + C_{m_0_B} + \\ C_{m_{\alpha_B}} + \frac{T}{qS_W} \left(\frac{\ell_{TH}}{C_K} \right) + C_{m_{\alpha_e}} + C_{m_{PROP}}$$

Longitudinal parameters pertinent to the trim calculations are listed below:

$$C_{m_0_W} = -0.028$$

C_K = keel length (26 feet)

$$C_{m_0_B} = -0.0018 \text{ per degree}$$

$$C_{m_{\alpha_B}} = +0.00021 \text{ per degree}$$

$$\frac{\ell_{TH}}{C_K} = -0.048$$

$$C_{m_{\alpha_t}} = C_{L_{\alpha_t}} \frac{X_t}{C_K} \frac{S_t}{S_W}$$

$$\alpha_t = \alpha_W - \epsilon - i_W \approx 0.7 \alpha_W - i_W$$

Elevator Deflection Required To Retrim in Event of Engine Failure

In order to provide clearance between the propeller and the cargo bed, it was necessary to mount the engine well above the bed. This high thrust line results in a nose-up moment in the event of sudden loss of power. The elevator deflection required to retrim to the original trim speed was determined as follows:

$$C_{m_T} = \frac{T}{q_S} \frac{Z_t}{C_K} = C_{m_{\delta_e}} (\Delta \delta_e)$$

where

$$C_{m_{\delta_e}} = C_{L_{\delta_e}} \frac{x_t}{C_K}$$

$$C_{m_T} = \frac{T}{q_S} \frac{Z_T}{C_K} = C_{L_{\delta_e}} \frac{x_t}{C_K} \frac{s_t}{s} (\Delta \delta_e)$$

where

$$\Delta \delta_e = \frac{T Z_T}{q C_{L_{\delta_e}} x_t s_t}$$

Total elevator deflection to retrim is then equal to:

$$\delta_{e_TRIM} = \delta_{e_FLOAT} + \Delta \delta_e$$

Figure 9H presents the elevator deflections required to retrim the aircraft, in the event of a complete loss of power, as a function of airspeed and for three center of gravity locations.

Stick-Fixed Longitudinal Static Stability

The stick-fixed longitudinal static margin was calculated from the following relations:

$$C_{m_C_L} = \frac{C_{m_\alpha}}{C_{L_\alpha}}$$

Values of C_{m_α} were obtained from the digital trim program discussed previously. C_{L_α} was determined as follows:

$$C_{L_\alpha} = C_{L_w} + C_{L_t} + C_{L_B}$$

$$C_{L_\alpha} = 0.0422 + 0.0020 + 0.0016 = 0.0458 \text{ per degree}$$

$C_m C_L$ is plotted in Figure 9I as a function of both lift coefficient and of speed, for three center of gravity locations.

Stick-Free Longitudinal Static Stability

A quantitative estimate of the stick-free longitudinal stability has not been made; however, the longitudinal static margin is expected to be slightly greater with controls free than with controls fixed. This increase in stability is a result of the positive C_h which induces the

elevator to float downward with increased angle of attack. The magnitude of the stability increase will, of course, be reduced by friction in the control system; however, the stick-free stability will never be less than that with controls fixed as long as C_h is positive.

Power-Off Emergency Landings

Standard landing procedure for the Model 164 will call for partial power throughout the approach for the following reasons:

1. Power can be used to establish the desired rate of descent during the approach.
2. Landing flares are accomplished with lower approach speeds due to the increased effective lift-to-drag ratio resulting from the added thrust.
3. Low touchdown rates of descent are obtained.

Conversely, power-off landings require higher approach speeds and rates of descent in order to insure a satisfactory flare. These approach conditions make it difficult to judge altitude and flight path, and for these reasons, power-off landings should be considered as emergency procedures unless subsequent flight tests prove the maneuver to be less critical than predicted. Power-off landings were investigated

during the analog simulation discussed previously. Figure 9J presents an analog trace of a typical power-off landing. The minimum touchdown rate of descent of 8 feet per second was obtained by initiating flare at a height of 50 feet. Full elevator deflection of 25 degrees was used. Approach speed was 55 knots. Studies have also shown that power-off landing velocities may be reduced by following the procedure listed below:

1. Establish glide speed as quickly as possible by use of longitudinal control.
2. Roll pitch-trim control back while maintaining glide speed by means of longitudinal control (stick forward).
3. Apply maximum up-elevator to flare.

The elevator deflection available to flare the aircraft is thus increased by the amount of deflection held during the approach.

Lateral-Directional Static Stability

The lateral-directional parameters $c_{Y\beta}$, $c_{n\beta}$ and $c_{\ell\beta}$ for the complete aircraft are presented in Figure 9K. These data are based on Ryan and NASA wind-tunnel tests of Flexible Wing models, and on flight test data obtained with the Ryan Manned Test Bed. The following equations defining vee-tail lateral-directional stability were used to obtain estimates of $c_{Y\beta}$, $c_{n\beta}$ and $c_{\ell\beta}$ due to the tail. The derivation of these equations can be found in reference 8.

$$c_{Y\beta_t} = -K c_L \frac{\sin^2 \Gamma}{\alpha_N}$$

$$c_{n\beta_t} = c_Y \left(\frac{x_t}{b} \right)$$

$$c_{\ell\beta_t} = c_Y \left(-\frac{z_t}{b} \right)$$

where K is a constant for computing slope of lift curve of a vee-tail in yaw (equal to 0.67 for Model 164 tail).

Longitudinal Dynamic Stability

Longitudinal dynamic stability was calculated by IBM 704 using stick-fixed, small perturbation equations. The data listed in Table 1 have been plotted as a function of velocity and are presented in this section for evaluation of the dynamic longitudinal characteristics.

TABLE 1
LONGITUDINAL DYNAMIC STABILITY DATA

Reference	Mode	Characteristic	Flight Conditions
Fig. 9L	Phugoid	Time to 1/2 ampl.	Aft center of gravity (F. S. 109), gross weight 2300 lb.,
Fig. 9L	Phugoid	Cycles to 1/2 ampl.	sea level, std. day
Fig. 9M	Phugoid	Damped freq.	
Fig. 9M	Phugoid	Damping ratio	
Fig. 9N	Short period	Time to 1/2 ampl.	
Fig. 9N	Short period	Cycles to 1/2 ampl.	

The small perturbation equations used in the analysis are based on equations developed in BUAER Report AE-61-4 Volume II, "Dynamics of the Airframe." The following assumptions were made:

1. The airframe is a rigid body.
2. The XZ plane is a plane of symmetry.
3. During steady state flight the airframe is flying with wings level, all components of velocity other than U_0 are zero, and the airframe is in unaccelerated flight.
4. Only small perturbations from the steady flight conditions are permitted.

The equations are:

$$\dot{U} = X_U U + X_W \dot{W} + X_{Wq} W + X_q \dot{\phi} + X_{\delta_e} \delta_e - g (\cos \gamma_0) \phi$$

$$\dot{W} = Z_U U + Z_W \dot{W} + Z_{Wq} W + (U_0 + Z_q) \dot{\phi} + Z_{\delta_e} \delta_e - g (\sin \gamma_0) \phi$$

$$\ddot{\Theta} = M_U \dot{U} + M_W \dot{W} + M_{W\dot{W}} + M_q \dot{\Theta} + M_{\delta_e} \delta_e$$

The symbol definitions are too lengthy to be reported herein. If required, these definitions may be found in Reference 5. The dynamic stability investigations indicate stable longitudinal characteristics throughout the speed range.

Lateral-Directional Dynamic Stability

The methods used to estimate lateral-directional dynamic stability are similar to those utilized for longitudinal dynamics, i. e., small perturbation equations solved by IBM 704. The stick-fixed lateral-directional perturbation equations, based on equations developed in Reference 5, are:

$$\dot{\beta} = Y_\beta \beta + Y_p \dot{\theta} + Y_r \dot{\psi} + Y_{\delta_\alpha} \delta_\alpha + Y_{\delta_r} \delta_r - \dot{\psi} + \frac{g}{U_0} (\cos \gamma_0) \theta + \frac{g}{U_0} (\sin \gamma_0) \psi$$

$$\ddot{\theta} = L_\beta \beta + L_p \dot{\theta} + L_r \dot{\psi} + L_{\delta_\alpha} \delta_\alpha + L_{\delta_r} \delta_r + \frac{I_{XZ}}{I_X} \dot{\psi}$$

$$\ddot{\psi} = N_\beta \beta + N_p \dot{\theta} + N_r \dot{\psi} + N_{\delta_\alpha} \delta_\alpha + N_{\delta_r} \delta_r + \frac{I_{XZ}}{I_Z} \dot{\theta}$$

See reference 5 for symbol definitions, if required.

Table 2 lists the data obtained from the lateral-directional perturbation program. These data are plotted versus velocity in Figure 9, details N and O.

TABLE 2
LATERAL-DIRECTIONAL DYNAMIC STABILITY DATA

Reference	Mode	Characteristic	Flight Conditions
Fig. 9O	Dutch roll	1/time to 1/2 ampl.	Aft cg (F. S.
Fig. 9O	Dutch roll	1/cycle to 1/2 ampl.	109), GW 2300
Fig. 9O	Spiral	1/time to 1/2 ampl.	lb., sea level,
Fig. 9P	Roll	1/time to 1/2 ampl.	std. day

The above data indicate stable dynamic stability in the dutch-roll and pure-roll modes, and mild instability in the spiral mode. The degree of spiral divergence, however, is within the acceptable limits for manned aircraft. In addition to the above data, the lateral-directional stability boundaries have been determined in the takeoff condition. These boundaries are determined from the aircraft's characteristic equation of motion, which has the form

$$A\lambda^4 + B\lambda^3 + C\lambda^2 + D\lambda + E = 0$$

The conditions of neutral dynamic stability are:

$$E = 0_2 \text{ (Spiral boundary)}$$

$$BCD - AD^2 - B^2 E = 0 \text{ (Dutch roll boundary)}$$

A complete discussion of the method of analysis can be found in Reference 7, Chapter 11. Solutions of the above equations were obtained by IBM 704 and are plotted in Figure 9Q in the $C_l - C_n$

$\beta - n_\beta$ plane. Figure 9Q shows that the aircraft will be operating far from dutch-roll instability, but that mild spiral instability will be present. The time to diverge to double amplitude was calculated to be 13 seconds, which is within the acceptable limits for manned aircraft.

STRESS ANALYSIS

STRUCTURAL DESIGN CRITERIA

Design Weights

Minimum flying weight	1189 pounds
Basic flight design gross weight	2300 pounds
Maximum flight design gross weight . . .	2300 pounds

Design Speeds

Level flight maximum speed (V_H)	56 knots
Limit speed (V_L)	84 knots
Speed for maximum gust intensity (V_G). .	50.5 knots

Ultimate Factor of Safety

The ultimate factor of safety is 1.5.

Maneuvering Load Factor

The maneuvering load factor is +2.5. See Figure 10.

Gust Load Factor. See Figure 10.

Vertical	$n_Z = +2.25$
Side	$n_Y = \pm 0.25$

Design Landing Load Factor at Center of Gravity

The design landing load factor at the center of gravity is 4.25.

Design Sink "p. ed

The design sink speed is 12.0 feet per second.

STRUCTURAL LOADS

Wing Keel and Leading Edges

Distribution of air loads along the wing keel and leading edges was made from test data set forth in NACA T. N. D-983. See Table 3 for summary.

Landing Gear

The landing gear and its attachments were designed to absorb the shock resulting from a descent at 12 feet per second, assuming wing lift to be 2/3 the gross weight. See Table 3 for summary.

Tail

Resultant tail loads were determined from Ryan analog simulation data. Chordwise distribution of air loads was made in accordance with CAM-3. Spanwise distribution was in accordance with NACA T. R. 921 and NACA W. R. L-212. See Table 3 for summary.

Engine Mount

The engine mount was designed to take the vertical, fore and aft, and side loads resulting from maneuvering, landing, gusts and propeller thrusts; it was also designed to take the moments due to engine torque and gyroscopic forces. See Table 3 for summary.

Cargo Platform and Body Structure

The cargo platform and body structure were designed to resist the loads imposed by the landing gear, engine mount structure, wing support struts, cargo load, control system and tail surfaces. See Table 3 for summary.

STRUCTURAL ANALYSIS

The capability of the various structural members to resist the imposed loads was demonstrated by calculations conforming to accepted engineering practice. Static proof loads representing the most severe design conditions were imposed on actual wing and tail structures to verify the calculations. Drop tests on the landing gear were made to demonstrate the ability of the shock absorbing system to dissipate landing shock loads. The margins of safety of all important structural members under the critical load conditions are summarized in Table 3.

WEIGHT DATA

Weight and Center of Gravity Calculations

The weight and center of gravity calculations are presented in Table 4 using reference data shown in Figure 11.

Loading and Burnoff

The XV-8A loading and fuel burnoff results are shown in Figure 12.

Results of Actual Weighing

The results of actual weighing are listed in Table 5. These results are based on the following:

Pilot ballast. 0.0 pound
Fuel. 0.0 pound
Oil. 15.0 pounds
Instrumentation wiring 15.0 pounds
Deck angle. 0.0 degree

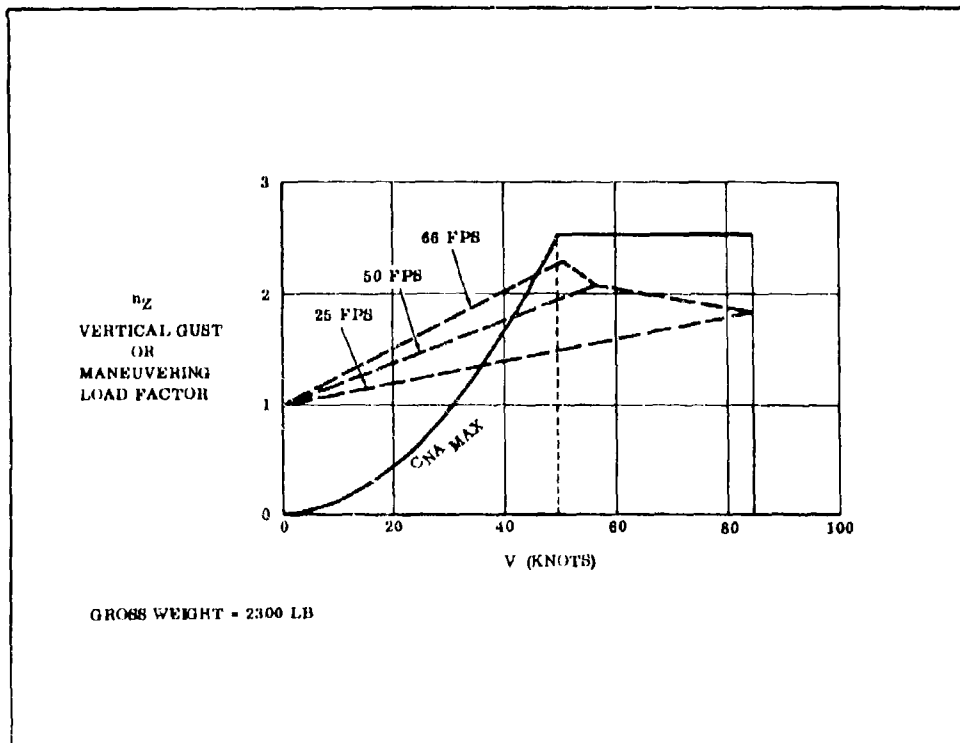


Figure 10. V-n Diagram for Symmetrical Flight

TABLE 3
SUMMARY - CRITICAL LOADS AND FACTORS OF SAFETY

Member and Location	Critical Condition	Applied Load(lbs.)	Allowable Load(lbs.)	Ultimate Factor of Safety
Leading edge (Sta. 60% aft of apex)	35° angle of attack	33,390	75,000	2.25
Leading edge (Sta. 42% aft of apex)	35° angle of attack	7,217	8,150	0.13*
Leading edge skin splice	35° angle of attack	113	173	1.58
Keel at main hinge point	Pos. Flt. 2. 5g gust sym	33,280	65,700	2.02
Keel at fw _c . cable attachment	Pos. Flt. 2. 5g gust sym.	47,200	76,500	1.62
Keel at aft cable attachment	Pos. Flt. 2. 5g gust sym.	35,600	76,500	2.15
Front wing support strut	Side load	7,680	14,050	1.83
Center wing support strut (Riveted end fitting)	30° angle of attack	1,760	4,240	2.41
Aft wing support strut (upper)	30° angle of attack	2,500	10,000	4.00
Aft wing support strut (lower)	30° angle of attack	7,040	15,000	2.13
Main landing gear axle	Side drift landing	105,000	218,000	2.07
Main landing gear spring (bending), Main landing gear spring (shear)	Tail down landing	82,700	113,200	1.37**
Nose landing gear drag brace	2-wheel braked roll	3,960	8,000	2.02
Nose landing gear socket	Side load	8,770	20,000	2.28
Nose landing gear strut	Spin up	32,600	52,500	1.61
Nose wheel fork (torsion in crown)	Spring back	113,000	247,000	2.18
Nose wheel fork (bending in crown)	Spring back	26,400	46,000***	-
Pivot-spreader bar to leading edge	Spring back	22,000	114,000***	1.66***
Spreader bar chord members:	Pos. flt.	31,800	150,000	4.71
Outer upper	Pos. flt.	4,675	10,450	2.24
Inner upper	Pos. flt.	12,200	20,300	1.66
Outer lower	Neg. flt.	510	930	1.82
Inner lower	Neg. flt.	510	930	1.82
Center lower	Neg. flt.	32,000	95,000	2.96

TABLE 3 (Continued)

Member and Location	Critical Condition	Applied Load (lbs.)	Allowable Load (lbs.)	Ultimate Factor of Safety
Spreader bar diagonals				
Outer	Pos. flt.	1, 940	3, 050	1. 57
Intermediate	Neg. flt.	510	930	1. 82
Inner	Neg. flt.	2, 530	6, 620	2. 61
Engine mount legs	Gust + thrust	4, 725	37, 000	7. 83
Engine mount diagonals (side members)	Thrust	7, 580	95, 000	12. 50
Engine mount diagonals (front and rear)	Side load	6, 050	15, 700	2. 60
Tail surface spar at root	Maneuvering	27, 045	40, 000	1. 48***
Ruddervator spar	Maneuvering	2, 310	5, 780	2. 50
Ruddervator rib at spar attachment	Maneuvering	4, 000	15, 770	3. 94
Control column (bending at root)	Pilot effort	64, 000	150, 000	2. 34
Control chain	Pilot effort	875	1, 700	1. 94
Platform long. beam compression flange	2. 5g sym.	9, 300	25, 000	2. 68
Platform edge beam compression flange	2. 5g sym.	18, 000	67, 000	3. 72
Platform skin beads	2. 5g sym.	3, 590	9, 450	2. 63

*Based on nonbuckling at limit load and no failure at ultimate

**Designed by deflection

***Combined factor

****This structure was a static test item. Spar caps were strengthened subsequent to marginal results of test. Resulting ultimate factor of safety greater than 1. 50

TABLE 4
WEIGHT AND CENTER OF GRAVITY CALCULATIONS

Item	Weight (lb.) (W)	Fus. Sta. (X)	Hor. Mom. (WX)	W. L. Vert. Mom. (Z) (WZ)
Cockpit area furnishings	35.66	24.8	885	39.2 1,397
Controls Instl.	53.32	57.9	3,088	32.1 1,711
Platform assembly	205.13	91.3	18,734	12.6 2,590
Nose landing gear instl.	42.84	2.6	110	-5.8 -248
Main landing gear instl.	82.50	127.7	10,532	-5.6 -462
Power plant instl.	411.41	148.2	60,983	48.6 20,007
Control surfaces	42.40	190.7	8,085	29.6 1,254
Wing instl.	122.74	113.3	13,904	146.3 17,952
Wing superstructure instl.	119.00	103.8	12,358	114.2 13,590
Final assembly	(1,115.00)	115.4	(128,679)	51.8 (57,791)
Pilot	170.00	40.0	6,800	44.1 7,497
Oil	15.00	147.6	2,214	51.4 771
Subtotal	(1,300.00)	105.9	(137,693)	50.8 (66,059)
Fuel	150.00	100.5	15,075	5.0 750
Subtotal	(1,450.00)	105.4	(152,768)	46.1 (66,809)
Cargo	850.00	99.0	84,150	25.0 21,250
Gross weight-maximum	2,300.00	103.0	236,918	38.3 88,059

TABLE 5
ACTUAL WEIGHING RESULTS

Reaction	Scale Reading (lb.)	Tare (lb.)	Net Weight (lb.)	Arm (in.)	Moment (in. -lb.)
L/H main gear	535	6.0	-	-	-
R/H main gear	520	0.0	-	-	-
Subtotal (both main)	1,055	6.0	1,049	129.19	135,520
Nose gear	102	0.0	102	1.75	179
Total	1,157	6.0	1,151	117.9	135,699

Weight Adjustments

Weight adjustments to configure to final assembly are listed in Table 6.

TABLE 6
WEIGHT ADJUSTMENTS

Item	Gross Weight (lb.)	Fuselage Sta. (in.)	Moment (in.)
As weighed	1,151	117.9	135,699
Less oil	15	147.6	2,214
Less Instl. wiring	15	80.0	1,200
Total	1,121	118.0	132,285

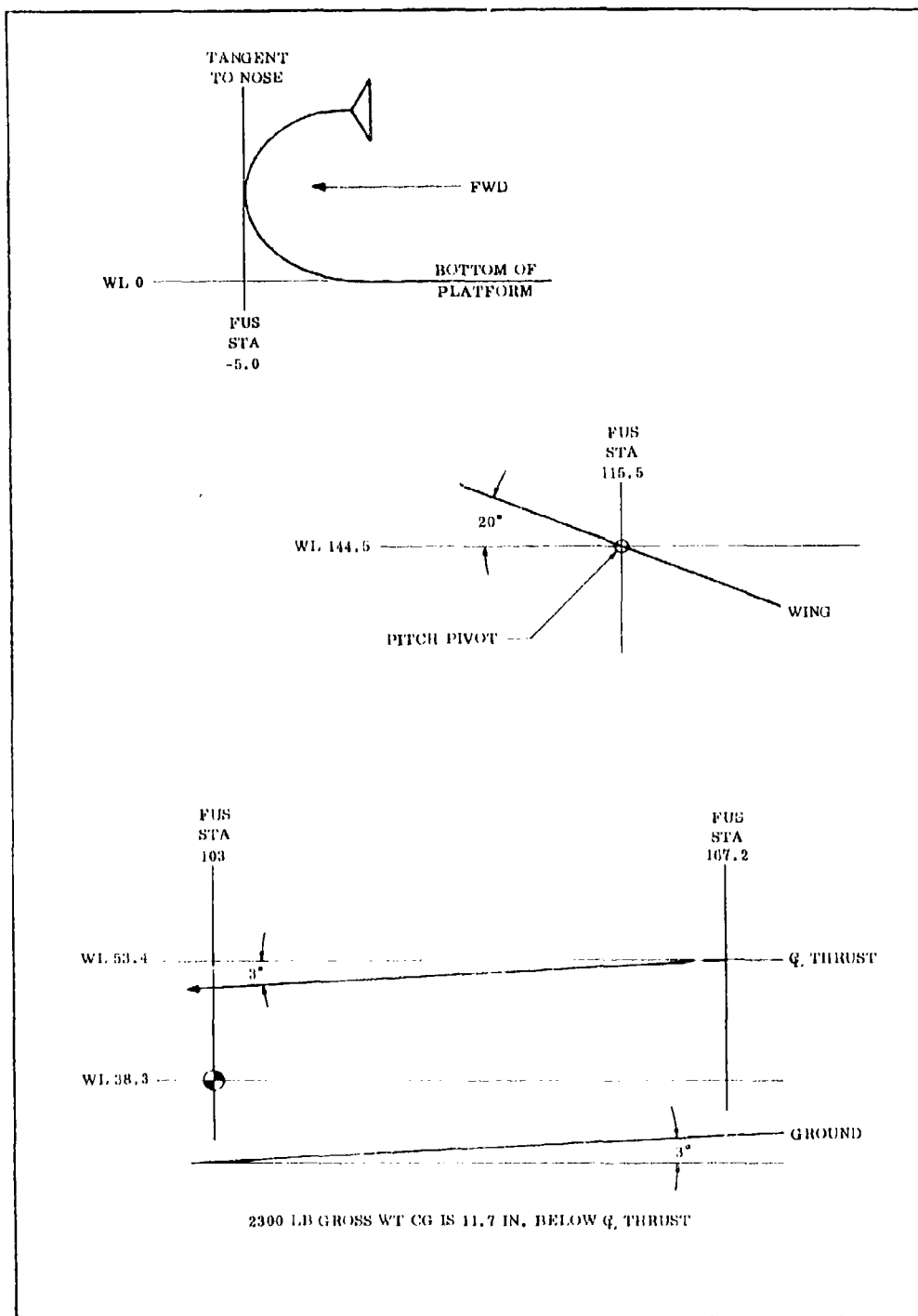


Figure 11. Reference Data for Weight and Center of Gravity Calculations

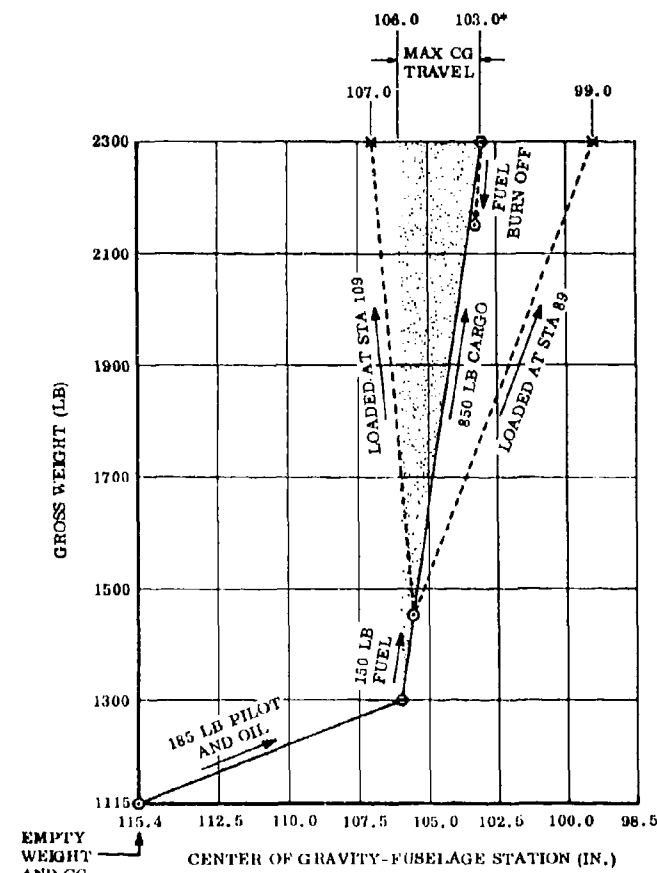


Figure 12. Loading and Burn-off Curve

STRUCTURAL TESTS

WING AND PLATFORM STRUCTURE

Test Vehicle

The wing and platform structure test vehicle was a completely rigged vehicle, less engine. The aileron cables were anchored to the bell-crank pivot bolts, to prevent aileron movement, because the aileron bellcranks were not available when the test was conducted. A test fabric was substituted for the production wing fabric.

Test Procedure

A proof load of 3,140 pounds (2.5 g) per semispan was applied to load distributing rods in each wing test fabric, 20.65 degrees forward and 13 degrees outboard, with reference to the plane of the leading edge and keel and the keel centerline, (Figure 13). The wing was at a 30-degree angle of incidence to the platform, which was inclined 11 degrees nose down, as shown in Figure 14. Loads were applied in 0, 20, 40, 60, 80, and 100 percent increments of the proof load, with returns to 20 percent after each increment over 60 percent to check for permanent set.

The test vehicle was tied to the ground at fuselage stations 56 and 120 to react the applied wing loads. The proof loads were applied to the keel and both leading edges through the wing test fabric, which was attached to the leading edge and keel in the same manner as the actual wing fabric. The test fabric was of sufficient width to reproduce the proper designed angles at the leading edges and keel. Proof loads were applied by a single hydraulic cylinder and a whiffle tree system attached to a load distributing rod in each wing section, (Figure 15). The total applied load was measured by a load cell.

A 330-pound side load was applied to the apex of the wing with a simultaneous 2,300-pound (1 g) wing load. The vehicle was tied to the ground, and measurements were taken as in the preceding test.

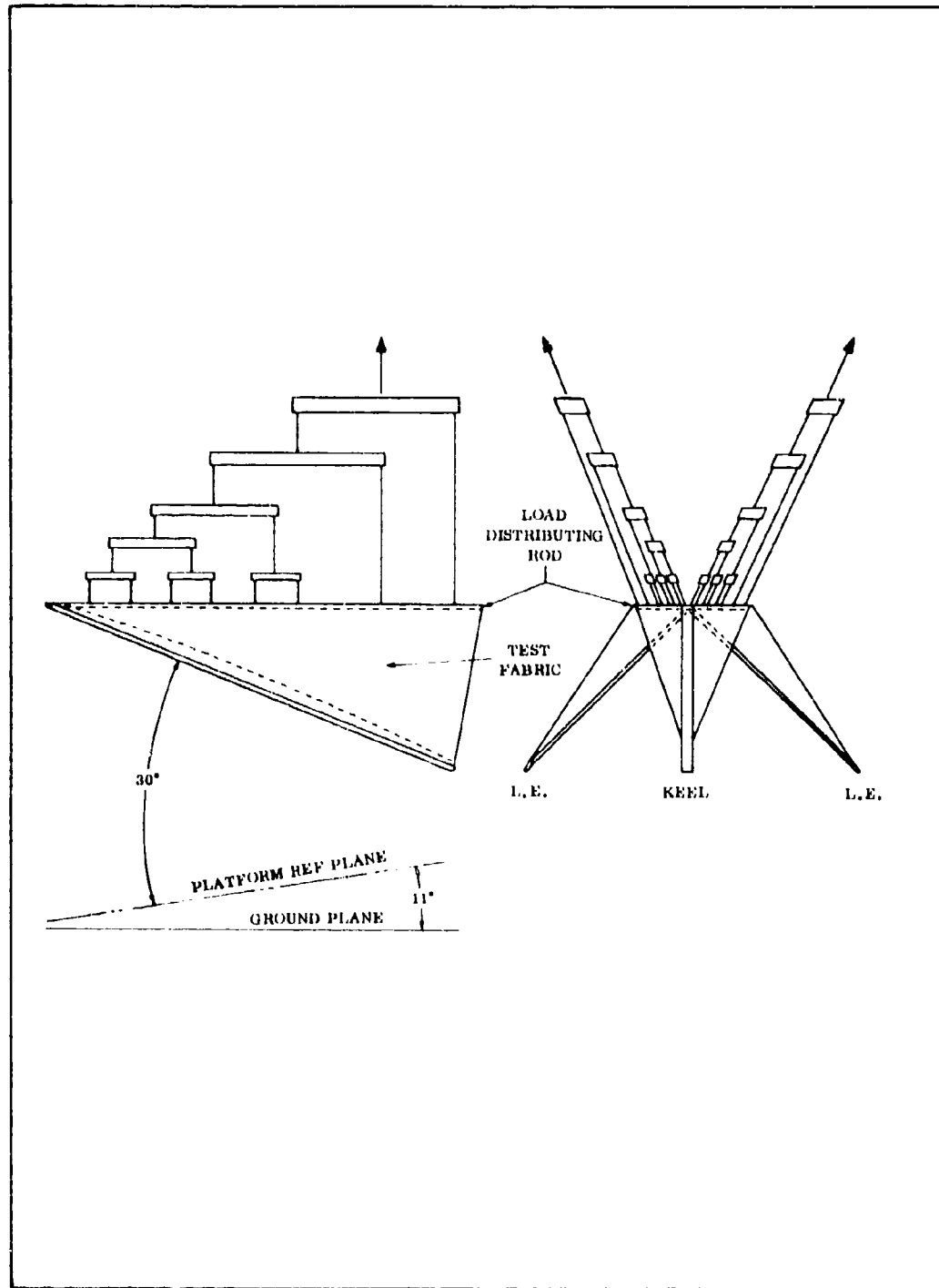


Figure 13. Whiffle Tree Configuration

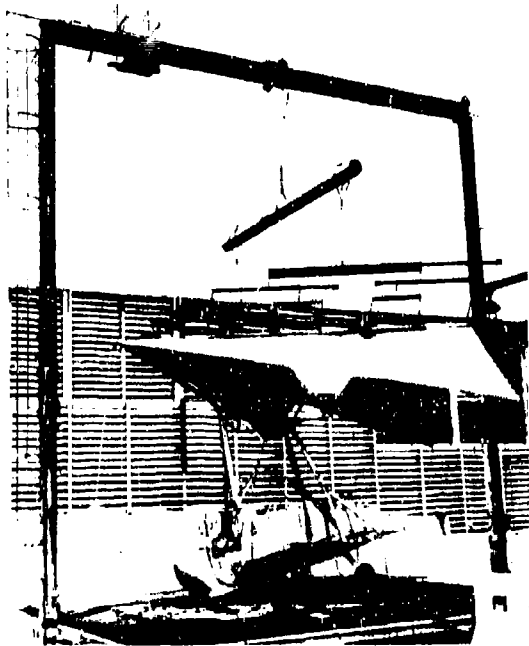


Figure 14. Static Test Setup

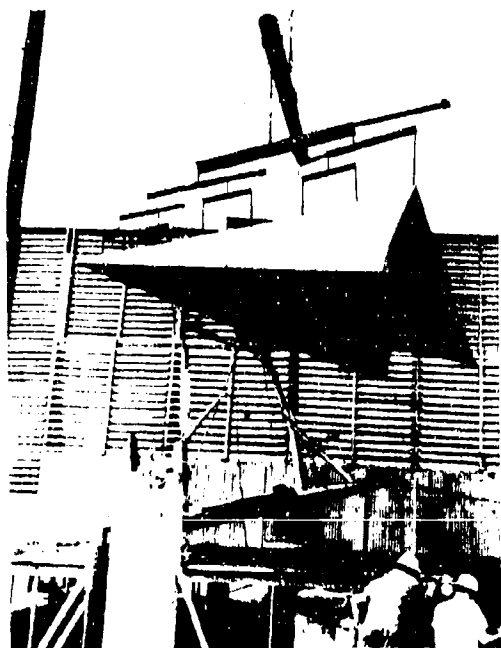


Figure 15. Keel Deflection

Test Results

The wing and platform structure satisfactorily withstood the applied static proof loads. Some bending of the aft section of the keel was observed at higher loads; however, no permanent set was discernible. See Table 7 for measurements taken and the values obtained. Records were taken on a recorder.

CONTROL SYSTEM

Test Vehicle

A completely rigged test vehicle was used to test the control system.

Test Procedure

The neutral and extreme positions of the pilot's controls and corresponding control surfaces were measured and recorded. Deflections were measured with a steel tape.

The steering pedals were loaded simultaneously with 250 pounds each, and deflections were recorded. A 200-pound load was applied to the brake pedal with the right-hand steering pedal fully depressed (Figures 16 and 17).

A load of 53 pounds was applied tangentially to the pitch control wheel in both directions with the keel restrained at the aft pitch cable attachment point and against the forward down stop. Deflections of the wheel and keel were recorded (Figure 18 and Table 8).

The ruddervator push-pull rods were anchored at their aft ends with the control column in the neutral position. A 200-pound load (100 pounds on each side of the wheel) was applied to the column in both directions and the deflections were recorded (Figure 17).

The wing was restrained at zero roll by attaching the roll stop cables to the platform tie-down rings. With the upper aileron bellcranks bottomed, a 1,126-inch-pound couple was applied to the wheel in both directions, and wheel deflections were recorded (Figure 17).

Test Results

The control system withstood the applied test loads. Deflections in all systems occurred through stretch in cables and/or deflection of the pulley brackets. No bending of any control equipment was observed.

TABLE 7
WING AND PLATFORM TEST DATA

Function and Location	Vertical Load Only 2.5 g	Vertical Load 1 g, Side Load 330 lb.
Forward Pitch Cable Tension	0	0
Aft Pitch Cable Tension	1,700 lb.	910 lb.
Bending, Keel at Pivot	11,000 p. s. i.	3,500 p. s. i.
Axial, Left Hand Fwd "V" Brace	0	2,400 p. s. i.
Axial, Right Hand Fwd "V" Brace	200 p. s. i. 200 p. s. i.	2,200 p. s. i. 2,200 p. s. i.
Axial, Left Hand Spreader Bar	7,900 p. s. i.	2,200 p. s. i.
Axial, Keel at Apex	2,000 p. s. i.	0
Vertical Bending, Left Hand Leading Edge at Pivot Ball	34,000 p. s. i.	12,200 p. s. i.
Lateral Bending, Left Hand Leading Edge at Pivot Ball	1,000 p. s. i.	1,000 p. s. i.
Axial, Left Hand Aft "V" Brace	1,000 p. s. i.	0
Axial, Right Hand Aft "V" Brace	2,000 p. s. i.	1,800 p. s. i.
Axial, Forward Center Strut	5,000 p. s. i.	0
Lateral Bending, Left Hand Leading Edge at Pivot Point	7,400 p. s. i.	2,600 p. s. i.

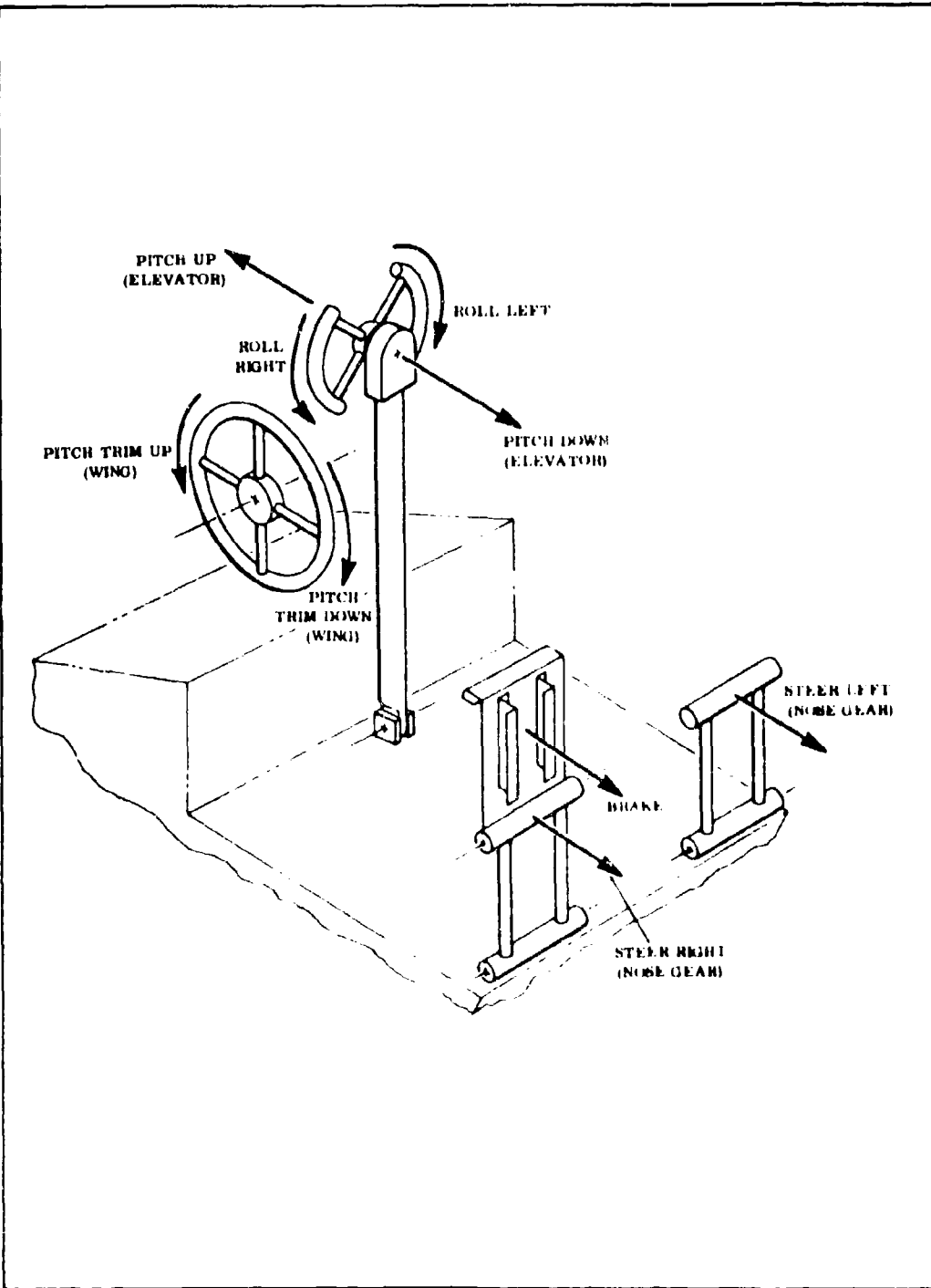


Figure 16. Cockpit Controls Proof Loading Test Configurations

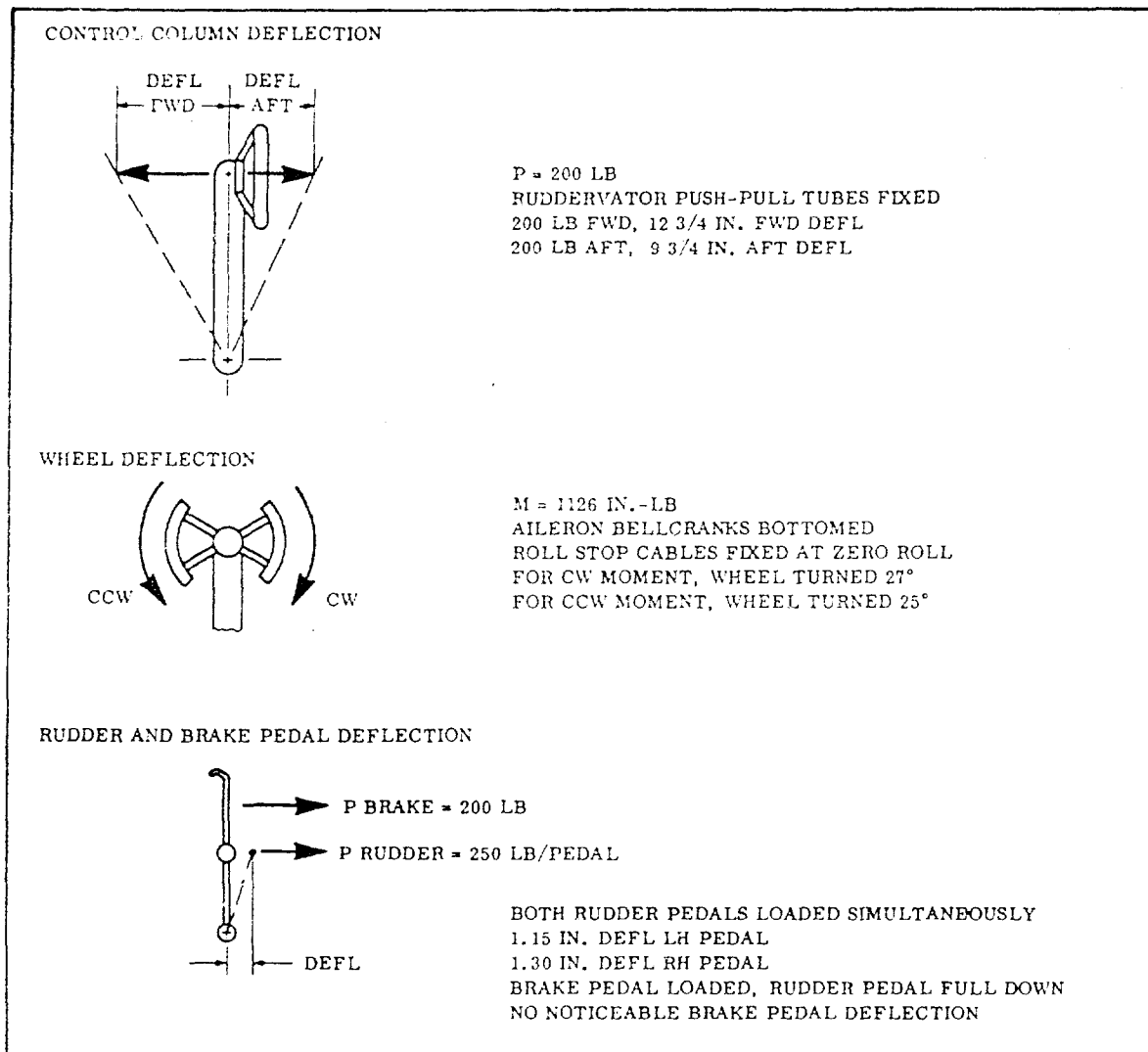


Figure 17. Control Column, Control Wheel, and Brake Pedal Deflection

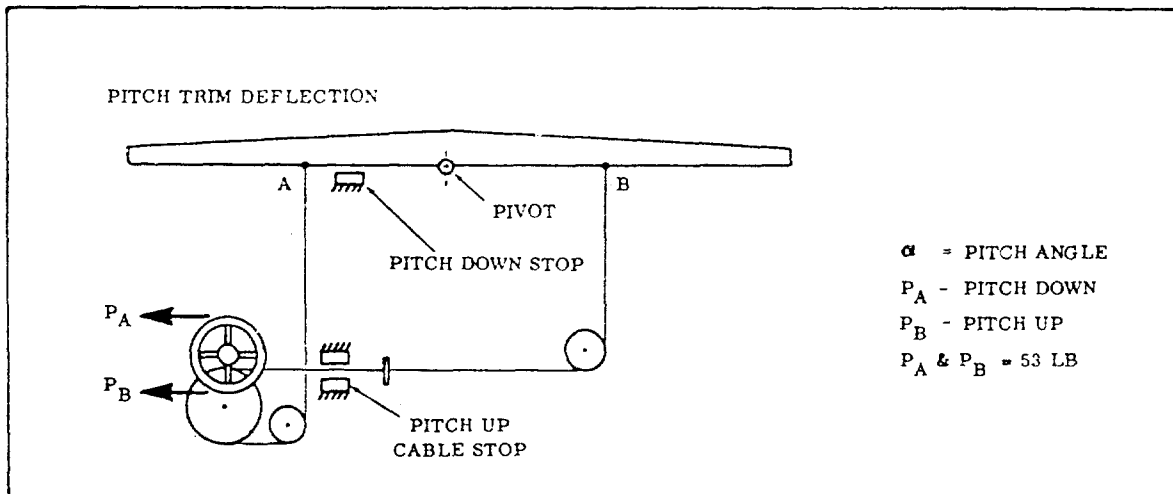


Figure 18. Keel Deflection Under Load

TABLE 8
KEEL DEFLECTION LOAD RESULTS

Pitch Angle (Deg.)	Load Applied	Point Restrained*	Keel Deflection Point A-Point B (in.)	Wheel Rotation
15	Pitch dwn.	B	2.5 dwn. 1.3 up	1½ turns
15	Pitch up	A	0.7 up 1.6 dwn.	1½ turns
0	Pitch dwn.	Pitch dwn. stop	0.26 dwn. 0.28 up	½ turn
30	Pitch up	Pitch up stop	0.25 up 0.25 dwn.	½ turn

*See Figure 18

TAIL ASSEMBLY

Test Structure

The tail assembly test structure was a complete left-hand ruddervator attached to the vehicle. The aft elevator bellcrank was locked in the neutral position during the test.

Test Procedure

The vehicle was inclined to orient the ruddervator in a horizontal attitude. Loads and deflections were measured at the positions shown in Figure 19. Five-pound shot bags were used to apply the test load. The shot bags were positioned as shown in Figure 20 for each increment while hydraulic jacks were supporting the ruddervator. After each loading, the jacks were lowered away from the surface, thus applying the load uniformly. The test structure was loaded in 20, 40, 60, 20, 80, 20, 90, 20, and 100 percent increments of the designed limit load.

Test Results

The ruddervator sustained 100 percent limit load for approximately 30 seconds, followed by a buckling failure of the lower surface of the fin. See Figures 21 and 22. The deflection and strain data are presented in Figure 23, details A through F.

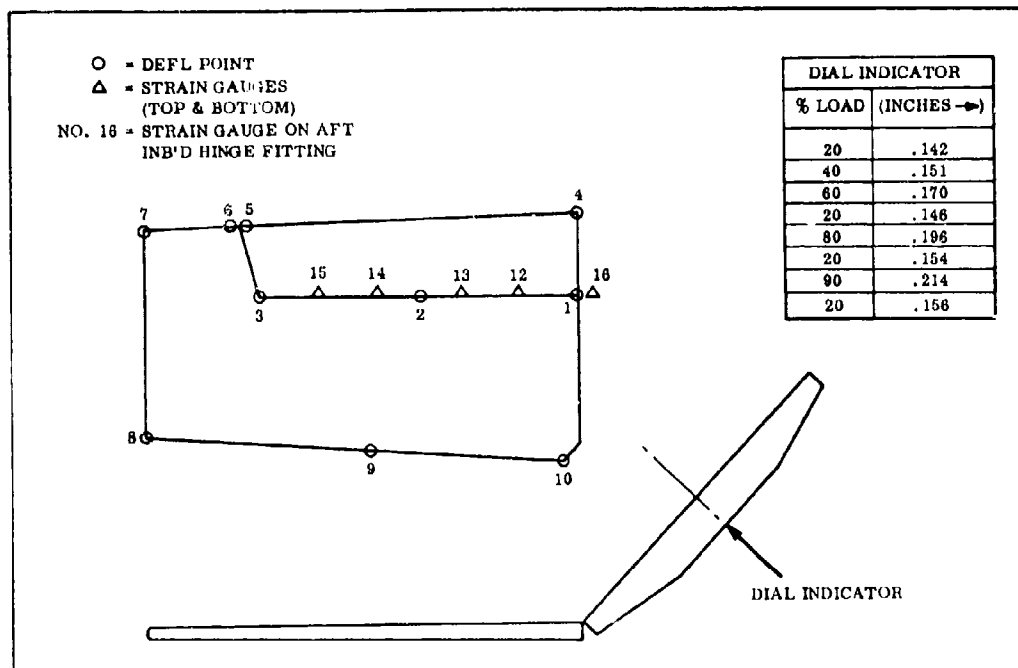


Figure 19. Deflection Point and Strain Gauge Locations, Ruddervator

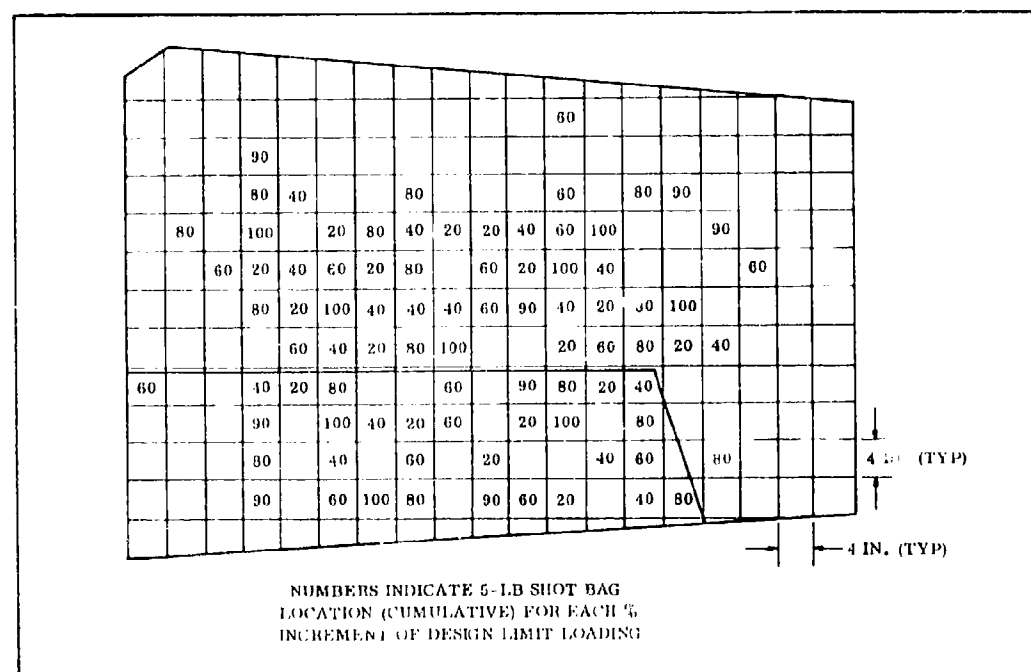


Figure 20. Shot Bag Configuration, Ruddervator



Figure 21. Ruddervator Failure

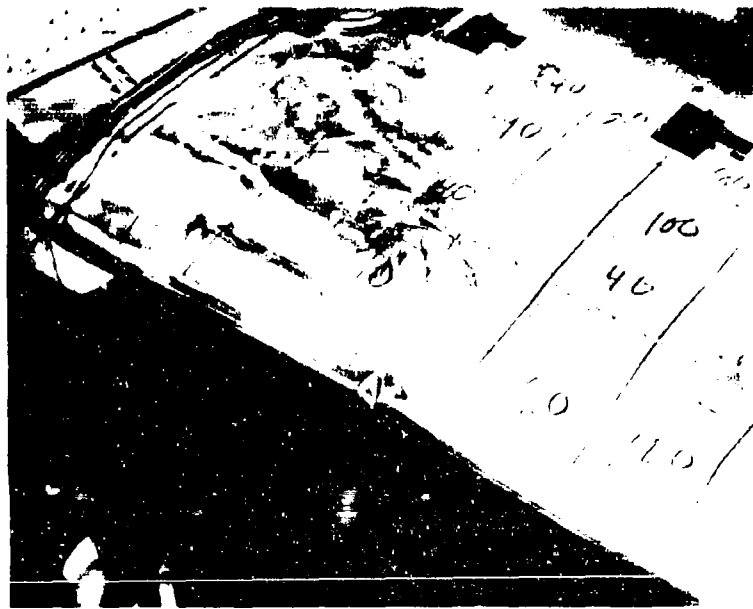
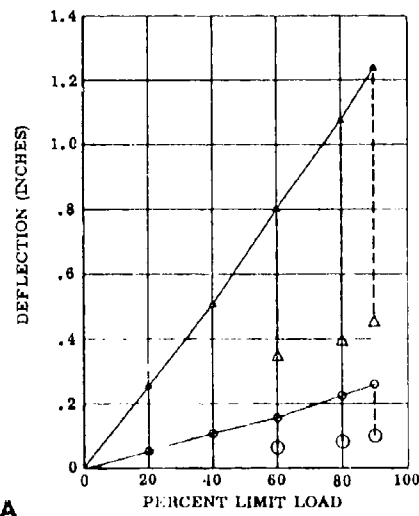


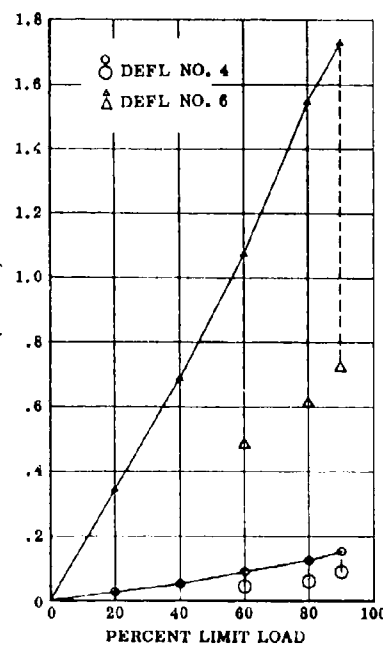
Figure 22. Ruddervator Failure, Shot Bags Removed

LARGER SYMBOLS INDICATE RETURNS TO 20% (TYP)

○ DEF'L NO. 1
△ DEF'L NO. 2

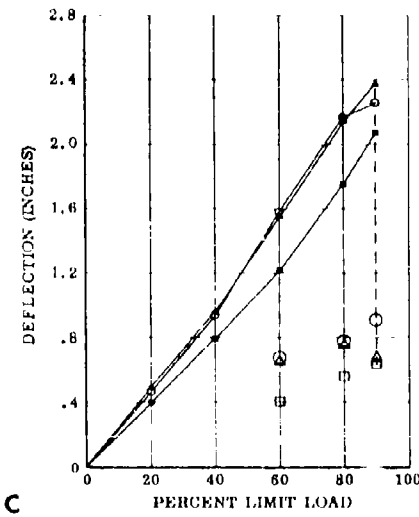


A

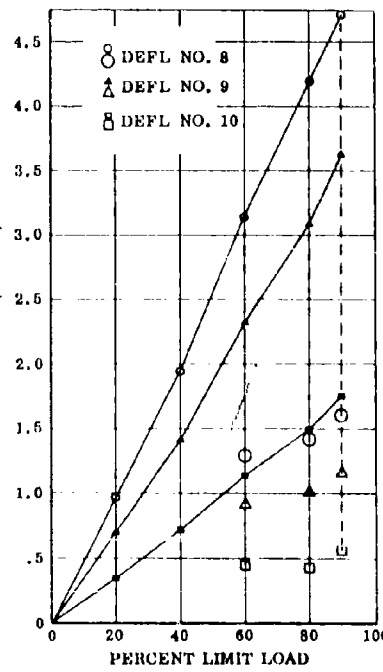


B

○ DEF'L NO. 5
△ DEF'L NO. 3
□ DEF'L NO. 7



C



D

Figure 23. Ruddervator Deflection Data (Sheet 1 of 2)

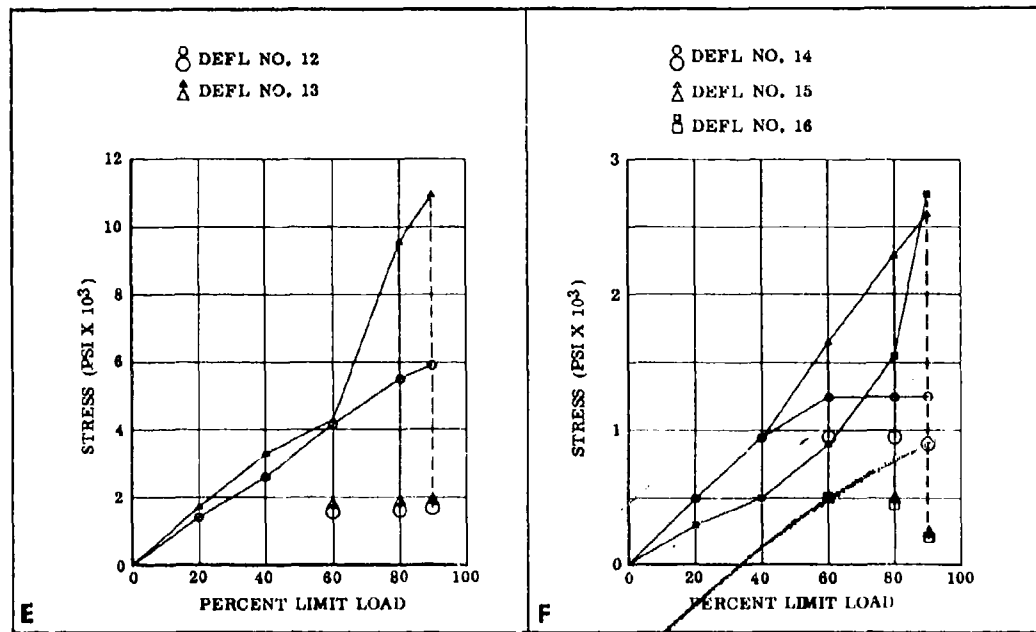


Figure 23. Ruddervator Deflection Data (Sheet 2 of 2)

DROP TESTS

Test Vehicle

The entire vehicle, less wing and support structure, was dropped under conditions set forth in the following paragraph. The center of gravity of the test vehicle was located at fuselage station 103. A 435-pound dummy engine was used, and the test vehicle drop weight was 1,635 pounds.

Test Procedure

The test vehicle was dropped from various heights and attitudes onto sloped and level surfaces to simulate the following landing conditions:

- 3-point landing
- 2-point landing
- Tail-low landing
- Nose-low landing
- Side-drift landing

The following drop configurations were used. Vehicle attitude refers to distance from wheels to ramps. A minus ramp angle indicates spring-back load.

Configuration 1 - Vehicle level, Main Landing Gear (M. L. G.) ramp -26.7 degrees, Nose Gear (N. G.) ramp -37.6 degrees. See Figure 24, detail A.

Configuration 2 - Vehicle and ramps level. See Figure 24, detail B.

Configuration 3 - Vehicle level, M. L. G. ramp -15 degrees, N. G. ramp level. See Figure 24, detail C.

Configuration 4 - Vehicle 7 degrees nose low, ramps level. See Figure 24, detail D.

Configuration 5 - Vehicle level, left-hand M. L. G. ramp 38.9 degrees, right-hand M. L. G. ramp 31 degrees, N. G. ramp level. See Figure 24, detail E.

The ramps were greased to simulate main gear wheel "run-out" which occurs during actual landings.

Test Results

The vehicle satisfactorily withstood all the drop conditions with no discernible damage. All accelerations were recorded, and an oscillograph recorded all strain gauge outputs. Data from recordings are contained in Tables 9 through 13.

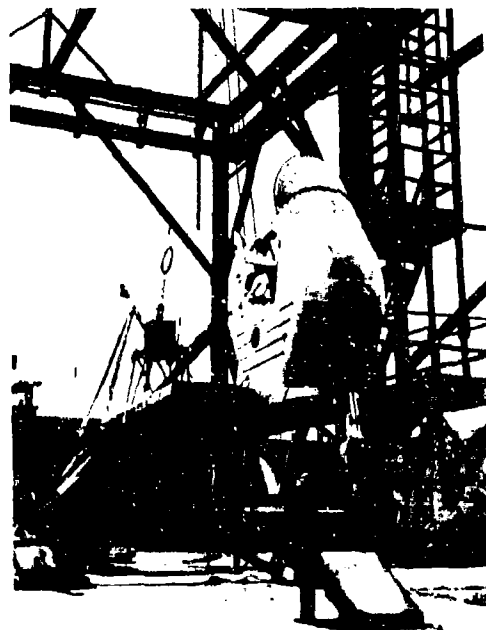
LANDING GEAR STATIC TESTS

Test Article

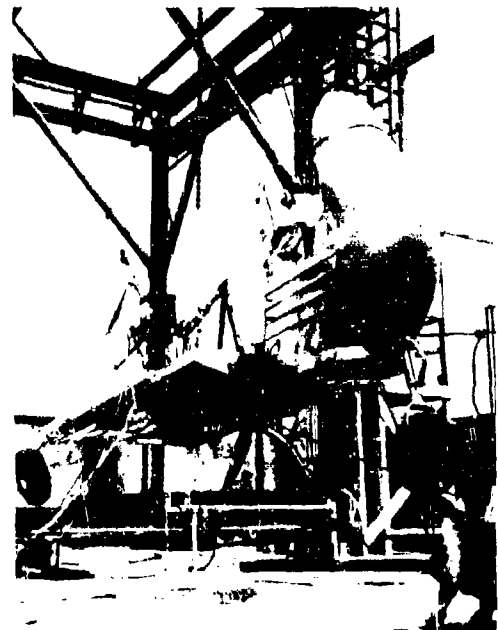
The test article consisted of a spring-axle assembly (Figure 25, detail A).

Test Procedure

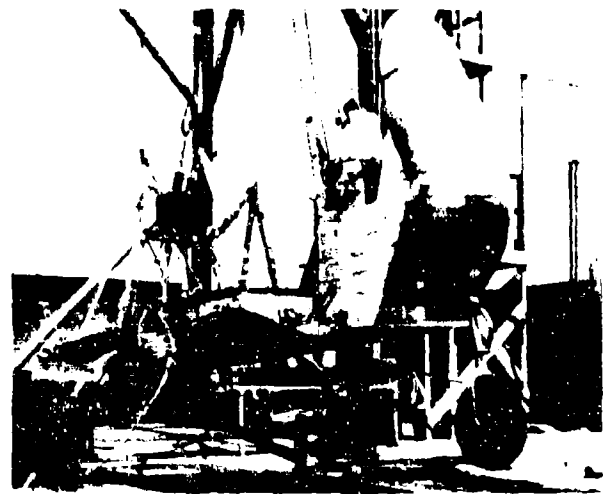
The spring-axle test assembly was mounted in a rigid jig in the same manner in which it attaches to the airplane. See Figure 25, detail B. A hydraulic cylinder was used to apply the load in increments of design limit, 5,350 pounds, until failure occurred. The axle deflections were visually measured with a graduated scale and the data recorder. Landing-gear loads were measured with strain gauges, which were located as shown in Figure 26.



Detail A

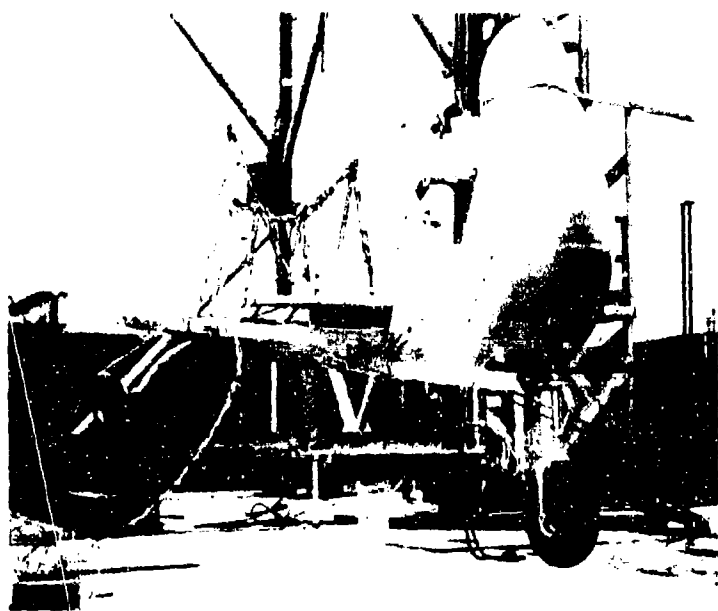


Detail B

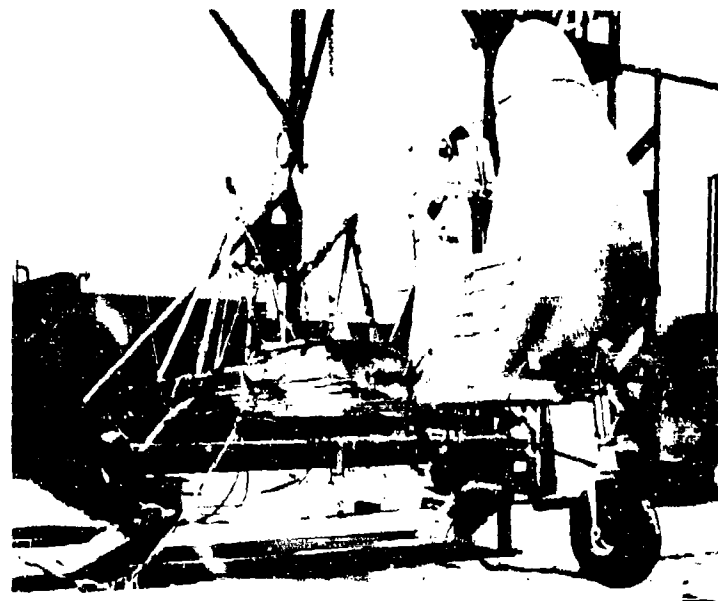


Detail C

Figure 24. Drop Test Configuration (Sheet 1 of 2)



Detail D



Detail E

Figure 24. Drop Test Configuration (Sheet 2 of 2)



Detail B



Detail D



Detail A



Detail C

Figure 25. Landing Gear Test Setup and Axle Failure

TABLE 9
DROP TEST CONFIGURATION NO. 1

Function and Location	Drop 1 Ht. 6 In.	Drop 2 Ht. 12 In.
Vertical Acceleration, Station 140	3.7 g above 0	3.2 g above 0
Longitudinal Acceleration, Station 140	2.7 g fwd.	3.3 g fwd.
Lateral Acceleration, Station 140	2.0 g	1.8 g
Vertical Acceleration, Nose Gear	3.4 g above 0 (first impact) 6.4 g above 0 (second impact)	4.8 g above 0 (first impact) 6.4 g above 0 (second impact)
Longitudinal Acceleration, Nose Gear	2.5 g fwd.	2.8 g fwd.
Platform Bending, Forward	5,000 p. s. i.	5,420 p. s. i.
Platform Bending, Aft	7,320 p. s. i.	7,320 p. s. i.
Axial Load Left Hand Engine Mount, Aft	4,080 p. s. i.	4,070 p. s. i.

TABLE 10
DROP TEST CONFIGURATION NO. 2

Function and Location	Drop 3 Ht. 6 In.	Drop 4 Ht. 12 In.	Drop 5 Ht. 18 In.	Drop 6 Ht. 21 In.	Drop 7 Ht. 26.9 In.
Vertical Acceleration, g above 0, Station 140	3.6 g	3.0 g	4.7 g	5.2 g*	6.0 g
Longitudinal Acceleration, Station 140	±0.5 g	1.0 g fwd.	1.8 g fwd.	2.4 g fwd.	2.0 g fwd.
Lateral Acceleration, Station 140	±1.8 g	2.0 g	±3.2 g	3.9 g	4.3 g
Vertical Acceleration, Nose Gear	3.2 g	5.6 g**	6.0 g***	5.0 g****	8.3 g
Longitudinal Acceleration, Nose Gear	±0.6 g	1.7 g fwd.	2.0 g	3.0 g fwd.	2.2 g fwd.
Platform Bending, Fwd.	1,250 p.s.i.	3,340 p.s.i.	5,000 p.s.i.	5,000 p.s.i.	5,410 p.s.i.
Platform Bending, Aft	2,150 p.s.i.	5,120 p.s.i.	6,220 p.s.i.	6,950 p.s.i.	8,420 p.s.i.
Axial Load Left Hand Engine Mount, Aft	5,500 p.s.i.	4,720 p.s.i.	5,350 p.s.i.	5,780 p.s.i.	5,570 p.s.i.

*With a 0.005 sec. spike of 6.3 g

**With a 0.01 sec. spike average peak 4.0 g above 0

***With 6.8 g - 0.01 sec. peak

****With a 0.005 sec. spike of 6.2 g

TABLE 11
DROP TEST CONFIGURATION NO. 3

Function and Location	Drop 8 Ht. 6 In.	Drop 9 Ht. 18 In.
Vertical Acceleration, Station 140	4.0 g above 0	4.6 g above 0 (first impact) 5.3 g above 0 (second impact)
Longitudinal Acceleration, Station 140	3.0 g fwd.	4.5 g fwd.
Lateral Acceleration, Station 140	2.1 g	2.5 g (first impact)
Vertical Acceleration, Nose Gear	4.0 g above 0 (first and second impact)	*
Longitudinal Acceleration, Nose Gear	2.8 g fwd.	4.0 g fwd.
Platform Bending, Forward	4,170 p. s. i.	6,250 p. s. i.
Platform Bending, Aft	6,220 p. s. i.	10,250 p. s. i.
Axial Load Left Hand Engine Mount, Aft	3,640 p. s. i.	8,570 p. s. i.

* (1st impact) 5.3 g with 0.01 sec. spikes to 7.5 g above 0 and 5.9 g below 0
 (2nd impact) 7.2 g with 0.01 sec. spikes to 8.3 g above 0 and 3.3 g below 0

TABLE 12
DROP TEST CONFIGURATION NO. 4

Function and Location	Drop 10 Ht. 0 In.*	Drop 11 Ht. 5 In.*	Drop 12 Ht. 8 In.*
Vertical Acceleration g above 0, Station 140	5.4 g	5.5 g	5.7 g
Longitudinal Acceleration, Station 140	1.0 g fwd.	0.9 g fwd.	0.8 g fwd.
Lateral Acceleration, Station 140	3.0 g (2nd impact)	± 1.5 g (1st impact) ± 2.5 g (2nd impact)	3.4 g (1st impact) 4.1 g (2nd impact)
Vertical Acceleration, Nose Gear, g above 0	2.0 g	2.5 g	3.0 g
Longitudinal Acceleration Nose Gear	0.5 g	0.8 g	0.7 g fwd.
Platform Bending, Fwd.	-	3,750 p. s. i.	2,920 p. s. i.
Platform Bending, Aft	7,300 p. s. i.	7,680 p. s. i.	8,050 p. s. i.
Axial Load Left Hand Engine Mount, Aft	4,930 p. s. i.	4,930 p. s. i.	6,000 p. s. i.

*Indicates height from nose wheel

TABLE 13
DROP TEST CONFIGURATION NO. 5

Function and Location	Drop 13 Ht. 6.73 In.
Vertical Acceleration, Station 140	3.8 g above 0
Longitudinal Acceleration, Station 140	± 1.0 g
Lateral Acceleration, Station 140	-2.8 g, -3.6 g
Vertical Acceleration, Nose Gear	4.1 g above 0
Longitudinal Acceleration, Nose Gear	1.2 g fwd.
Platform Bending, Forward	2,920 p. s. i.
Platform Bending, Aft	4,020 p. s. i.
Axial Load Left Hand Engine Mount, Aft	4,280 p. s. i.

Test Results

The axle failed just after 150 percent of designed limit load was reached. Figure 25, details C and D show the nature of the failure and also indicate secondary damage incurred when the spring impacted the broken end of the axle onto the concrete under the jig. The strain gauge and deflection data appear in Figures 27 and 28.

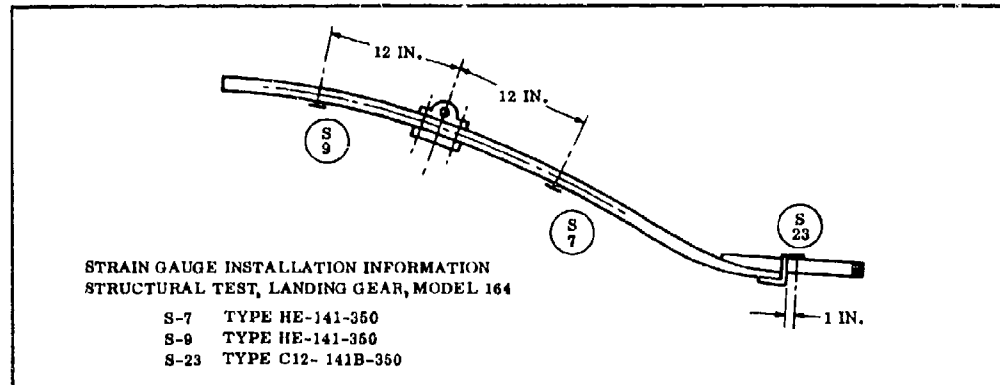


Figure 26. Landing Gear Test, Strain Gauge Locations

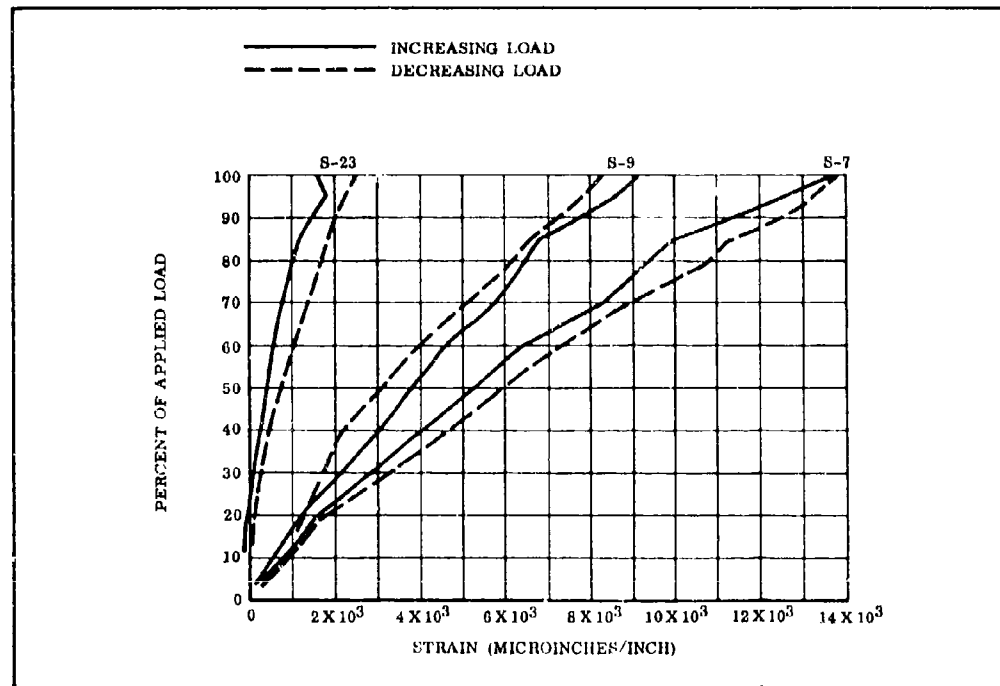


Figure 27. Landing Gear Test, Load Vs. Strain

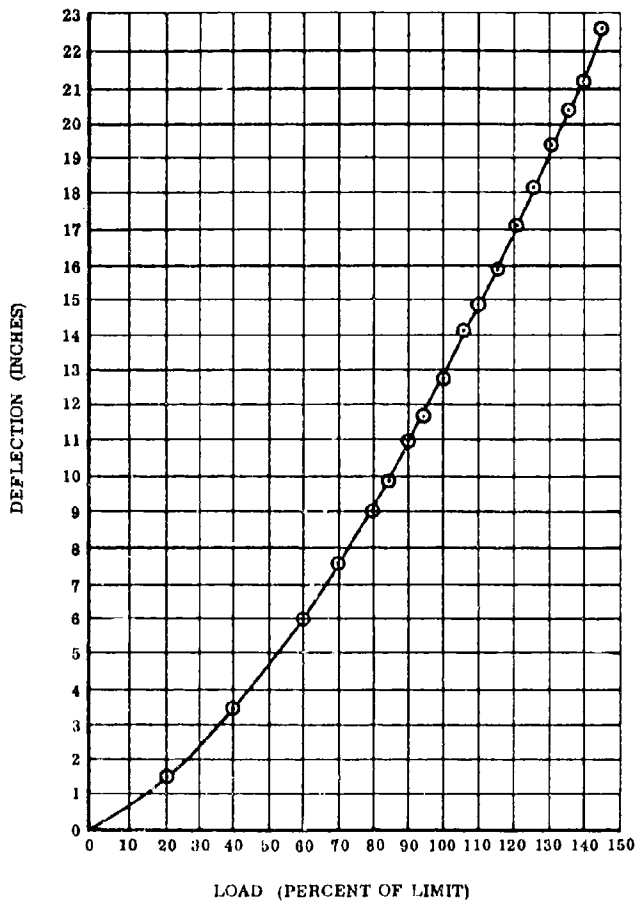


Figure 28. Landing Gear Test, Load Vs. Deflection

FLIGHT-TEST EVALUATION

INSTRUMENTATION

The two aircraft were instrumented as set forth in Ryan Report No. 62B021. Measurements were taken for proof of design from a stand-point of loads, stresses, performance, stability and control information which will be used in the overall evaluation of the aircraft. The first aircraft completed was instrumented for structural static tests. When these tests were completed, it was instrumented for flight tests.

Flight Test

Both aircraft were instrumented for flight test to determine control system displacement and forces, accelerations, airspeed, altitude, and g forces in the X, Y, and Z axes. Displacements were measured with potentiometers, and cable tensions were measured with load links. Accelerometers were used to measure acceleration, g forces, and vibrations. Low-pressure transducers were used for altitude and airspeed measurements. Engine operation, r.p.m., and temperature were also measured and recorded. Records were taken on a 26-channel oscilloscope during the taxi and initial flight tests to determine acceleration forces, control surface position, and control forces. As the test progressed, additional measurements were taken to determine stress levels in the structural members of the aircraft. Two standard 12-volt storage batteries connected in series were used as a power source for instrumentation. The recording instrumentation and associated equipment, including signals conditioning boxes, were installed on removable plywood pallets secured to the aircraft cargo bed with the cargo tie-down rings.

GROUND FUNCTIONAL TESTS

General

The two instrumented aircraft were given complete ground functional tests to insure satisfactory operation of the power plant and control system. The tests performed were:

1. Power plant operation and control.
2. Fuel, oil, and cooling system checks.

3. Flight control and trim system characteristics.
4. Controls proof test.
5. Braking system check.
6. Aircraft weight and balance.

Power Plant Operation and Control

The power plant and its controls were checked to determine engine performance, control settings and adjustments. Engine performance and operation of controls were satisfactory; as necessary, the mixture control was set, the idle cutoff was adjusted, and the magneto operation was performed. The propeller pitch setting was determined and set to obtain 2,700 r.p.m. with full throttle. Induced engine vibration was not excessive.

Fuel, Oil, and Cooling System Checks

A complete check of the fuel, oil, and cooling system was performed to determine the fuel tank capacity, wobble pump pressure, fuel pressure at engine pump outlet and at injectors, oil pressure, and accuracy of the fuel quantity and fuel pressure gauges. The fuel tank capacity is 25 gallons, with the fuel quantity gauge being calibrated accordingly. Instrumentation measurements were taken for cylinder head temperature, barrel temperature, oil pressure and oil temperature at a sustained r.p.m. of idle, 1,000, 1,200, 1,500, 1,800, 2,000 and 2,200. All measurements were satisfactory, with none of the temperature and pressure ratings being exceeded.

Flight Control and Trim System Characteristics

The following items were inspected and/or checked for proper installation prior to subjecting the vehicle to tests of any kind:

1. All fasteners for security; i.e., pulley brackets, cable unions, control mounting, etc.
2. All movable joints and hinges for excessive play, loose bushings, undue friction, etc.

3. Alignment of attached components; i.e., cable pulleys, control surfaces, foot pedal/nose wheel, control wheel/aileron wing, etc.

All discrepancies noted were corrected prior to performing tests.

Controls Proof Test

Prior to application of proof loads, the extreme ranges of the control system were measured with a steel tape. These measurements were taken of both the pilot's controls and associated control surfaces, with elevator control measurements being taken at the center and both extremes of pitch trim. The following loads were applied to the pilot's controls with the control surfaces mechanically locked in the neutral position and hydraulic cylinders used to apply the loads:

1. A 53-pound load was applied tangentially to the top of the pitch trim control wheel in both directions.
2. Two 100-pound loads were simultaneously applied at the rim, normal to the plane of the main control wheel, and diametrically opposite horizontally. Loads were applied in both directions. Load point deflections were measured at 40, 60, 80 and 100 percent of the applied load.
3. Two 80-pound tangential loads were applied simultaneously to diametrically opposite points on the rim of the main control wheel as a couple.
4. A 300-pound load was applied to the right-hand rudder pedal with the nose wheel locked in the neutral position.
5. A 300-pound load was applied to the brake pedal with the left-hand rudder pedal locked. Maximum deflections of the brake pedal and right-hand rudder pedal were measured.

The control system withstood the applied test loads satisfactorily.

Braking System Check

The complete braking system was checked for brake pedal operation, for excessive pedal movement, and for leaks. Operation of the braking system was satisfactory.

Aircraft Weight and Balance

Aircraft weight and balance was determined by using three platform scales. The as-weighed condition included the empty aircraft with full oil and instrumentation wiring only. The aircraft was weighed in the following conditions prior to the first taxi operations:

Platform Angle	N. W. Oleo Strut	Wing Incidence
6.0 deg.	Fully extended	0.0 deg.
0.0 deg.	Snubbed	0.0 deg.
0.0 deg.	Snubbed	26.0 deg.
20.25 deg.	Fully extended	0.0 deg.

The results of this initial series of weighings were as follows and constituted the basis for weight and balance calculations throughout the remainder of the program:

Gross Weight 1,151 pounds
Horizontal Arm 117.9 inches
Vertical Arm. 54.5 inches

The recommended center of gravity limits for the XV-8A in the fully loaded condition are from fuselage station 97 to 109 inches.

It was found during the aircraft weighing operation that variation in wing incidence angle had no effect on horizontal center of gravity location.

TAXI TESTS

Low Speed

The low-speed ground handling characteristics are very good. The response to nose wheel steering inputs was instantaneous and positive, and required only light pedal forces. Minimum radius turns of 20 feet can be accomplished. No significant sway, lean or heeling was evident during relatively fast turns. The vehicle is highly maneuverable even when operating on unprepared surfaces. Braking action is satisfactory, although fairly high pedal force is required. There is little or no pedal free play. Abrupt brake application or hard steady application did not induce any landing gear chatter, oscillation or excessive deflections.

No significant brake heating was apparent during any of the test operations. The brakes are adequate to hold the aircraft static against power application up to 2,710 r. p. m. 90 to 95 percent of takeoff power. At higher r. p. m. the wheels remain locked and the aircraft will skid forward. No adverse or unnatural control procedures or techniques were encountered as a result of having a single toe brake pedal configuration on the right nose wheel steering pedal. The behavior of the fiber glass main landing gear struts was excellent. Approximately 900 r. p. m. is required to initiate a taxi roll from a standing start.

High Speed

Lateral canting of the wing downwind during a crosswind taxi requires high lateral control force inputs on the part of the pilot to hold the wing level. It was noted that, when taxiing at speeds in excess of 15 miles per hour, these forces tend to lessen, which can be attributed to the servo effect of the leading edge tip ailerons. Elevator control effectiveness was not in evidence at taxi speeds up to approximately 33 miles per hour at a wing incidence angle of 20 degrees, and only a slight degree of effectiveness was observed at 28 degrees of wing incidence. The elevator control forces were very light. The aircraft became light on the gear at approximately 33 miles per hour calibrated airspeed, and some lateral rocking was present. Nose wheel shimmy was absent even with the aircraft light on the main gear. Directional response to lateral control inputs was evaluated at wing incidence angles of 20 and 24 degrees with the nosewheel steering pedals unrestrained. Negligible response to the control inputs was noted at speeds up to 30 miles per hour calibrated airspeed. Divergent oscillation of the nose wheel was observed as a resulting phenomenon to these inputs if the pedals were left free. Even at low taxi speeds, a light tap on the pedal would induce a divergent nose wheel oscillation with the pedals free. This condition was eliminated by the addition of a shimmy damper to the nose gear. No lateral-directional coupling was evident when the landing gear was firmly on the runway. Some brake fading was apparent when braking to a stop from approximately 33 miles per hour calibrated airspeed.

Crosswind Taxi Operations

Taxi operations were evaluated in moderately gusty crosswinds ranging from 8 to 15 knots. S-turns were executed at a speed of approximately 10 miles calibrated airspeed. The control force required to hold the wing from canting downwind was excessive. As these tests progressed, the wing incidence angle was increased from zero degree in

2-degree increments. The lateral control forces increased steadily to the point where at 16 degrees wing incidence, it became very difficult to move the wing in the upward direction. Minimum lateral control force is required at 0-degree wing incidence angle; however, a considerable amount of wing lobe flutter is present at this condition which may not be conducive to a long service life of the fabric. It was also noted that while taxiing at a wing angle of approximately 20 degrees, there was no tendency for the aircraft to heel excessively even with the wing canted over to the stop.

HANDLING QUALITIES

Nose Wheel Lift-Offs (Basic Configuration)

High-speed taxi runs were made at wing incidence angles of 20 to 24 degrees in an attempt to achieve nose wheel lift-off at a mid center of gravity location at speeds up to 43 miles per hour calibrated airspeed. In all cases the main gear broke ground before or, at best, simultaneously with the nose gear. Lateral control forces were light, and no response to any longitudinal control inputs was observed. Additional tests were conducted at wing incidence angles of 20 to 24 degrees to attain nose wheel lift-off at the aft center of gravity location. The speeds attained ranged from 20 to 43 miles per hour calibrated airspeed, in 5-mile-per-hour increments. Nose wheel lift-off could not be accomplished on any of the aforementioned runs.

Aircraft Lift-Offs (Basic Configuration)

The first lift-off was made at a wing incidence angle of 24 degrees at the aft center of gravity with 2200 r. p. m. at a calibrated airspeed of approximately 46 miles per hour. The aircraft became airborne through power effects rather than elevator effectiveness, and no attitude change was apparent following lift-off. The lateral control was satisfactory; forces were light and within the capability of one-hand control. Longitudinal control was ineffective. The landing was accomplished by power retardation rather than aft stick movement. Additional lift-offs were conducted at wing incidence angles of 24.5, 25.5, 26, 26.5 and 27 degrees at the aft center of gravity location to determine handling qualities. All lift-offs occurred with essentially a constant body attitude. Lateral control was acceptable, but the control forces involved were too high when compared to a conventional airplane. Longitudinal control was unacceptable even for an emergency condition, in that large control

inputs produced only very small pitch changes after a considerable time lag. The only difference noted, when changing the incidence angle from 24.5 to 26.5 degrees, was a reduction in lift-off speed by 2 miles per hour, from 46 to 44 miles per hour calibrated airspeed. At the wing incidence angles of 26.5 to 27 degrees, control was even more marginal, especially in pitch. Lift-off occurred at approximately 43 miles per hour calibrated airspeed in a manner similar to that described above.

A high rate of descent to touchdown produced a pitch-up about the main gear sufficient to scrape the elevator trailing edges on the runway when in a full-down position. One additional run was made at the mid center of gravity location which exhibited completely unacceptable characteristics. The aircraft attempted to fly off with the nose gear skipping on and off the runway. Longitudinal control inputs were completely ineffective in alleviating this condition. All remaining operations were conducted at the aft center of gravity limit. Lift-offs were also conducted at incidence angles of 20 and 22 degrees at the aft center of gravity location. Lift-offs occurred between 50 and 60 miles per hour calibrated airspeed. Elevator effectiveness appeared better than at the higher incidence angles because of the higher lift-off speeds, but was still unacceptable. Landings were extremely touchy by reason of the lack of longitudinal control and the higher landing speeds, with the landing a questionable item until the main landing gear was firmly on the runway.

High-Speed Taxi (Auxiliary Elevator)

Additional high-speed taxi runs were conducted after the addition of an auxiliary wooden elevator mounted at the aft end of the bed between the original elevators. Total elevator area was thus increased by 1,750 square inches by this additional surface. These runs were made at airspeeds over the range from 33 to 52 miles per hour calibrated airspeed at incidence angles of 16 and 18 degrees, during which the pilot pulsed the elevator. No vibrations were induced and no adverse characteristics were noted. One taxi run was accomplished at 46 miles per hour calibrated airspeed to observe the effect of trailing edge battens on the wing tip flutter. No flutter was observed during this taxi run.

Nose Wheel Lift-Offs (Auxiliary Elevator)

Nose wheel lift-off was attempted at wing incidence angles of 20 and 22

degrees at speeds up to 53 miles per hour calibrated airspeed. The nose wheel could not be lifted off at this aft center of gravity position. In order to augment the elevator control power, a flexible cloth seal was added between the aft end of the bed and the auxiliary elevator, and the engine ejector hole in the bed was skinned over. Test results were the same as for the auxiliary elevator alone during the one operation conducted in this configuration.

Aircraft Lift-offs (Auxiliary Elevator)

Several lift-offs and flights were accomplished at 24.5 degrees wing incidence angle at airspeeds between 50 and 55 miles per hour calibrated airspeed. Although the nose wheel lift-off was not attained, a positive attitude change capability was achieved. Elevator control power was still insufficient to achieve an initial main gear touchdown at landing speed, 49 miles per hour calibrated airspeed. Large longitudinal control displacements were required to produce attitude and subsequent altitude changes; however, the associated time lag was not objectionable. Platform attitude was nose-up during these operations. The auxiliary elevator was lightened from 31 to 21 pounds by the drilling out of lightening holes and skinning the surface with fabric. Taxi and takeoff operations indicated no appreciable effect due to lightening of the elevator. No pitch-trim changes were evident at lift-off as engine r. p. m. was progressively increased from 2,300 to maximum r. p. m. for takeoff. A slight amount of left wheel application is required at lift-off to counteract torque at maximum r. p. m. Shorter ground rolls and steeper climb angles resulted from increase in r. p. m. for lift-off. Slight control wheel buffet was observed which was attributed to trailing edge flutter near the wing tips. Lateral battens, 61 inches in length, were added to the left-hand and right-hand outboard wing panels parallel to the trailing edges to eliminate wing fabric flutter. No flutter or control wheel vibration was noted during the resulting lift-off and runway flight. Additional aircraft lift-offs were made at incidence angles of 26.5 and 27.5 degrees at lift-off speed of 46 and 42 miles per hour calibrated airspeed respectively. Longitudinal control was unacceptable at 26.5 degrees and nonexistent at 27.5 degrees incidence angle. The aircraft was unstable during the landing at 27.5 degrees incidence angle.

PERFORMANCE

Some preliminary level-flight performance data at wing incidence angle of 24.5 degrees are presented in Figure 29. These data are preliminary in nature and are uncorrected in view of the limited number of data

points obtained. Indications are that these performance parameters will be equal to or will exceed predicted values. These level-flight data points were obtained with an H-23 helicopter as a chase-pace vehicle.

STABILITY AND CONTROL

The first traffic pattern flight was made with maximum r. p. m. (2,850) for takeoff. Lift-off occurred at approximately 50 miles per hour calibrated airspeed, and the ground run was estimated to be 350 feet into a 6-knot, 40-degree crosswind. A climb was made to 180 feet in altitude, and power was retarded to 2,400 r. p. m., which resulted in a stabilized airspeed of 54 miles per hour calibrated airspeed at 100 feet. One traffic pattern flight was accomplished during which shallow turns were made. The lateral and longitudinal control forces were light; although the lateral forces were too high for a good harmony of control, they were sufficiently light to permit one-hand control. A slight right-hand wing heaviness became apparent during the flight. Post-flight inspection revealed that the right-hand wing bolt rope had failed. Fluttering of the wing fabric was present over the outer three feet of each wing panel. No difficulty was encountered with the crosswind, and a good landing was made. A fixed tab having a 15-inch span and 2.5-inch chord was added to the auxiliary elevator at a 15-degree depression angle. Six traffic pattern flights were accomplished. Some adverse yaw was encountered during S-turns at 56 miles per hour calibrated airspeed. In general, the aircraft handles satisfactorily. The maximum longitudinal forces encountered at an incidence angle of 24.5 degrees were 15 to 20 pounds push and pull over the speed range from 43 to 68 miles per hour calibrated airspeed. Left-wing heaviness appeared to increase with speed, as did the lateral control forces required to correct the situation. Considerable trailing edge wing flutter was encountered in the outer three feet of wing span which was fed back through the tip ailerons to the control wheel. Descent during landing was completely arrested by use of up elevator, requiring no power change. The rate of deflection was excessive, a momentary pause in level flight being required prior to reestablishment of the touchdown rate of descent. One pattern flight was made with the trailing edge battens installed at an airspeed of 55 miles per hour calibrated airspeed. The batten installation appeared to eliminate the wing trailing edge flutter.

Aircraft Lift-Offs (Wing Pitch Control System)

The auxiliary elevator was removed and the programmed wing pitch

LEVEL FLIGHT
PRESSURE ALTITUDE \approx 550 FT

SYMBOL	I_w	FTO	OAT	GROSS WEIGHT
	24 1/2"	13	95° F	1900 LB

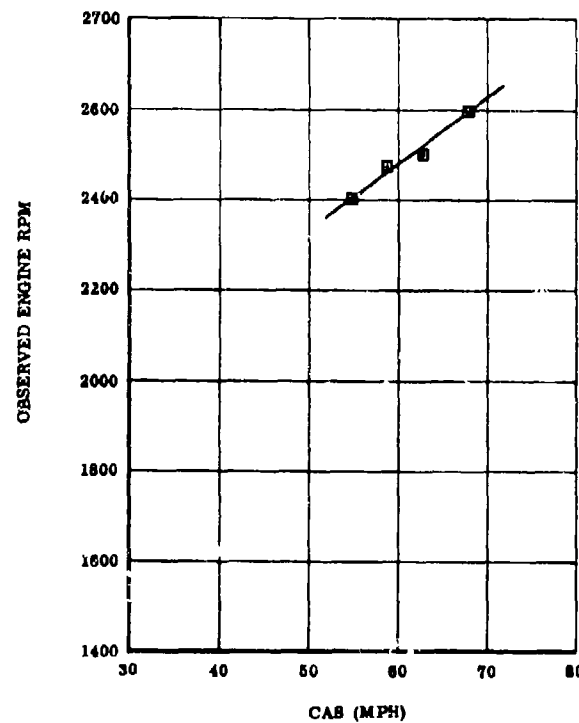


Figure 29. Performance Data, Level Flight

control system was incorporated for evaluation. This system programmed a ± 1.5 -degree wing incidence change from trim upon full (19 degrees) forward or aft stick deflection. Tests showed that the resultant control forces were high. The ability to accomplish altitude changes was essentially the same as with the auxiliary elevator configuration except that the auxiliary elevator provided a more positive attitude response. One other operation was conducted using the wing pitch control system together with the sealed auxiliary elevator. The same schedule of taxi runs was conducted as was the case for the wing pitch control system alone (an incidence angle variation of from 16 to 24.5 degrees over the airspeed range of from 46 to 52 miles per hour calibrated airspeed). Longitudinal stick forces were still too high (40 to 50 pounds). This configuration was more responsive than with the wing pitch control system alone; however, the control forces were objectionably high.

Trim Change

An attempt was made to evaluate wing incidence change (Δi_w) as a means of changing body attitude. A decrease of 90 degrees of pitch control wheel ($1/4^\circ \Delta i_w$) resulted in an immediate descent to touchdown. The significance of this result was somewhat masked by the close proximity of the aircraft to the ground. During subsequent tests the trim wheel was rotated forward and aft to a maximum of 180 degrees for a short period of time. No apparent trim change was evidenced due in part to the relatively small wing incidence angle change and the short period of time that the new trim position was held.

Lateral Control

The incorporation of re-sized lateral control bellcranks did produce a decrease in lateral control wheel force, which made one-hand control acceptable. There was no apparent decrease in lateral control effectiveness, and the sensitivity appeared to remain unchanged. Additional tests were conducted following the incorporation of the auxiliary elevator. Aircraft response to lateral control wheel force was good. The control forces and wheel displacement were satisfactory during shallow banks and turns, and the aileron stops were not contacted during these limited maneuvers, indicating that wing tilt was following aileron deflection sufficiently to preclude full aileron travel in order to accomplish the maneuvers executed. A light was incorporated in the cockpit to glow when full aileron travel had been reached. The light was not seen to glow.

Bolt Rope Effect

Two lift-offs were made at a wing incidence angle of 24.5 degrees at the aft center of gravity location with the trailing edge bolt rope disconnected. No difference in body attitude was noted, and the only discernible difference in characteristics, which could be attributed to bolt rope removal, was a slight control column buffet.

Simulated Malfunctions

Aileron cable failure was simulated by first disconnecting one aileron cable and then both aileron cables with the wing incidence angle set at 24.5 degrees. Three taxi runs and short lift-offs were accomplished with one aileron cable disconnected. This condition produced an increase in lateral control forces, and the wing had to be tilted opposite to the side having the inoperative aileron. The handling qualities were such that the vehicle could probably be recovered and landed should a cable failure occur. One taxi run was made with both ailerons disconnected. Lateral control forces were high, and approximately ± 30 degrees of lateral control wheel input produced no response. This condition is marginal and would probably cause damage to the aircraft during a landing.

OPERATIONAL TECHNIQUES

General

Techniques for performing the various operational functions with the Flexible Wing Aerial Utility Vehicle follow (it is not intended that these techniques will enable untrained or inexperienced personnel to operate the vehicle):

Starting Engine

After checking the vehicle for readiness, start the engine as follows:

1. Set the fuel mixture control to the FULL RICH position.
2. Advance the throttle control to the 1/8- to 1/4-inch position.

3. Rotate the propeller several turns by hand.

WARNING

Always stand clear while turning the propeller. When the engine is hot, or when the ignition switch is in the BOTH, LEFT, or RIGHT position, the propeller may kick or the engine may start, causing injury to personnel.

4. Pump the wobble pump until fuel drips from the fuel injector overflow lines on the engine.
5. Turn the ignition switch to the BOTH (magnetos) position.
6. Signal the ground crew to crank the engine with the propeller.
7. If the engine fails to start, after several attempts, turn the ignition switch to OFF, place the throttle in the full open position, and turn the engine over several turns with the propeller to clear the cylinders.
8. Repeat steps 2, 4, 5, and 6.
9. After the engine is started, adjust the throttle to idling speed (900 to 1,000 r. p. m.).

Engine Ground Operation

After the engine has started, assure that oil operating pressure is within limits, and warm up the engine by operating the engine at 900 to 1,000 r. p. m. for at least 1 minute; follow this warmup by one at 1,200 r. p. m.

Engine Ground Test

After the engine oil temperature has reached 75 degrees Fahrenheit (23.8 degrees centigrade), increase engine speed to 1,700 r. p. m., and perform the following steps:

1. Move magneto switch and tachometer switch to "R" position and note the engine r. p. m.

2. Move magneto switch and tachometer switch to BOTH, then to the "L" position and note the engine r. p. m. Maximum r. p. m. drop in the "L" and "R" positions should not exceed 125 r. p. m., nor should there be greater than 50 r. p. m. difference between the r. p. m. at "L" or "R" positions.
3. Return magneto switch to BOTH position.
4. Slowly and smoothly increase engine r. p. m. to maximum. Check for r. p. m. approaching maximum, engine running smooth, and oil pressure between 30 and 60 p. s. i.
5. Return throttle control to idle position.

Taxi

Check steering and brake controls before taxiing the vehicle. Taxi speeds should be relatively slow, especially where crosswinds are greater than 5 to 8 knots. In order to reduce "heeling" tendencies in crosswinds, apply lateral control into the wind. This may best be accomplished by leading the anticipated crosswind with wheel control such that the wing is tilted into the wind before the crosswind is actually encountered. Failure to follow this procedure may cause the wing to be picked up by the wind with subsequent excessive heeling of the entire vehicle. Little more than idling r. p. m. should be required to start the vehicle moving and maintain a satisfactory taxi speed.

Takeoff

The Flexible Wing Aerial Utility Vehicle is designed to take off from semiprepared or rough fields in short distances. To take off, proceed as follows:

1. Set the brakes.
2. Check the fuel mixture control at RICH and increase engine r. p. m. to maximum.
3. Release the foot brakes and commence takeoff, using nose wheel steering to maintain a straight ground run. Aircraft will fly itself off, with little or no aircraft rotation involved.
4. Use the pitch trim handwheel to trim to a 45-knot climb airspeed.

5. Reduce power and fuel mixture to that consistent with the desired climb speed. Trim speed as required.
6. In takeoffs in crosswind, use lateral control to lower windward wing leading edge into the wind to prevent heeling and drift; maintain heading by means of nose wheel steering.

Climb

Following takeoff, power may be held at the maximum of 2,800 r. p. m. for maximum climb performance. With a wing trim setting of 24.5 degrees incidence angle and an indicated airspeed of 45 to 50 miles per hour indicated airspeed, the vehicle is in good balance as very little aft stick force is required. The climb flight path is relatively steep under light to moderate gross weight conditions (up to 1,900 pounds).

Descent to Landing

Recommended speed during approach to landing is 45 to 47 miles per hour indicated airspeed, with the minimum of 42 miles per hour indicated airspeed for 1,900 pounds gross weight. To provide a flight path which is not too steep for a comfortable flare to landing touchdown, approximately 2,100 r. p. m. should be maintained during the glide.

Landing

Landing is best accomplished by accurately adjusting the flare maneuver to arrive at the bottom of the flare one or two feet above the runway surface and reducing power slowly to idle. If the flare maneuver is executed too high, with the power setting for glide (2,100 r. p. m.), the airspeed will fall below that required for minimum longitudinal control (approximately 37 miles per hour indicated airspeed), and the sink rate will be too great for a satisfactory landing. In such a case, power should be EASED ON to control the descent rate to touchdown.

After Landing

Following touchdown, the vehicle may be decelerated in a very short distance by applying brakes until wheel skid is felt. There is no tendency for the vehicle to diverge in direction if the nose wheel is centered prior to its contact with the ground. Once all wheels are firmly on the surface, excellent control for roll-out and taxi exists.

Engine Shutdown

Shut down the engine after taxiing to the parking area as follows:

1. Place the throttle control in IDLE position.
2. Place the mixture control in IDLE cutoff position.
3. Turn the ignition switch to OFF.

MAINTENANCE REQUIREMENTS

GROUND SUPPORT EQUIPMENT

The equipment originally provided for ground support during the test program consisted of a tow bar, two wheel chocks, one 8-foot step ladder, and two 10-foot aluminum poles for support of the leading edges during the folding operation. During the test program it was found that considerable difficulty was encountered when attempting to insert the quick-release pins in the spreader bar joints after extending the wing from the folded position. This operation has been greatly facilitated by providing the quick-release pins with long tapered extensions which serve as drift pins to bring the parts into proper alignment as the pins are pushed into place. When towing the vehicle with the wings folded, it is necessary to pad the sheet metal leading edges where they contact the tubular steel roll control structure. Removable pads have been provided which can be attached or removed from the roll control structure by means of quick-release pins. These pads are now considered to be a necessary item of ground support equipment.

SPECIAL TOOLS REQUIRED

It was found that a special wrench was needed to tighten the ignition cable attachments at the lower spark plugs. This was made by slotting one side of a standard 7/8-inch-deep socket wrench. All other assembly and maintenance operations on the vehicle were accomplished with standard tools.

BIBLIOGRAPHY

REFERENCES

1. Campbell, J. P., "Summary of Methods for Calculating Dynamic Lateral Stability and Response and for Estimating Lateral Stability Derivatives," N. A. C. A. Report 1098, 1952.
2. Gray, V. I., "Representative Operating Charts of Propellers Tested in the N. A. C. A. 20-Foot Propeller Research Tunnel," N. A. C. A. W. R. L-286, 1943.
3. Hoerner, S. F., "Fluid Dynamic Drag," 1958.
4. Liddell, R., "Wind-Tunnel Investigation of Rounded Horns and of Guards on a Horizontal Tail Surface," N. A. C. A. ARR No. L4J16, 1944.
5. Northrop Aircraft Inc., "Dynamics of the Airframe," BUAER Report AE-61-4, Volumes II and IV, 1952.
6. Pass, H., "Analysis of Wind-Tunnel Data on Directional Stability and Control," N. A. C. A. TN 775, 1940.
7. Perkins, C. and Hage, R., "Airplane Performance, Stability and Control," John Wiley & Sons, Inc., 1960.
8. Purser, P. E., "Experimental Verification of a Simplified Vee-Tail Theory and Analysis of Available Data on Complete Models with Vee-Tails," N. A. C. A. ACR No. L5A043, 1945.
9. Ribner, H., "Formulas for Propellers in Yaw and Charts of the Side Force Derivative," N. A. C. A. Report 819, 1945.
10. Ryan Report No. 63B021, "Flexible Wing Aerial Light Utility Vehicle," Volumes I through V, Ryan Aeronautical Company, San Diego, California, May 1963.

11. Sacks, A., "Aerodynamic Forces, Moments and Stability Derivatives for Slender Bodies of General Cross Section," N. A. C. A. TN 3283, 1954.
12. Sears, R., "Wind-Tunnel Data on the Aerodynamic Characteristics of Airplane Control Surfaces," N. A. C. A. ACR No. 3L08, 1943.
13. Sivells, J., "Tests in the 19-Foot Pressure Tunnel of a Rectangular N. A. C. A. 0012 Horizontal Tail Plane with Plain and Horn-Balanced Elevators," N. A. C. A. ARR No. 4, 1942.

HANDBOOKS

Pilot's Handbook for the Flexible Wing Aerial Utility Vehicle XV-8A (Ryan Model 164), March 1964.

MANUFACTURER'S SPECIFICATION

Continental Motors Corp., Detail Specification for Continental Aircraft Engine Model IO-360-A, April 25, 1962.

DISTRIBUTION

US Army Materiel Command	9
US Army Mobility Command	5
US Army Aviation Materiel Command	5
US Strike Command	2
Chief of R&D, DA	3
US Army Transportation Research Command	64
USATRECOM Liaison Officer, US Army R&D Group (Europe)	1
US Army Natick Laboratories	1
US Army Engineer R&D Laboratories	3
US Army Limited War Laboratory	2
Army Research Office-Durham	1
US Army Test and Evaluation Command	2
US Army Combat Developments Command, Fort Belvoir	1
US Army Combat Developments Command Aviation Agency	2
US Army Combat Developments Command Armor Agency	1
US Army Combat Developments Command Transportation Agency	2
US Army Combat Developments Command Quartermaster Agency	2
US Army Combat Developments Command Experimentation Center	1
US Army War College	1
US Army Command and General Staff College	1
US Army Aviation School	2
Deputy Chief of Staff for Logistics, DA	1
US Army Infantry Center	4
US Army Aviation Test Board	2
US Army Airborne, Electronics and Special Warfare Board	4
US Army Aviation Test Activity	2
Army Liaison Officer, Special Air Warfare Center	1
Air Force Flight Test Center, Edwards AFB	1
Air University Library, Maxwell AFB	1
Commandant of the Marine Corps	2
Marine Corps Liaison Officer, US Army Transportation School	1
NASA-LRC, Langley Station	6

Manned Spacecraft Center, NASA	2
NASA Representative, Scientific and Technical Information Facility	2
Research Analysis Corporation	1
National Aviation Facilities Experimental Center	3
Canadian Liaison Officer, US Army Transportation School	1
Defense Documentation Center	20
Ryan Aeronautical Company	5
ARFO (LA)	2
ARFO (ME)	2
RDFU-T	2
RDFU-V	2
ARPA (For Project AGILE)	2
11th Air Assault Division	1
Yuma Test Station	1
Hq USATDS	2
US Army Board for Aviation Accident Research	1

Unclassified

Security Classification

DOCUMENT CONTROL DATA - R&D

(Security classification of title, body of abstract and indexing annotation must be entered when the overall report is classified)

1 ORIGINATING ACTIVITY (Corporate author) Ryan Aeronautical Company San Diego, California		2a REPORT SECURITY CLASSIFICATION AT 1 Unclassified
3 REPORT TITLE XV-8A Flexible Wing Aerial Utility Vehicle		2b GROUP N/A
4 DESCRIPTIVE NOTES (Type of report and inclusive dates) Final Report August 1964 to January 1965		
5 AUTHOR(S) (Last name, first name, initial) Landgraf, F. and Girard, P.F.		
6 REPORT DATE February 1965	7a TOTAL NO OF PAGES 96	7b NO OF REFS 15
B. CONTRACT OR GRANT NO. DA 44-177-AMC-874(T)	9a ORIGINATOR'S REPORT NUMBER(S) USATRECOM 64-74	
C. PROJECT NO. Task 1D121401A14172	9b OTHER REPORT NO(S) (Any other numbers that may be assigned this report) 65B003	
10 AVAILABILITY LIMITATION NOTICES All distribution of this report is controlled. Qualified DDC users shall request through Secretary of Defense, ATTN: ARPA-AGILE, Washington, D. C. 20310 Release or announcement to the public is not authorized.		
11 SUPPLEMENTARY NOTES Sponsored by: Advanced Research Projects Agency	12 SPONSORING MILITARY ACTIVITY US Army Transportation Research Command Fort Eustis, Virginia	
13 ABSTRACT This final report is based on interim report 64B08 of contractor. Contract number was DA 44-177-AMC-874(T), ARPA Order 294-62 Amendment No. 3, unclassified. This report discusses procedures and accomplishments of the design, fabrication and the test program of the XV-8A vehicle and		
<ol style="list-style-type: none"> 1. Investigates the construction of a Flexible Wing Light Utility Vehicle, simple to operate, and capable of transporting a 1,000-pound payload for a distance of 100 miles at a speed of 50 miles per hour. 2. Covers the design, building and testing of two vehicles. 3. Concludes that the vehicles as described are feasible, and recommends further tests. 		

DD FORM 1 JAN 64 1473

Unclassified

Unclassified
Security Classification

Unclassified

Security Classification



DEFENSE ADVANCED RESEARCH PROJECTS AGENCY

3701 NORTH FAIRFAX DRIVE
ARLINGTON, VA 22203-1714

November 20, 2001

Ms. Kelly Akers
Defense Technical Information Center
8725 John J. Kingman Road
Suite 0944
Ft. Belvoir, VA 22060-6218

Dear Ms. Akers:

This is to advise you that the following documents have been reviewed and/or declassified and released under the Freedom of Information Act.

- Document Number: AD 803668
Unclassified Title: Sailwing Wind Tunnel Test Program
Report Date: September 30, 1966
- ✓ • Document Number: AD 461202
Unclassified Title: XV-8A Flexible Wing Aerial Utility Vehicle
Report Date: February 1, 1965
- Document Number: AD 460405
Unclassified Title: XV-8A Flexible Wing Aerial Utility Vehicle
Report Date: February 1, 1965
- Document Number: AD 431128
Unclassified Title: Operational Demonstration and Evaluation of the Flexible Wing Precision Drop Glider in Thailand
Report Date: March-July 1963
- Document Number: AD 594 137L
Unclassified Title: Communist China and Clandestine Nuclear Weapons-Input Substudies A-J, SRI Report
Report Date: October 1970
- Document Number: AD B 176711
Unclassified Title: Overlay and Grating Line Shape Metrology Using Optical Scatterometry
Report Date: August 31, 1993

If you have any questions, please contact Mr. Fred Koether, our Declassification Specialist, at (703) 696-0176.

TEZCON, 4 DEC 2001,
MR. KOETHER STATED
THAT ABOVE DOCUMENTS
ARE APPROVED FOR
PUBLIC RELEASE
Jany Novak

Sincerely,

for Douglas J. Fairhurst
Nancy M. Kassner
Director
Security and Intelligence Directorate